The sounds of the stars

Asteroseismology

- New eyes to see the invisible stellar interiors
- Development of Helioseismology to Asteroseismology
  - Various physical conditions/environment
  - evolution stage, stratification, chemical compositions, rotation, magnetism, binarity, planets

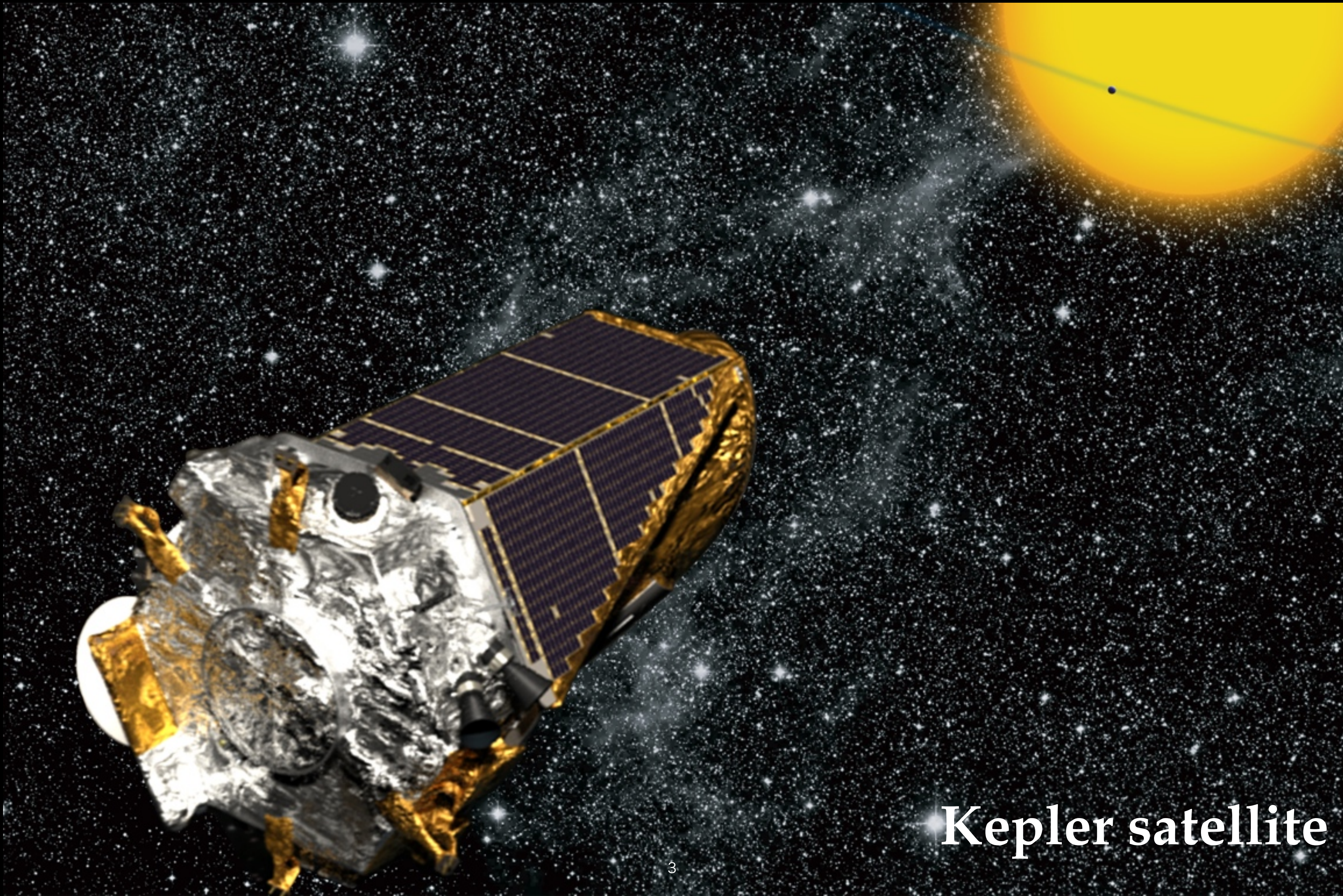
Kepler satellite

Transit Light Curves

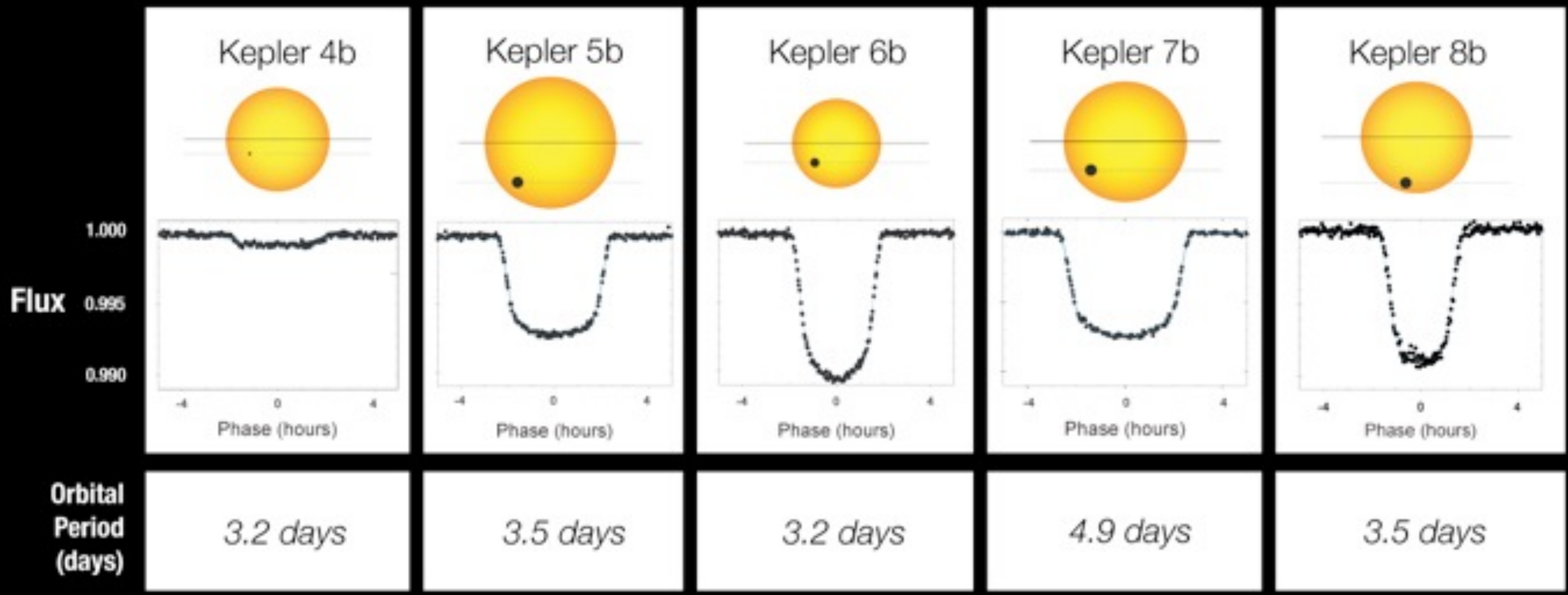

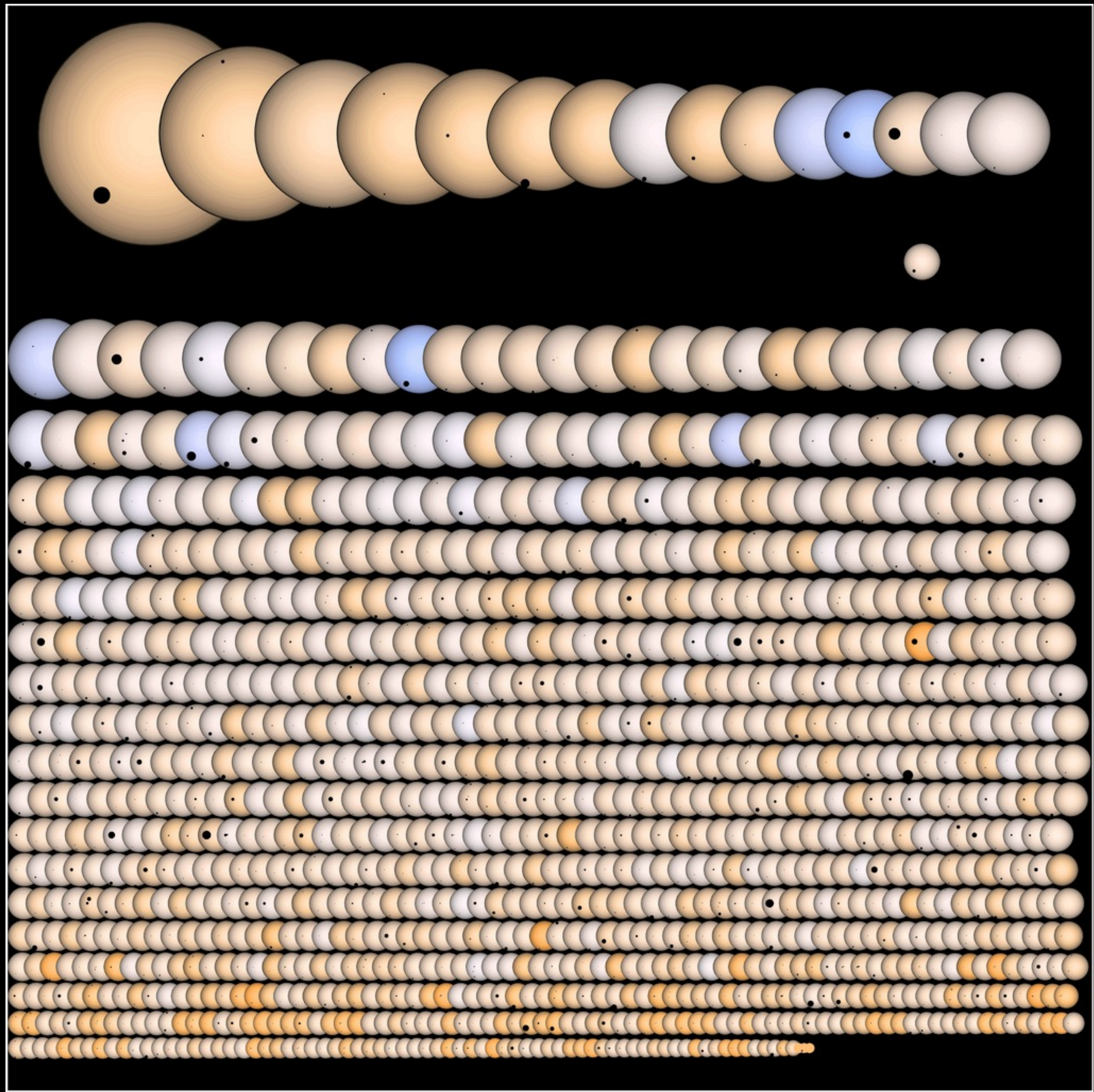

Keplerian revoltion

- Almost continuous observations over 4 years

- Observations from Space

  no atmospheric sintillation

  no day-night gaps

- Extremely high precision; $\Delta L/L \sim 10^{-6}$

1960's

today

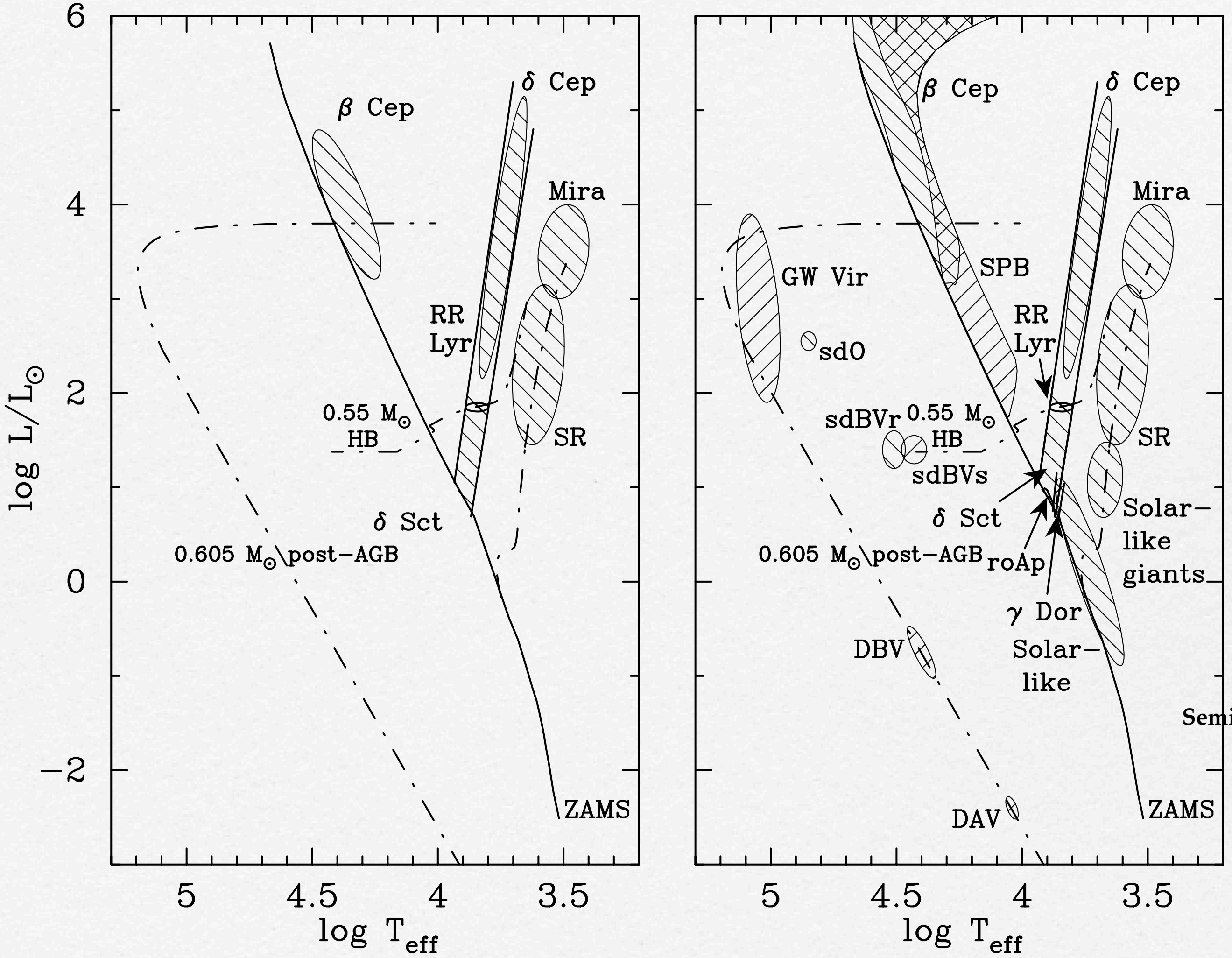

$\Delta L(t)$

$\widetilde{L}(\omega)$

\\\\\\ : p-mode

////// : g-mode

Semiregular -> solar like

Handler, G. 2012, ASPC, 462, 111

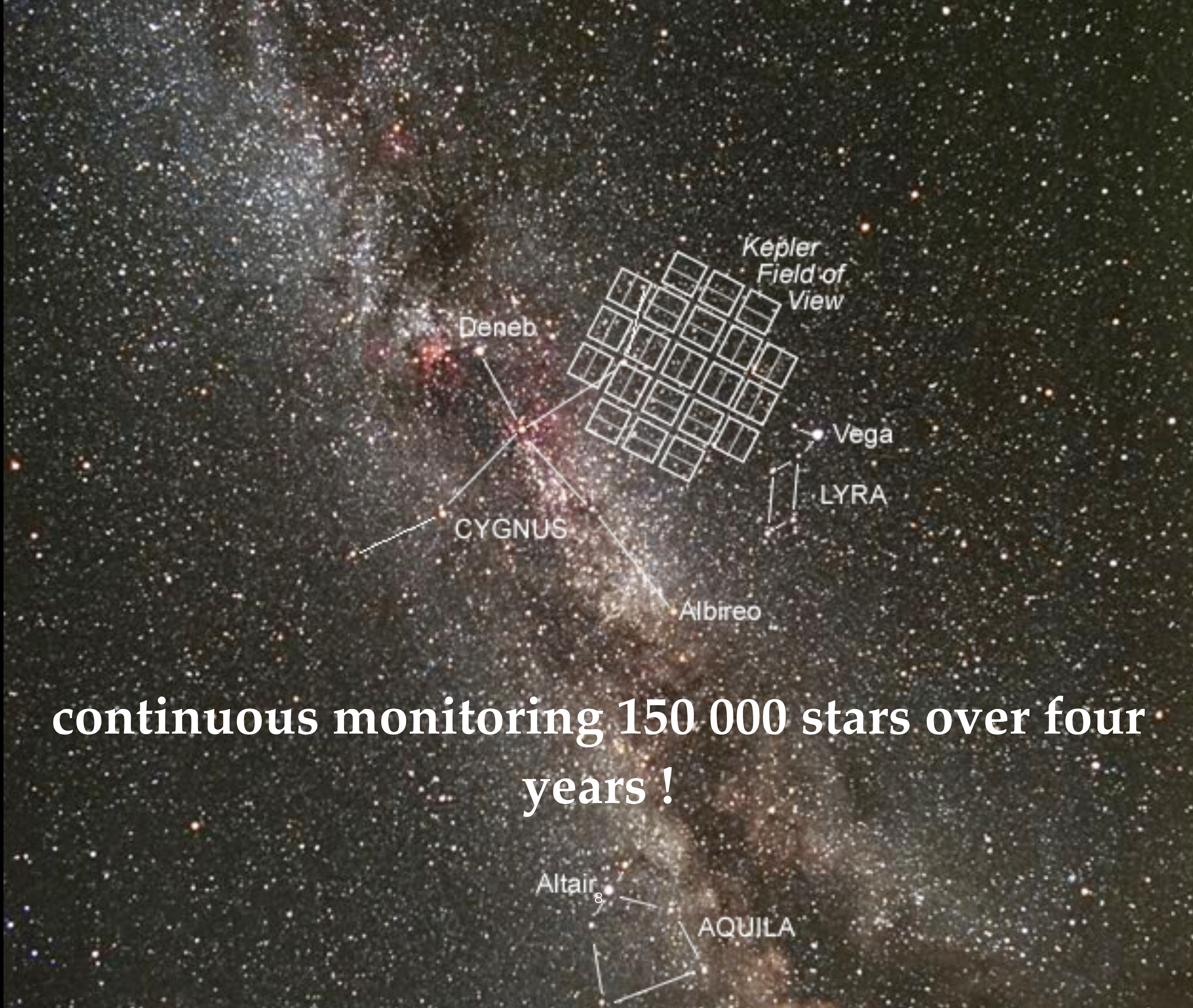

continuous monitoring 150 000 stars over four years !

Helioseismology

New eyes to see
the invisible interior of the Sun

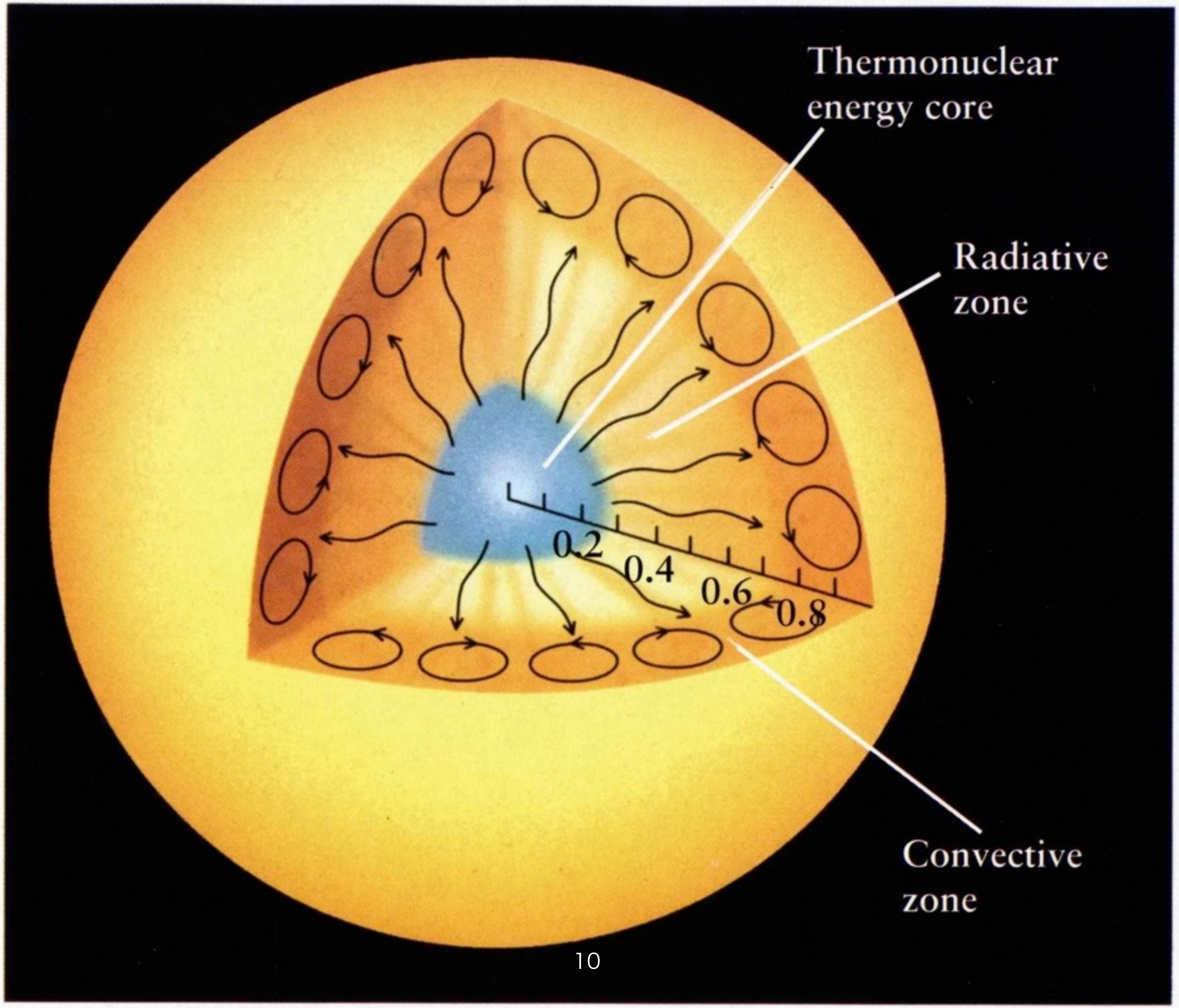
Thermonuclear
energy core
Radiative
zone
Convective
zone
0.2
0.4
0.6
0.8

Robert B. Leighton

(Sep 10, 1919 – March 9, 1997)

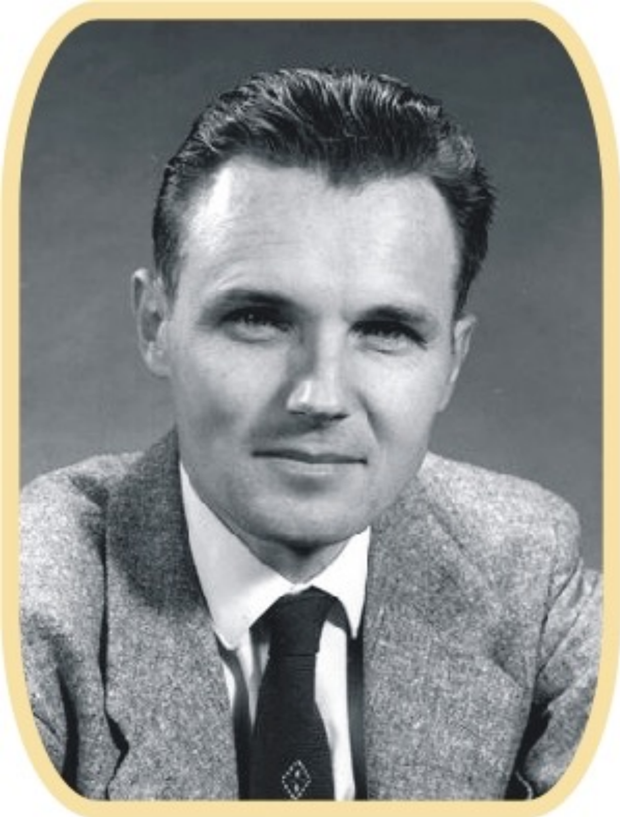

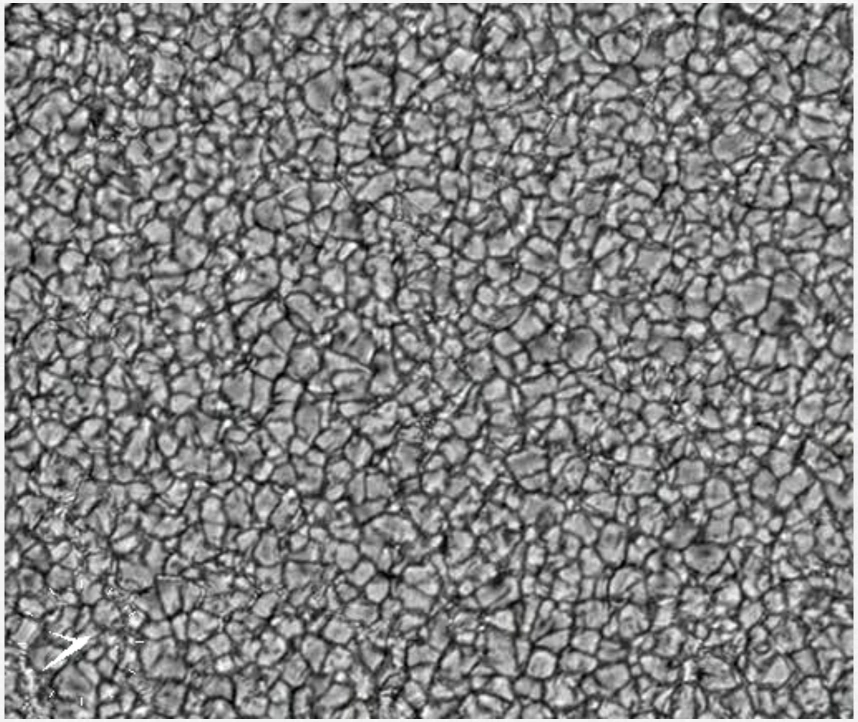

Aiming to study turbulence ...

Discovery of Solar 5-minute Oscillation

and

Supergranulation (1960)

Doppler velocity measurement

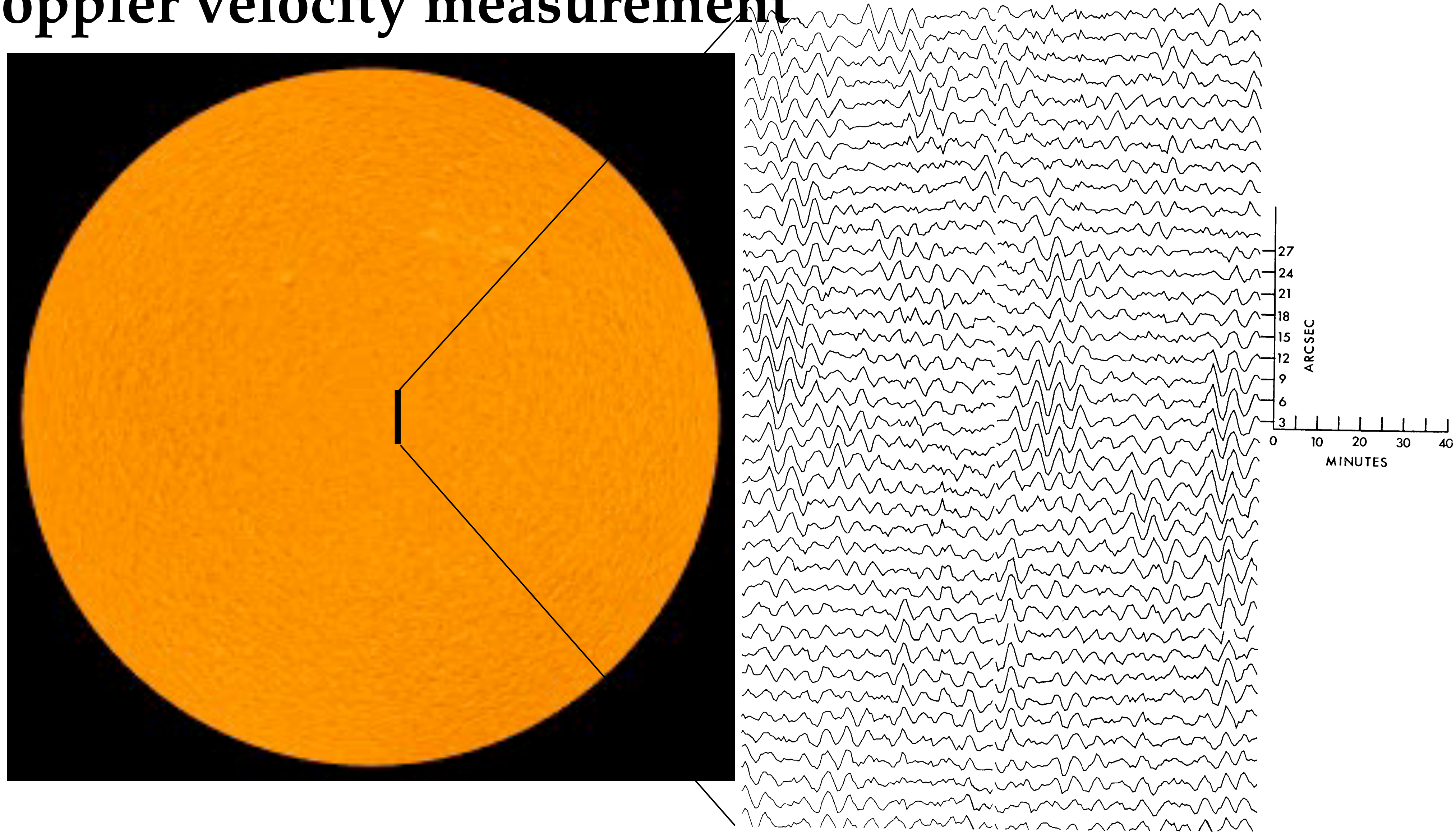

Musman, S. & Rust, D.M. 1970, Sol. Phys., 13, 261

mass conservation

$$\frac{\partial \rho}{\partial t} + \nabla \cdot (\rho v) = 0$$

momentum conservation

$$\rho \left(\frac{\partial}{\partial t} + v \cdot \nabla \right) v = \rho f - \nabla p - \rho \nabla \Phi$$

energy conservation

$$\rho T \left(\frac{\partial}{\partial t} + v \cdot \nabla \right) S = \rho \varepsilon - \nabla \cdot F$$

$$\rho = \rho_0(r) + \rho'(r,t)$$

$$v = v_0(r) + v'(r,t)$$

$$p = p_0(r) + p'(r,t)$$

$$r = r_0 + \xi$$

$$\rho(r,t) = \rho_0(r) + \rho_1(r,t) + \rho_2(r,t) + \ldots$$

Lagrangian displacement

$$r\,(t,r_0) = r_0 + \boldsymbol{\xi}(t,r_0)$$

Lagrangian velocity

$$v = \mathrm{d}r/\mathrm{d}t$$

where

$$\mathrm{d}/\mathrm{d}t := \partial/\partial t + (v_0 \cdot \nabla)$$

is Lagrangian derivative

Eulerian view: coordinates fixed

$$f\,(r,t) = f_0\,(r) + f'\,(r,t)$$

Lagrangian view: mass element fixed

$$f\,(r_0,t) = f_0\,(r_0) + \delta f\,(r_0,t)$$

$$= f_0(r - \xi) + \delta f\,(r_0,t)$$

$$= f_0(r) - (\xi \cdot \nabla) f_0(r) + \delta f\,(r_0,t)$$

$$r\,(t,r_0) = r_0 + \xi(t,r_0)$$

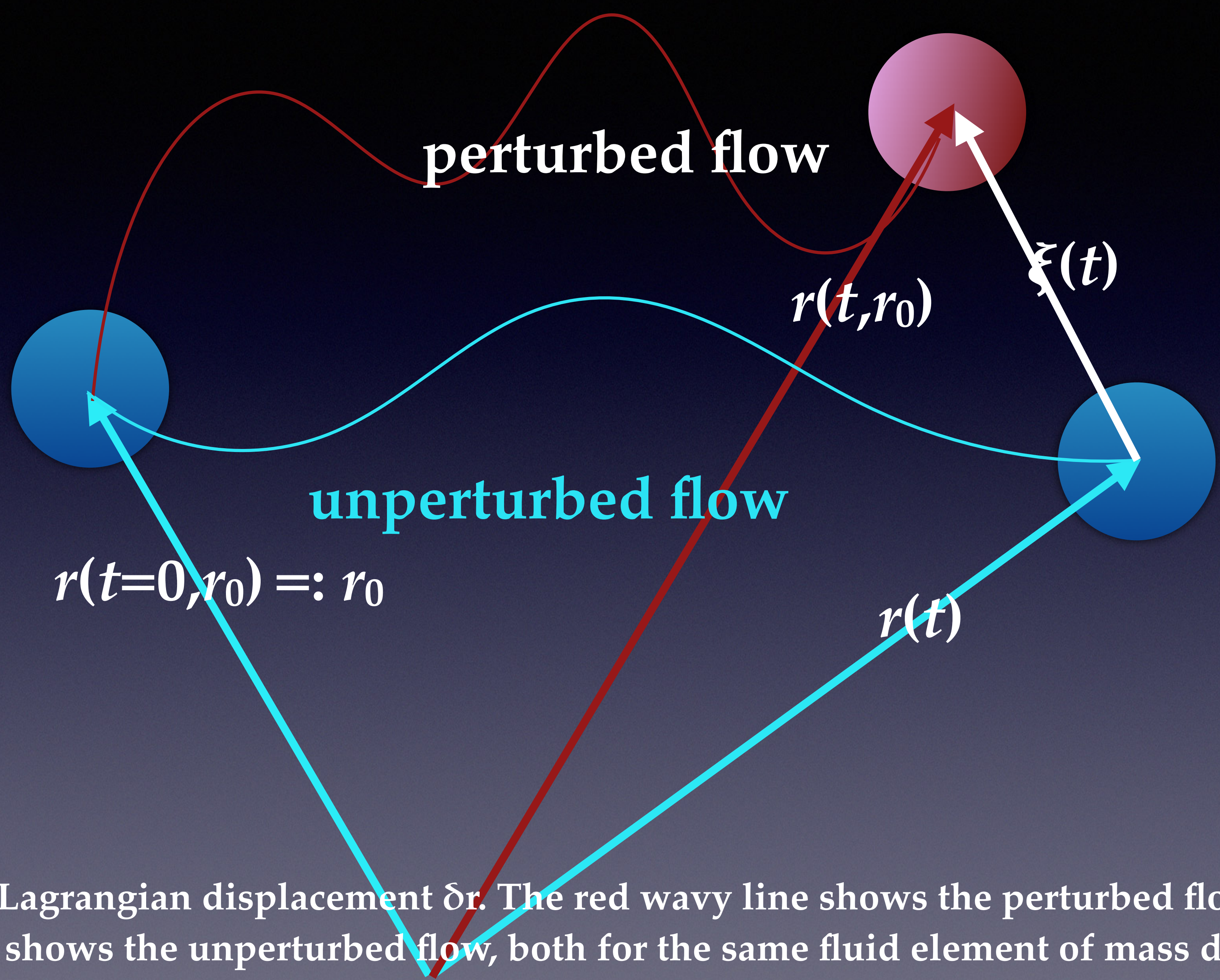

Illustration of Lagrangian displacement δr. The red wavy line shows the perturbed flow, and light-blue line shows the unperturbed flow, both for the same fluid element of mass dm.

Lagrangian perturbation: mass element fixed

Eulerian perturbation: coordinates fixed

$$\therefore\ \delta f\,(r_0,t) = f'\,(r,t) + (\boldsymbol{\xi} \cdot \nabla) f_0(r)$$

To first order,

$$\boxed{\delta f\,(r,t) = f'\,(r,t) + (\boldsymbol{\xi} \cdot \nabla) f_0(r)}$$

Time scales

Dynamical timescale : $\tau_{\rm dyn} = (GM/R^3)^{1/2}$

Thermal timescale : $\tau_{\rm th} = \int c_{\rm v} T {\rm d}m/L$

$\tau_{\rm dyn} \lll \tau_{\rm th}$

Motion is almost adiabatic, that is,
$\delta S = 0$, or equivalently,

$$\boxed{\delta p/p = -\Gamma_1 \delta\rho/\rho}$$

$$\frac{\partial \rho'}{\partial t} + \nabla \cdot (\rho_0 v') = 0$$

$$\rho_0 \frac{\partial v}{\partial t} + \nabla p' + \rho_0 \nabla \Phi' + \rho' \nabla \Phi_0 = 0$$

$$\frac{\delta p}{p_0} = \gamma \frac{\delta \rho}{\rho_0}$$

$$\frac{\partial p'}{\partial t} - c_0^2 \frac{\partial \rho'}{\partial t} - \rho_0 c_0^2 \left(\frac{d \ln \rho_0}{dr} - \frac{1}{\Gamma_1} \frac{d \ln p_0}{dr}\right) v_r = 0$$

plane parallel isothermal atmosphere

$$\rho \quad \propto \quad \exp(-z/H_\rho)$$
$$c^2 = \gamma\, p/\rho$$

Set

$$\boldsymbol{\xi}, \frac{p'}{\rho}, \frac{\rho'}{\rho_0} \propto \exp\left(\frac{z}{2H_\rho}\right) \exp(i\boldsymbol{k}\cdot\boldsymbol{x} + i\omega t)$$

to derive a dispersion relation:

$$\omega^4 - \omega^2\left(c^2k^2 + \omega_{\rm ac}^2\right) + N^2c^2k_{\rm h}^2 = 0$$

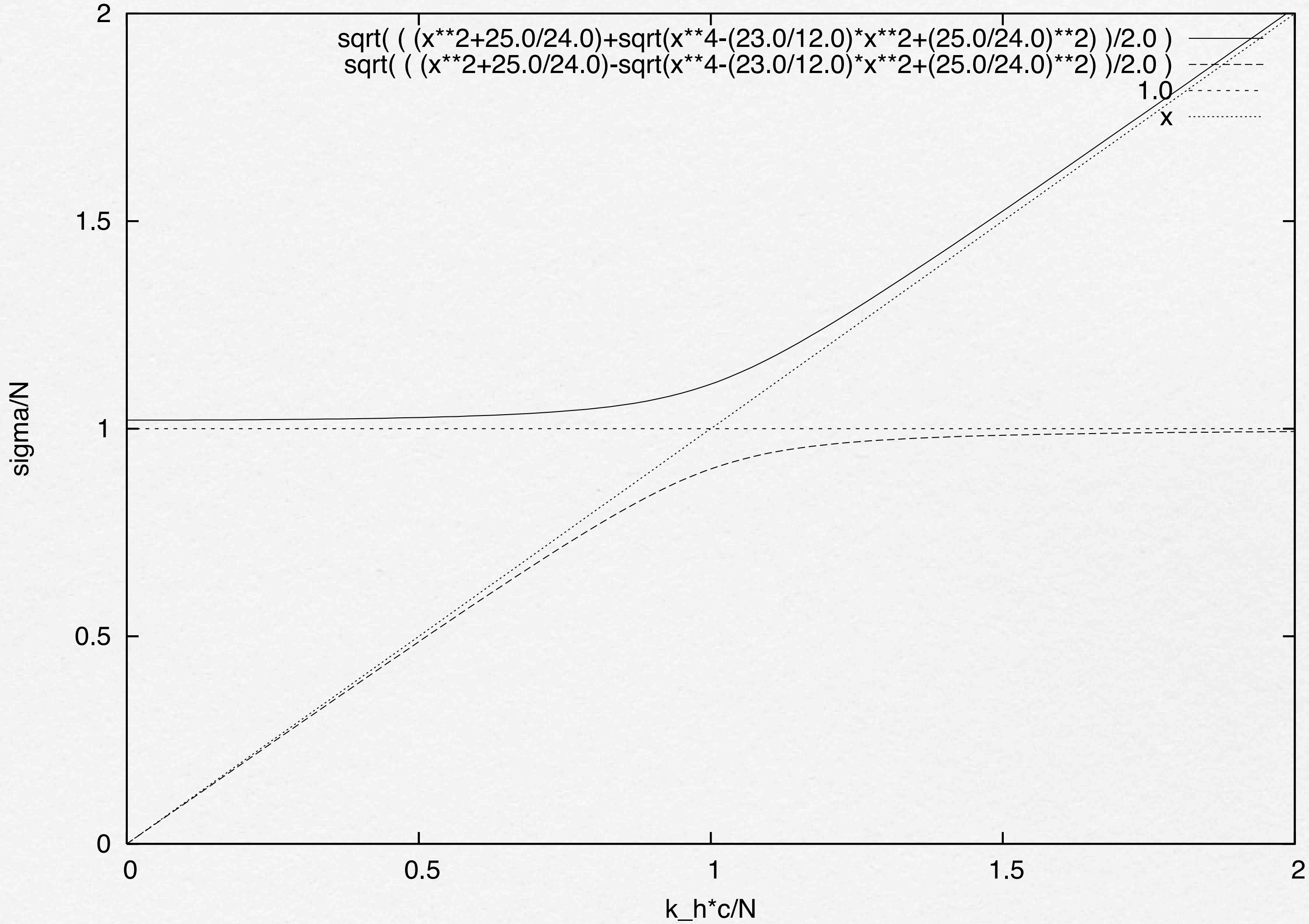

sqrt(((x**2+25.0/24.0)+sqrt(x**4-(23.0/12.0)*x**2+(25.0/24.0)**2))/2.0)
sqrt(((x**2+25.0/24.0)-sqrt(x**4-(23.0/12.0)*x**2+(25.0/24.0)**2))/2.0)
1.0
x
sigma/N
k_h*c/N
0
0.5
1
1.5
2

Two types of modes

- Acoustic waves
- restoring force = gaseous pressure
- high frequency
- stellar envelope

- Gravity waves
- restoring force = buoyancy
- low frequency
- stellar deep core

Observational development

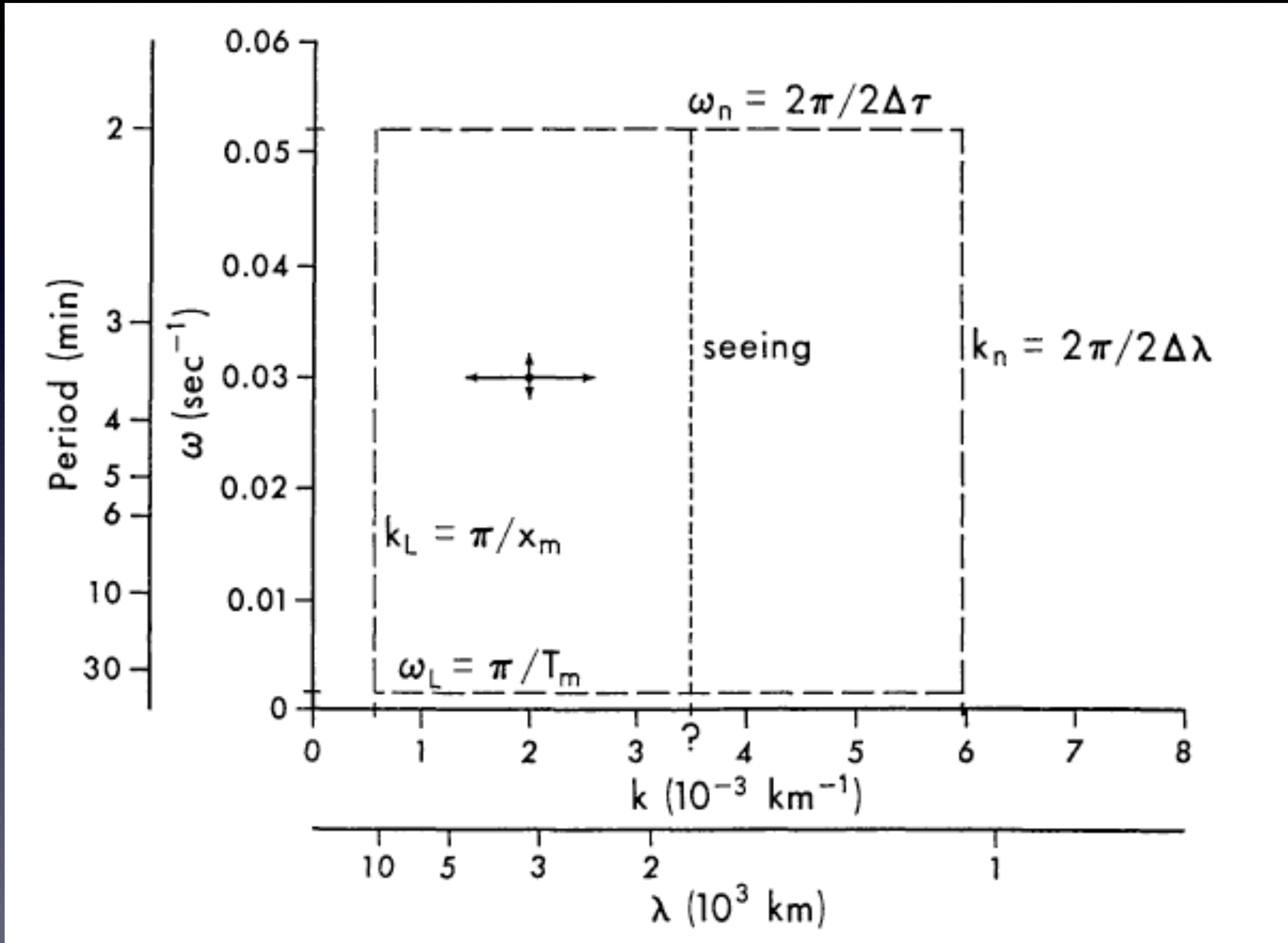

Frazier, E.N. 1968, Zs.f.Astrophysik, 68, 345

Observational development : Fourier analysis

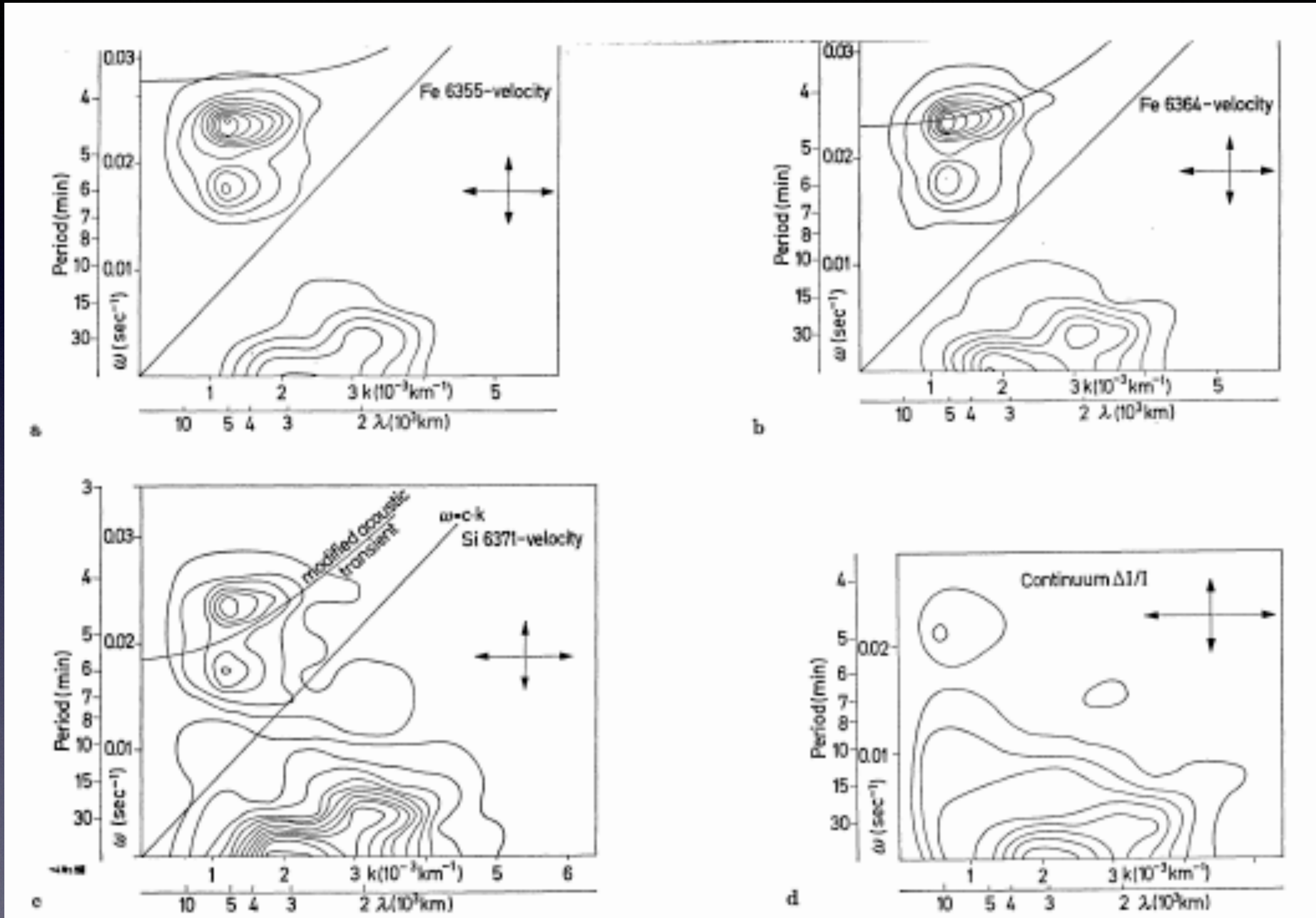

Frazier, E.N. 1968, Zs.f.Astrophysik, 68, 345

Observational development : wider view

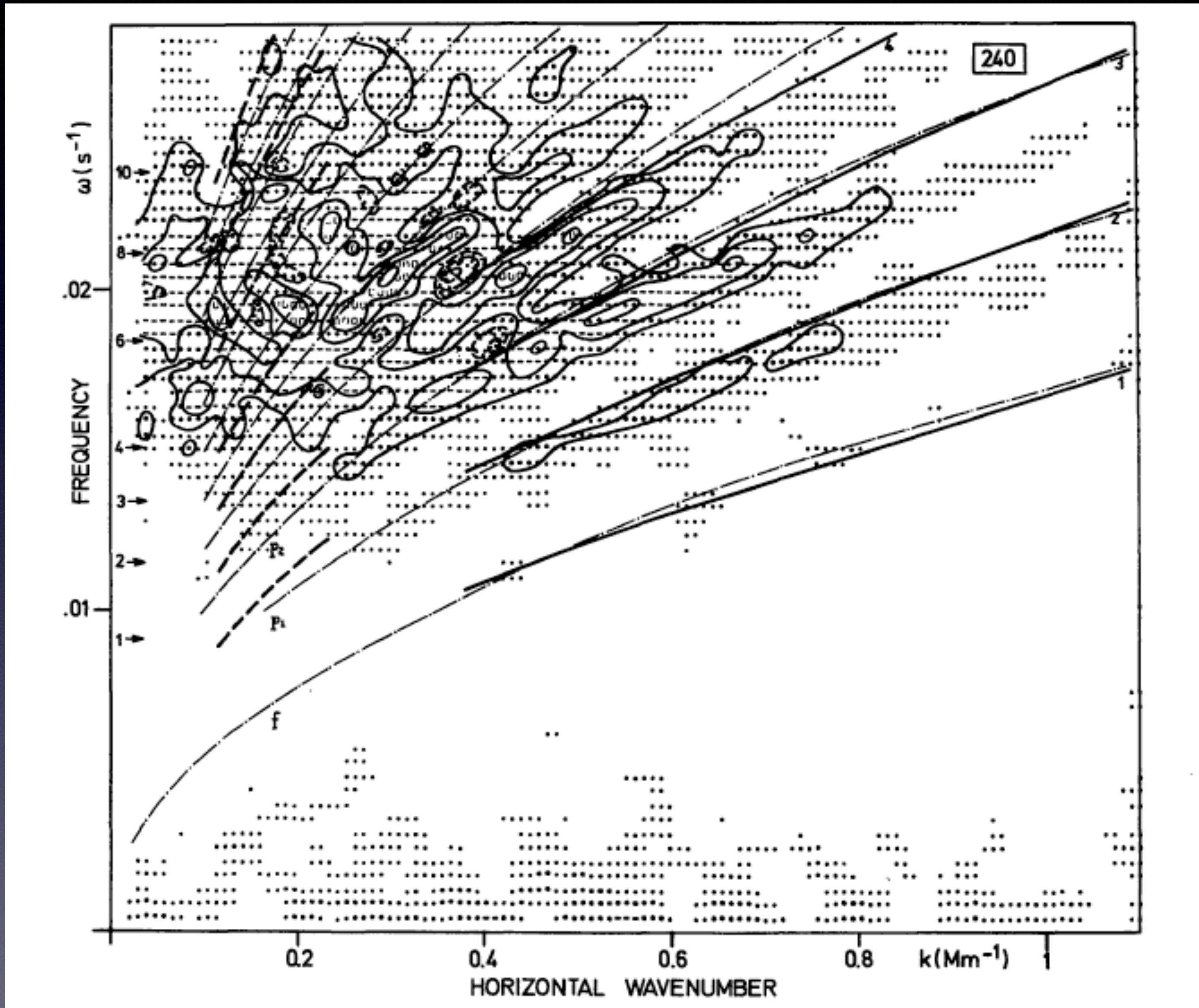

Deubner, F.-L. 1975, A&A, 44, 371.

- Deubner's observation shows a set of ridges, which was in good agreement with the theoretical computation done by Ando & Osaki (1975).
- However, agreement is not perfect. Observed ridges have higher frequencies.
- This means that the sound speed of the real Sun is higher than the model.
- Since T_{eff} is fixed, this means that the temperature gradient is higher in the real Sun.
- This means the convection zone of the real Sun is deeper than expected.

Excitation mechanisms

- Self-excitation
  - Thermal overstability:

    opacity mechanism working in an ionization zone
  - Stochastic excitation due to turbulence:

    waves generated by turbulence resonate in the cavity of a whole star

- Tidally forced oscillation

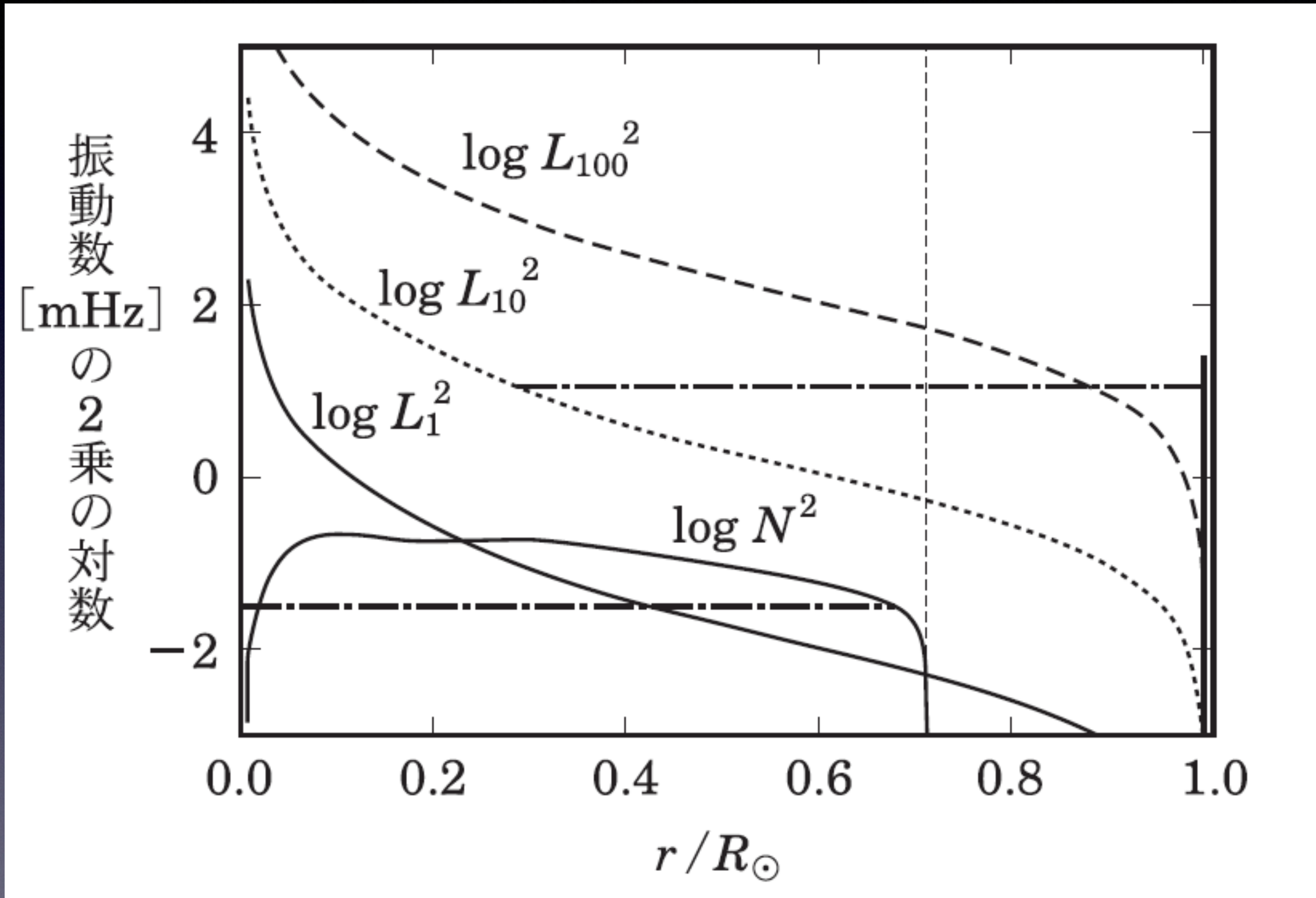

振動数[mHz]の2乗の対数
4
2
0
−2
log L_{100}^2
log L_{10}^2
log L_1^2
log N^2
0.0
0.2
0.4
0.6
0.8
1.0
$r/R_\odot$

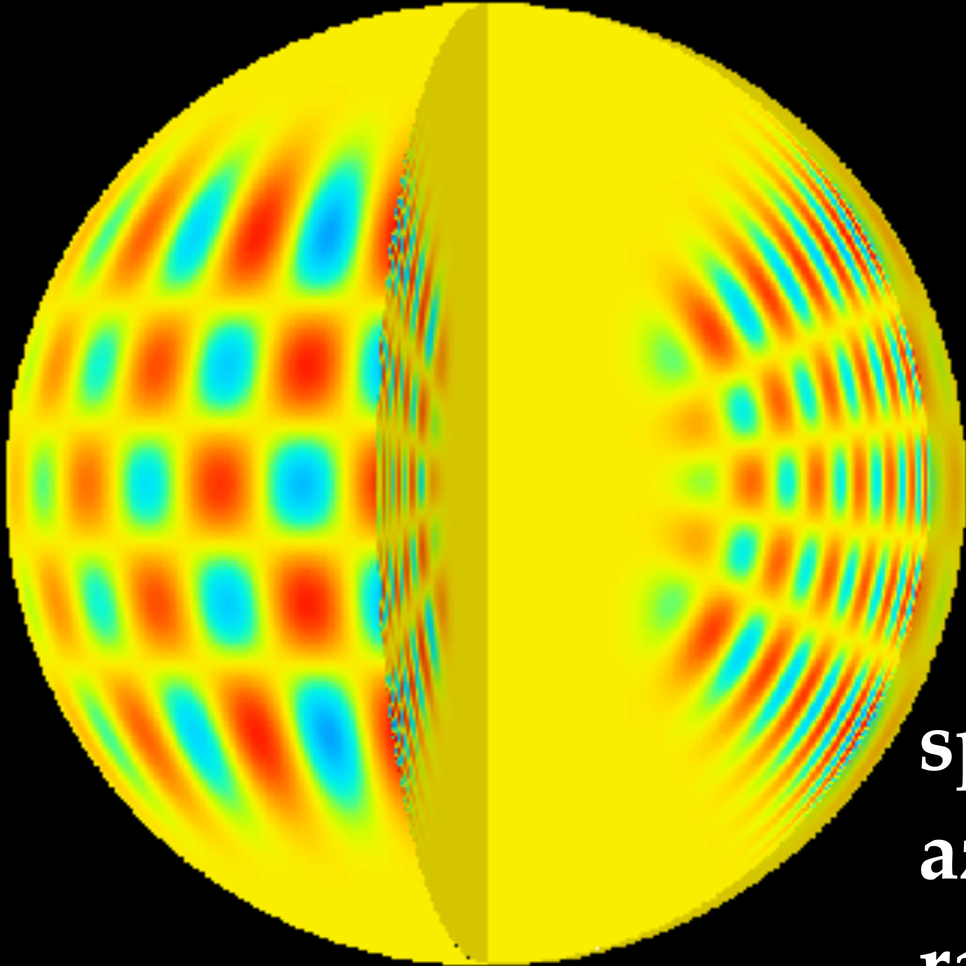

spherical degree
azimuthal order
radial order *n*

Eigenmode: $Y_{lm}(\theta,\phi)\ \exp(i\omega_{lmn}t)$

Observational development : narrow-band filter

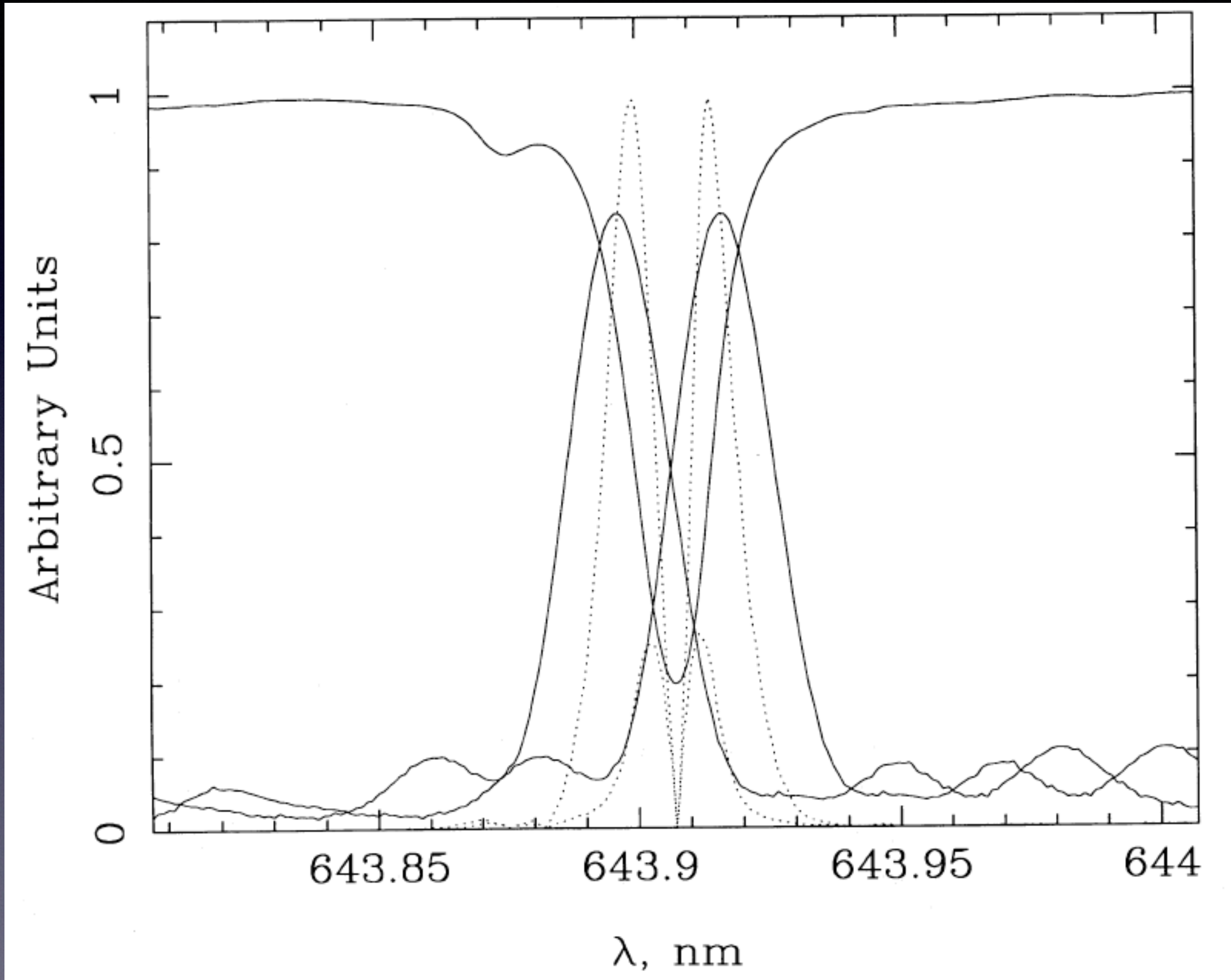

Libbrecht, K.G. 1988, ApJ, 334, 510.

Observational development : 2D disk image

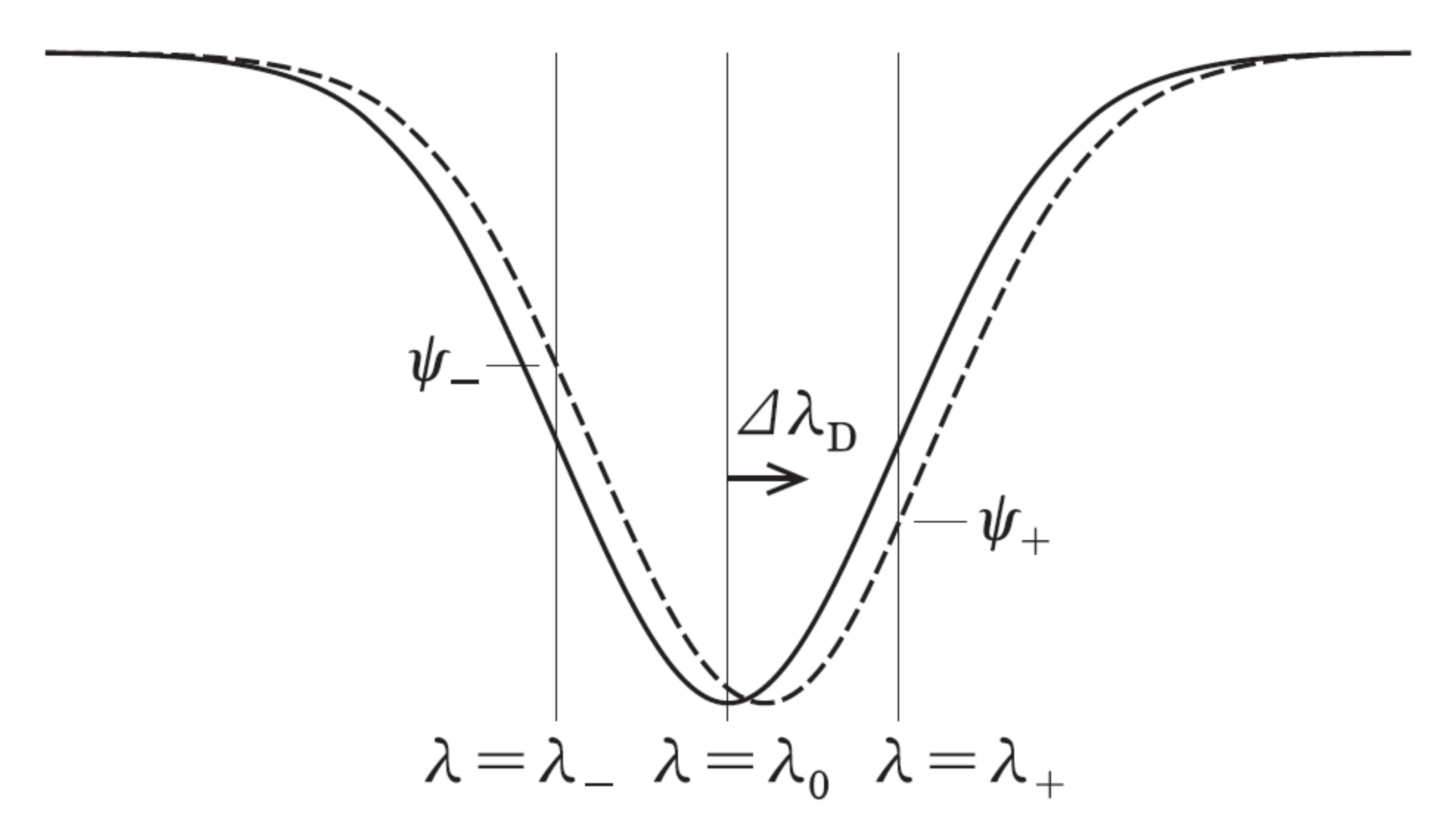

Solar oscillation $= \sum a_{lmn} Y_{lm}(\theta,\phi) \exp(i\omega_{lmn}t)$

spherical harmonic analysi

$\longrightarrow (l, m)$

Fourier transform

$\longrightarrow (a_{lmn} , \omega_{lmn}$

Observational development : high to middle range of *l*

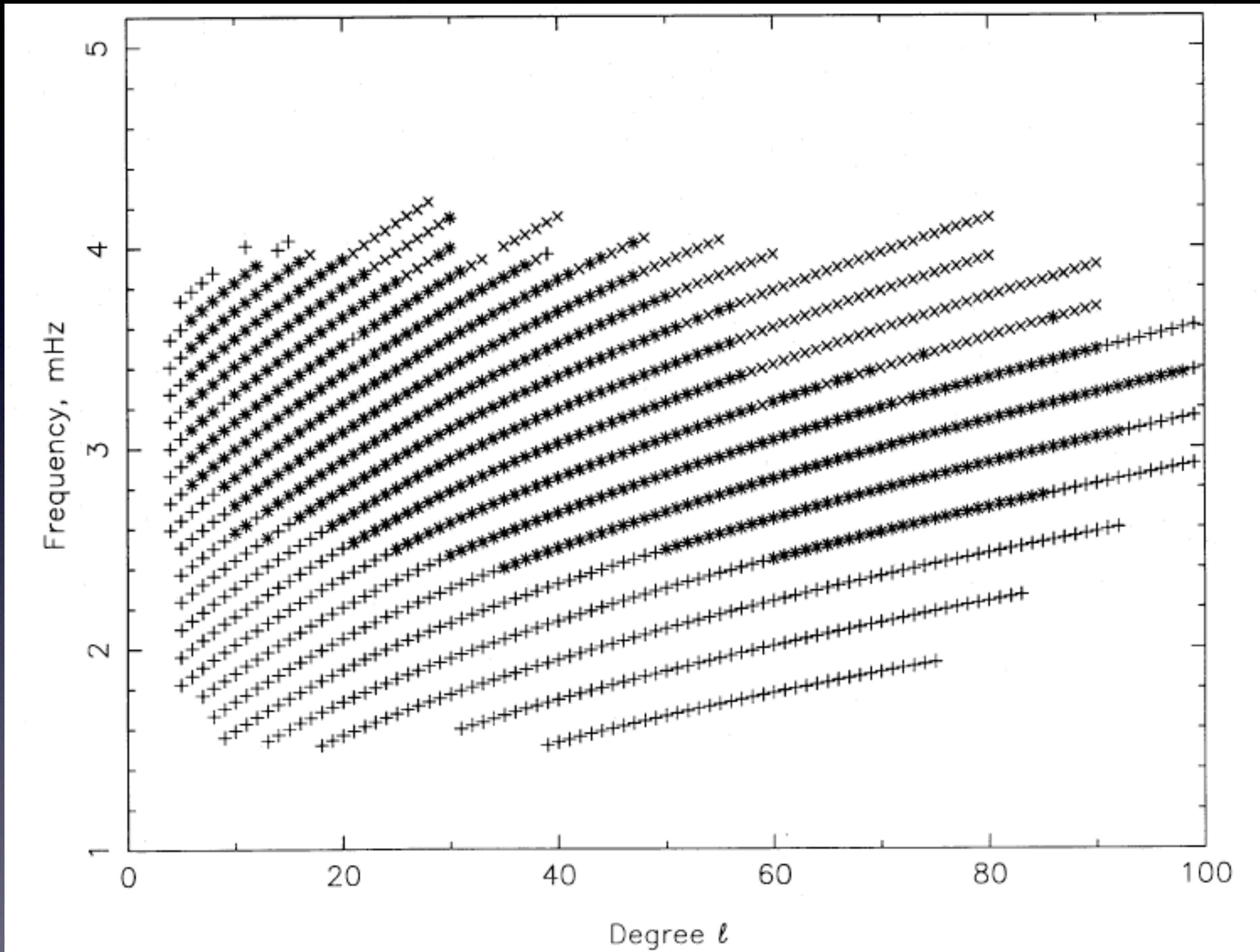

Duvall, T.L., Jr., Harvey, J.W., Libbrecht, K.G., Popp, B.D. & Pomerantz, M.A. 1988, ApJ, 324, 1158.

Total Solar Irradiance

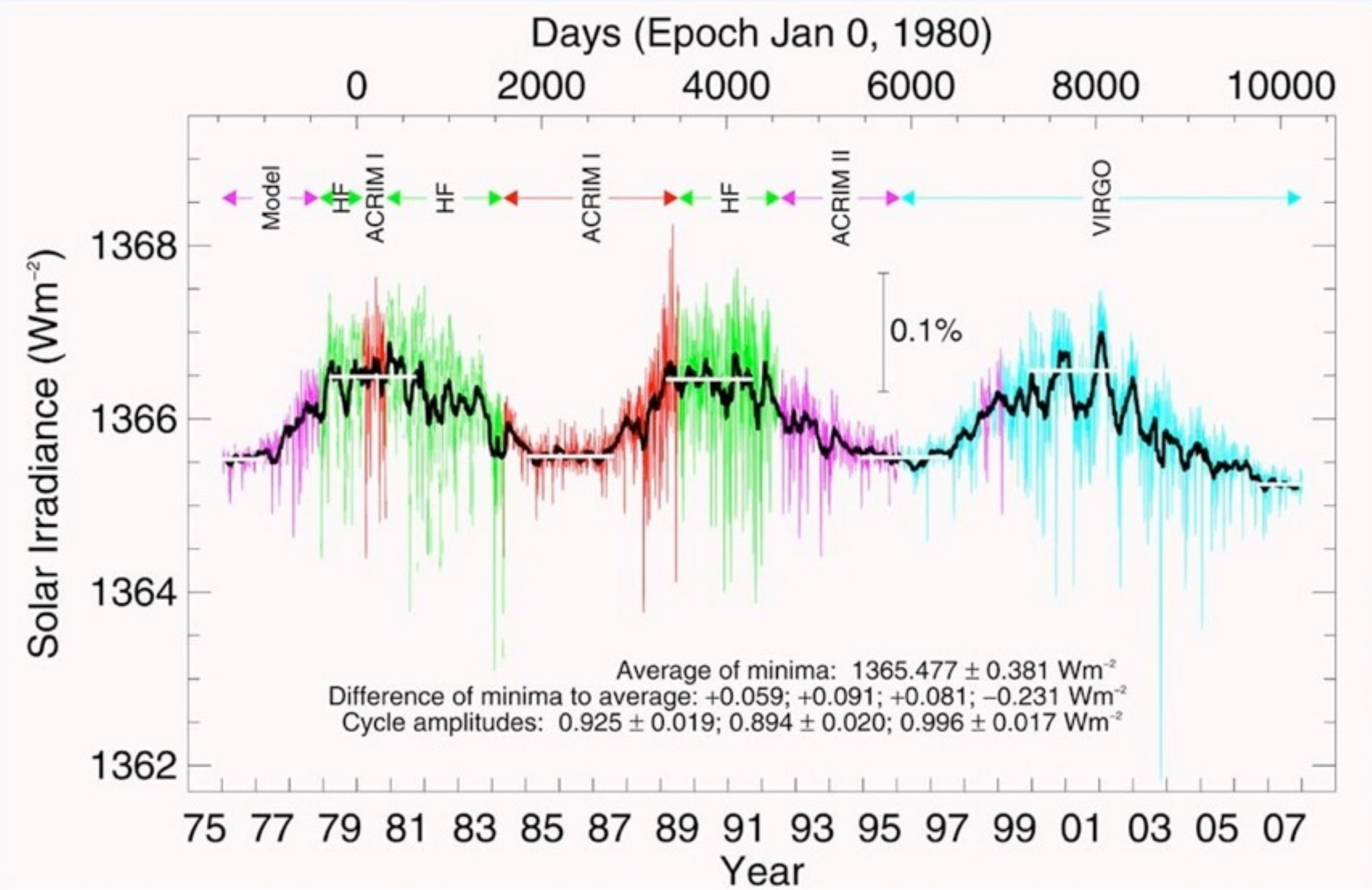

Figure from C. Fröhlich

- TSI is lower this minimum than the previous two
- Unexpected change after a greatly disputed increase in the previous minimum
- Few mechanisms exist for magnetic changes in the basal solar luminosity

Observational development : Brightness variation

clear comb structure = evidence for low degree *l* high order *n* p-modes

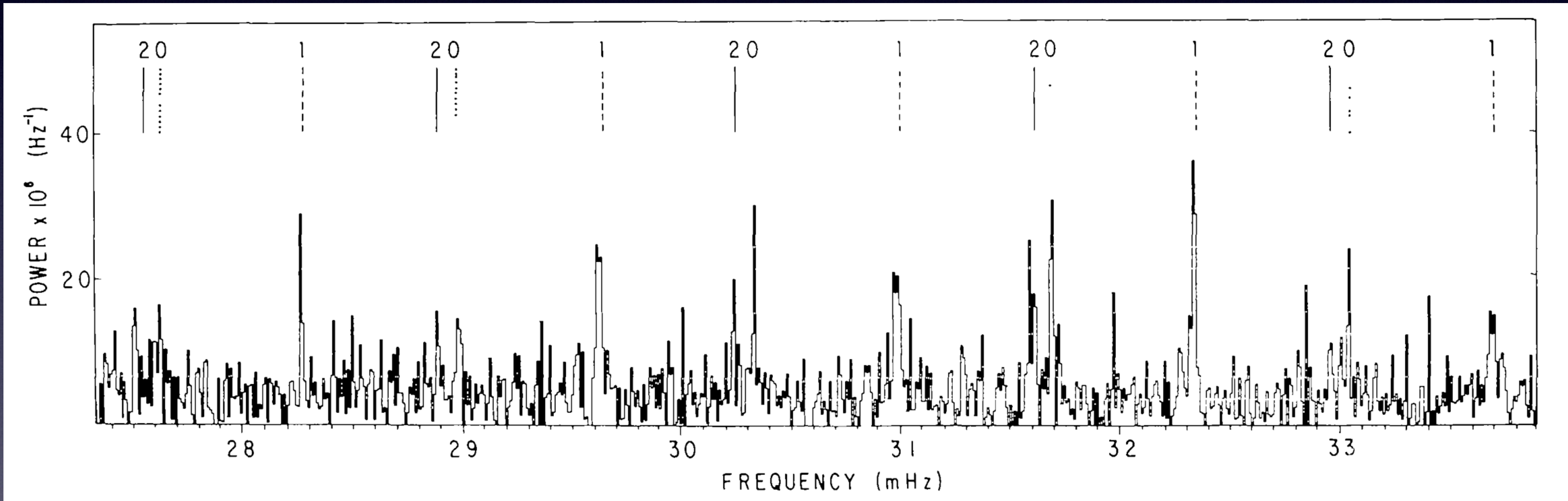

Woodard, M. & Hudson, H. 1983, Solar Phys., 82, 67.

Doppler measurement with integrated light

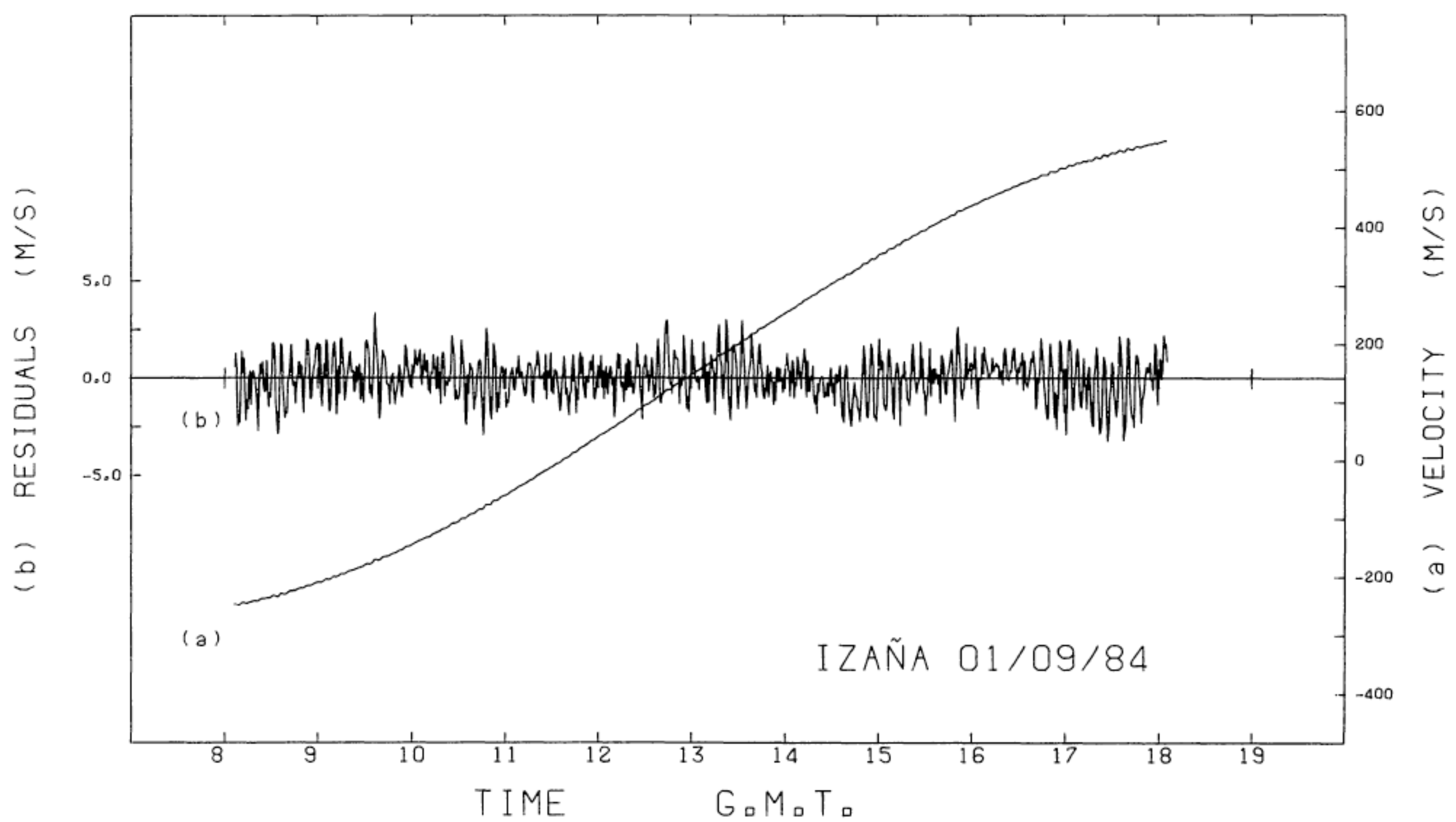

Palle, P.L., Perez, J.C., Regulo, C., Roca Cortes, C., Isaak, G.R., McLeod, C.P. & van der Raay, H.B. 1986, A&A,169, 313.

Doppler measurement with integrated light

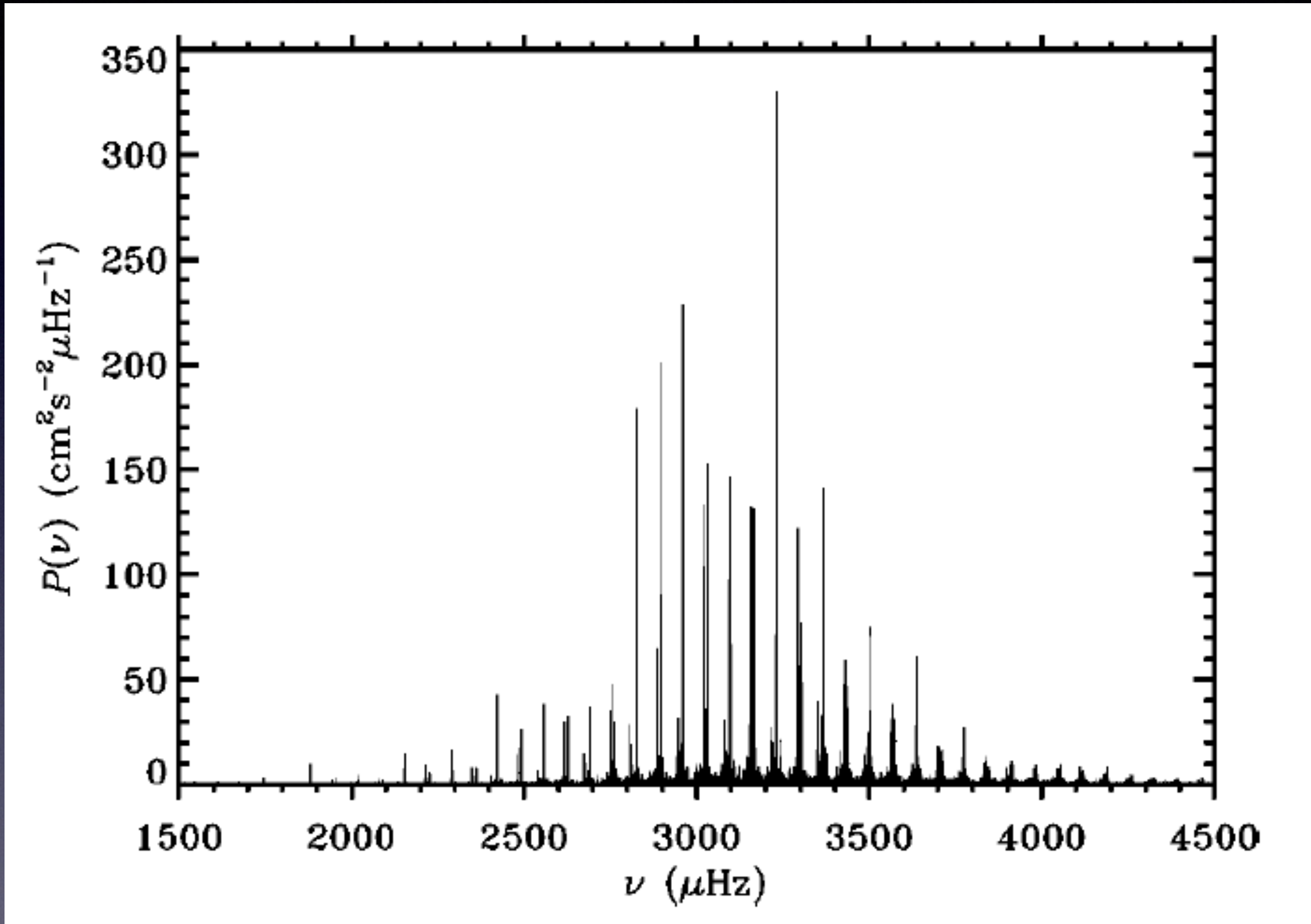

clear comb structure = evidence for low degree *l* high order *n* p-modes

Echelle diagram $\nu_{nl} = \Delta\nu\ (n+l/2+\varepsilon)$

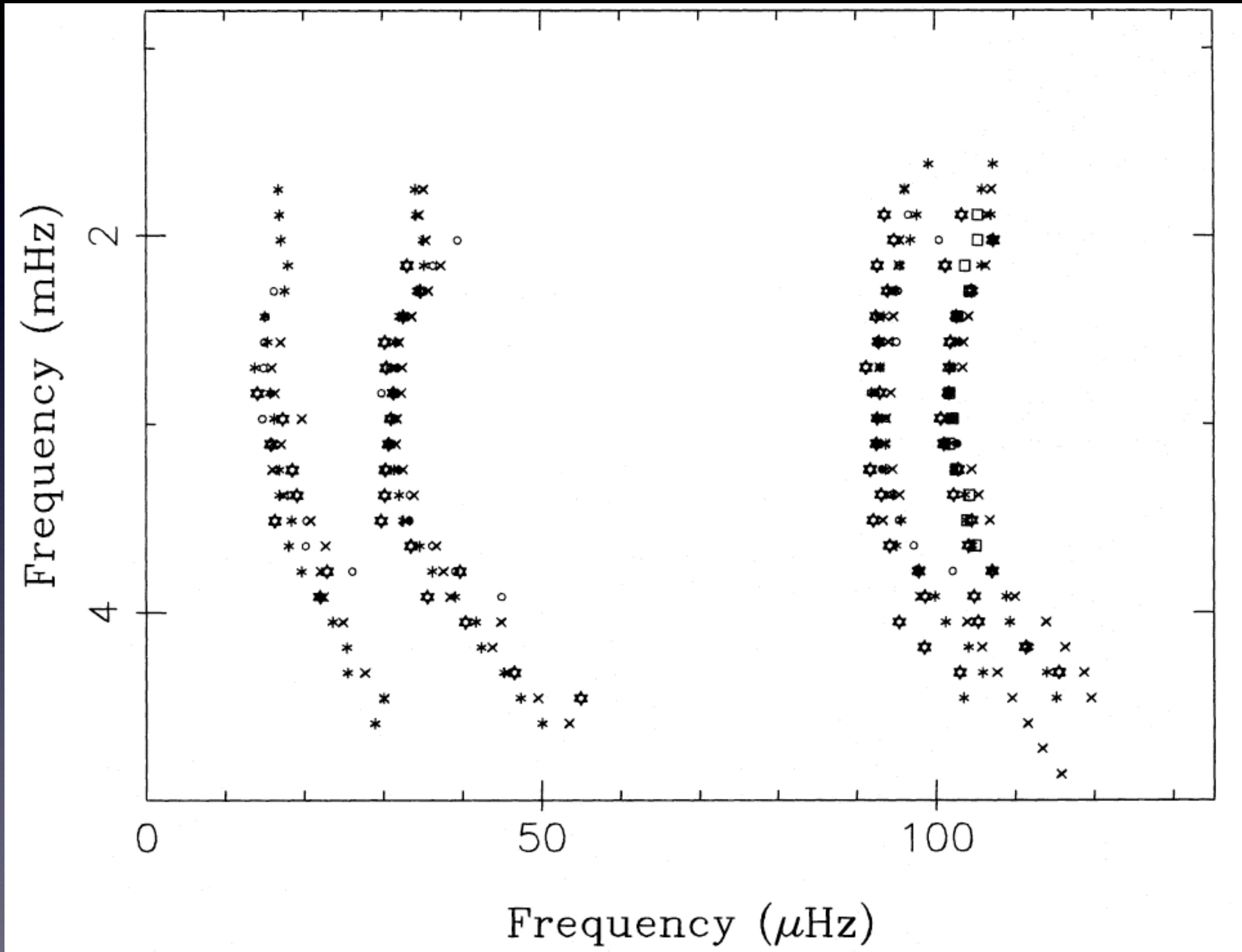

Gelly, B., Fossat, E., Grec, G. & Schmider, X.-F. 1988, A&A, 200, 207.

Echelle diagram $\nu_{nl} = \Delta\nu\,(n + l/2 + \varepsilon)$

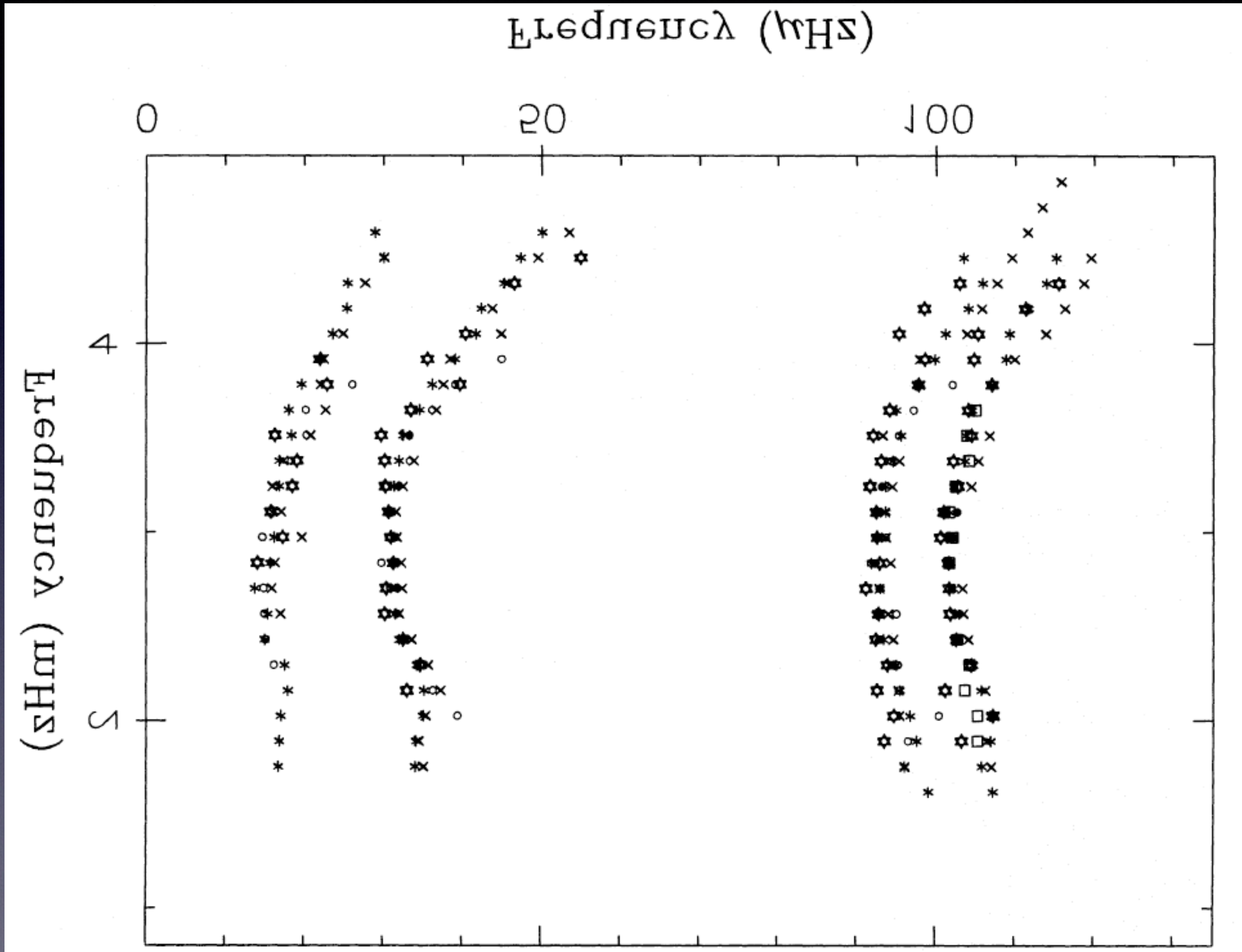

Gelly, B., Fossat, E., Grec, G. & Schmider, X.-F. 1988, A&A, 200, 207.

Observational development : high precision

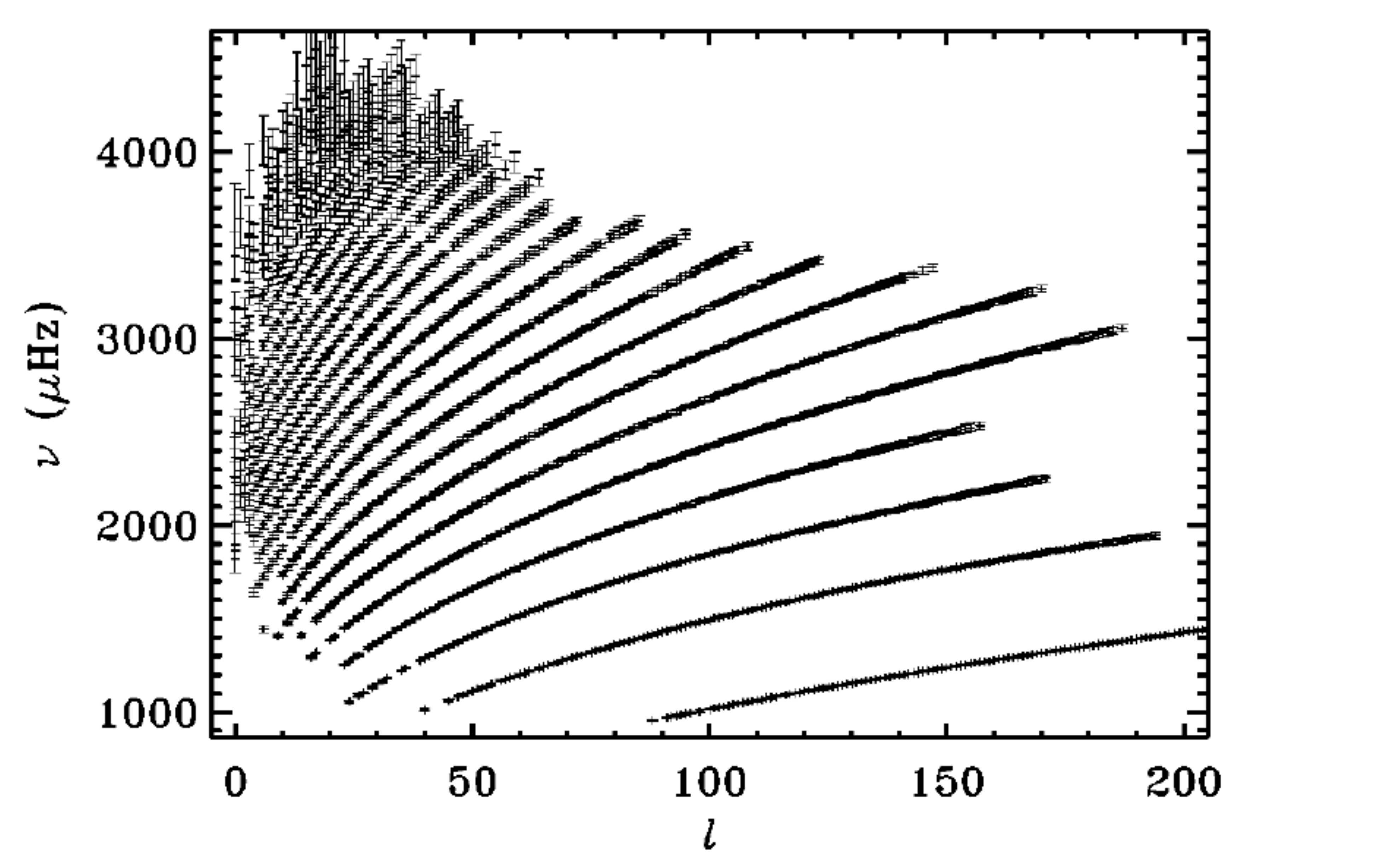

Libbrecht, K.G., Woodard, M.F. & Kaufman, J.M. 1990, ApJS, 74, 1129

Observational development : high precision

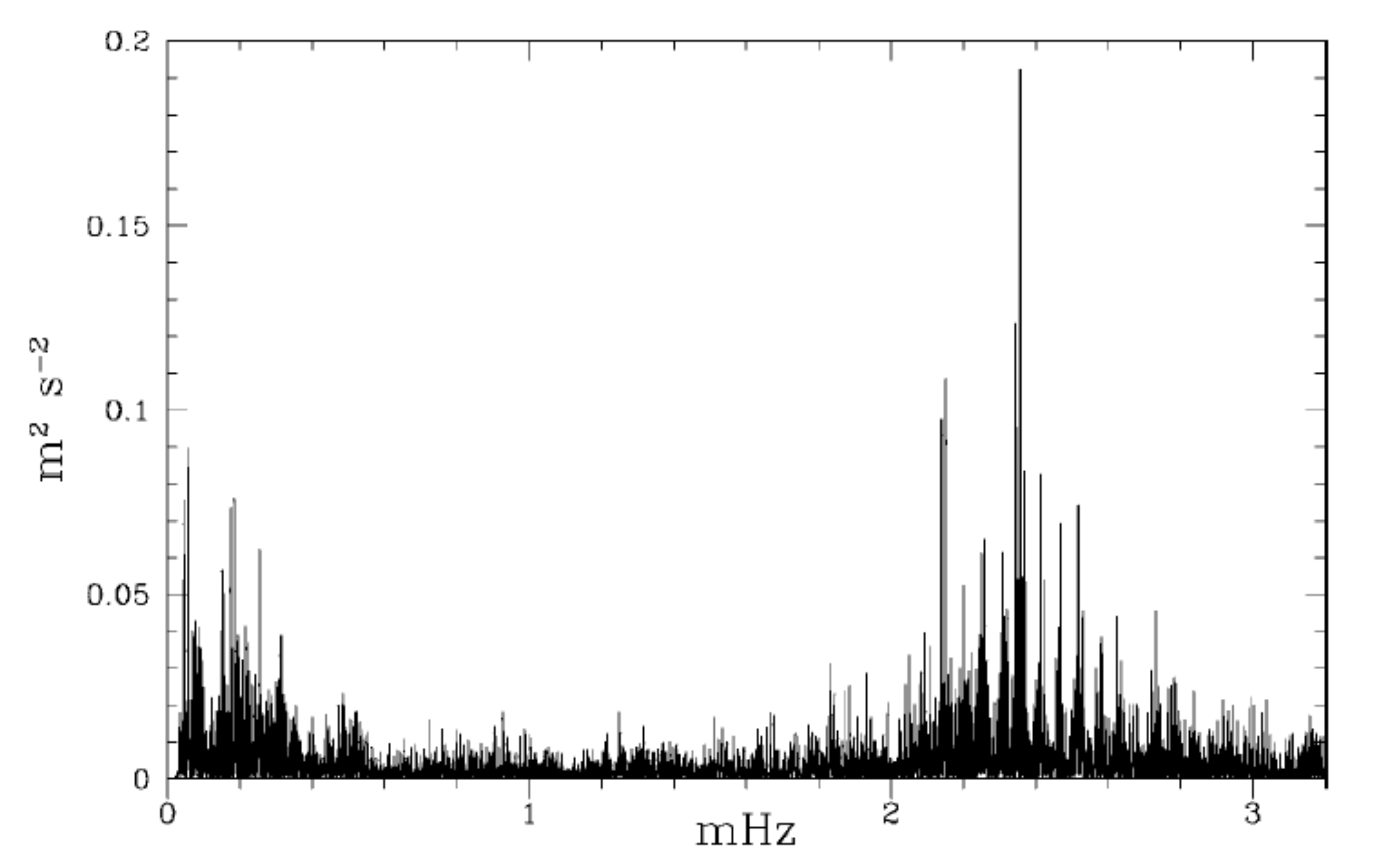

Observational development : ultra-high precision

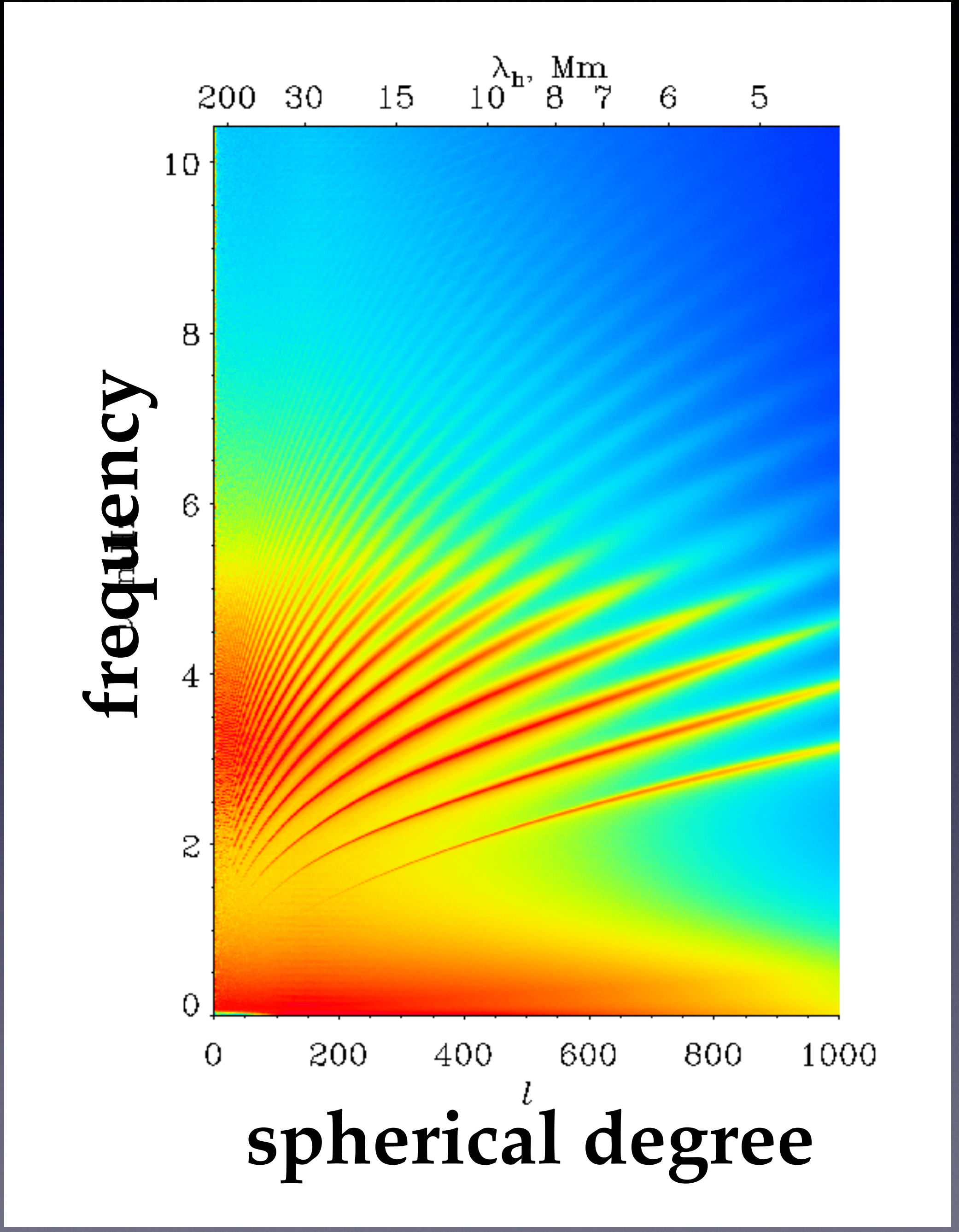

SOHO/MDI

color code: amplitude

In order to global structures, we need to zoom out.

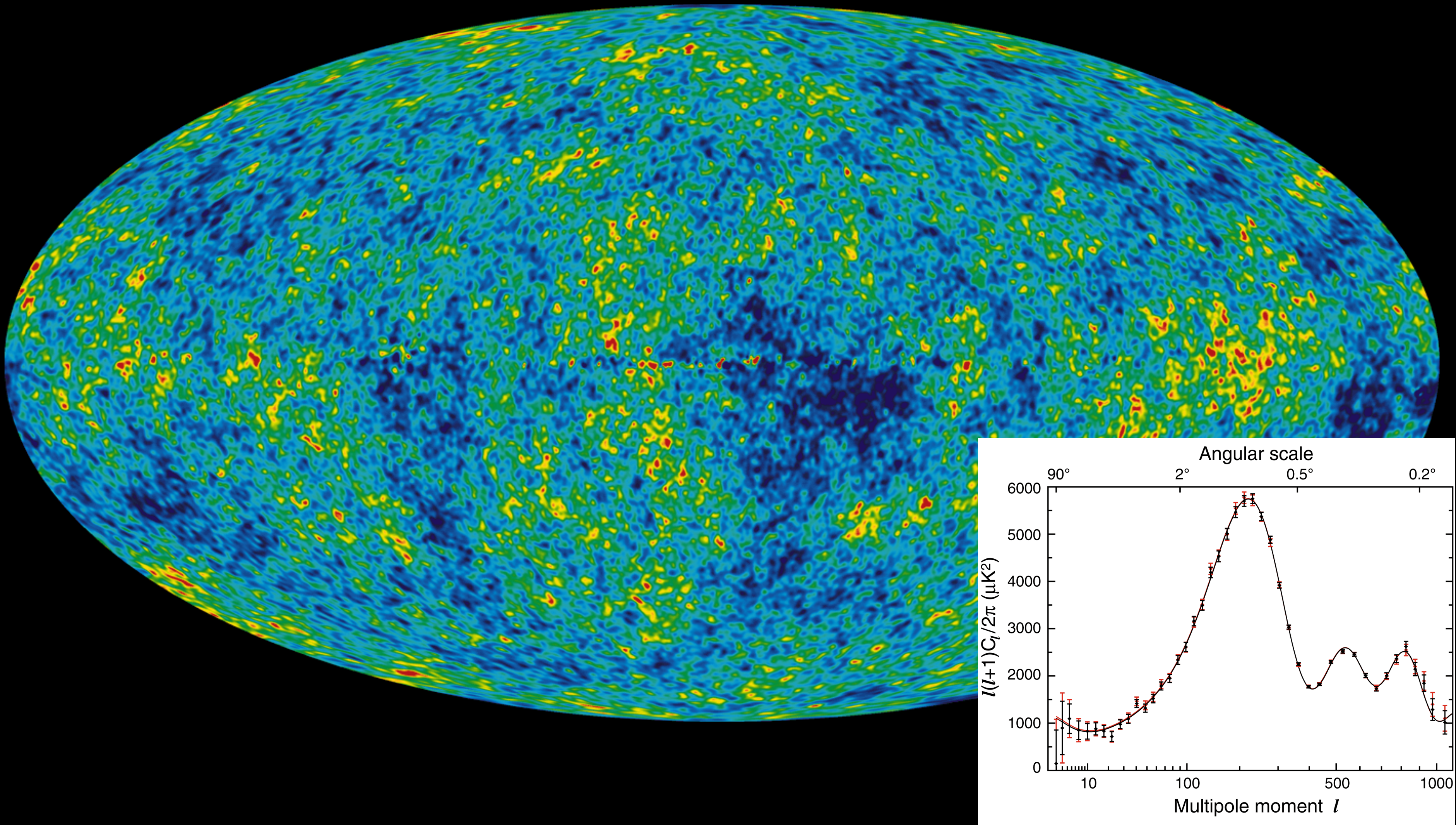

http://lambda.gsfc.nasa.gov/product/map/current/m_images.cfm

Observed oscillation is a superposition of p-modes of the Sun.

Total number of the detected modes is $n x l x m \sim 10 x 10^3 x 10^3$

Quantitatively different from traditional study of pulsating stars

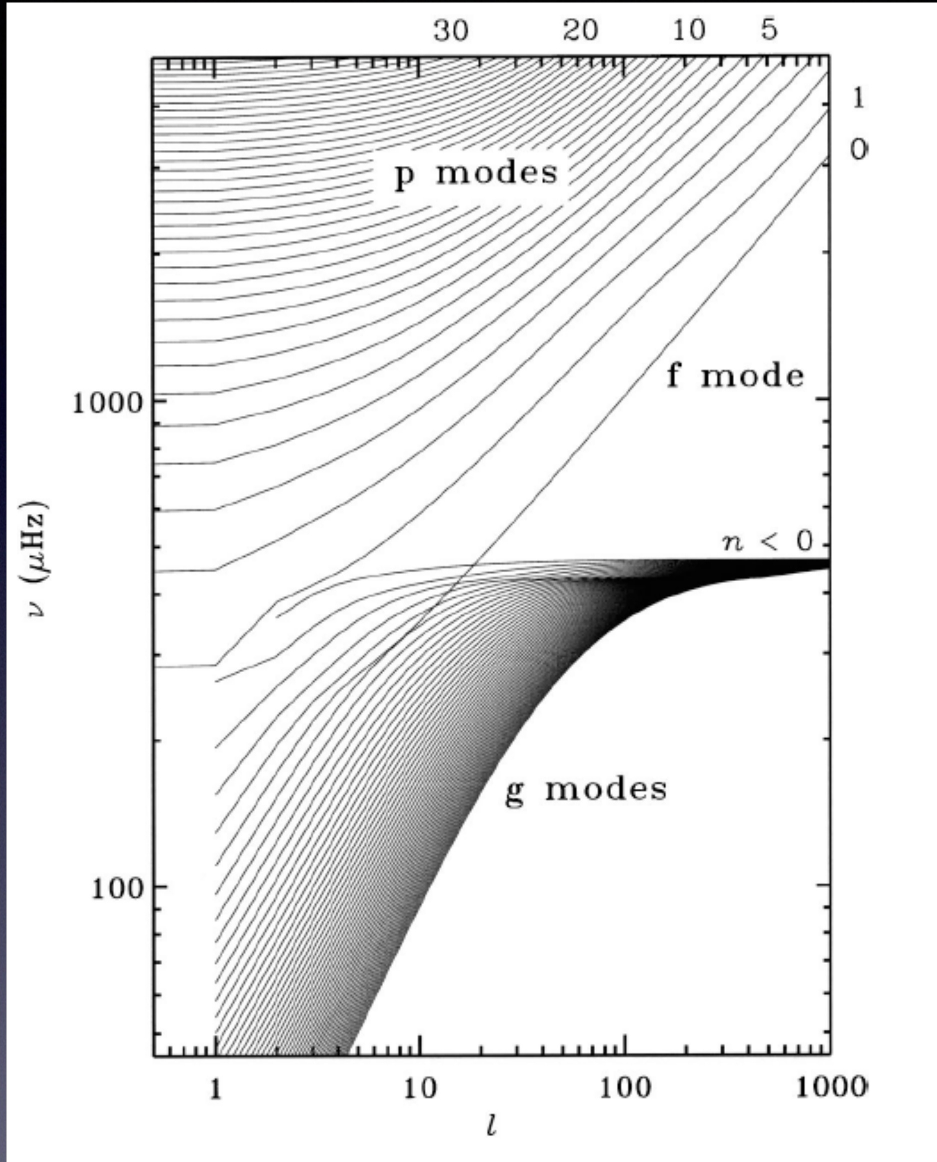

Forward problem approach:

- Make a series of equilibrium models with some parameters.
- Compute eigenvalues of each model.
- Find the best fitting model by comparing the computed eigenvalues and the observed ones.

$$\frac{\partial^2 \xi}{\partial t^2} = -\mathcal{L}(\xi)$$

$$\omega^2 \xi = \mathcal{L}(\xi; c^2, \rho)$$

- No guarantee, or no hope, for uniqueness

Inverse problem approach:

$$\omega^2 \xi = \mathcal{L}(\xi; c^2, \rho)$$

Integral equation for inverse problem:

$$\omega^2 = \int \xi^* \cdot \mathcal{L}(\xi)\, dm / \int |\xi|^2\, dm$$

$$\delta\omega^2 = \int \xi^* \cdot \left[\left(\frac{\partial \mathcal{L}}{\partial c^2}\right) \delta c^2 + \left(\frac{\partial \mathcal{L}}{\partial \rho}\right) \delta \rho \right] dm$$

- **Assume a good model and compute its eigenvalues**
- **Take differences from the observed frequencies as the LHS**
- **Solve the above equations as algebraic equations**

Sound speed profile inside the Sun

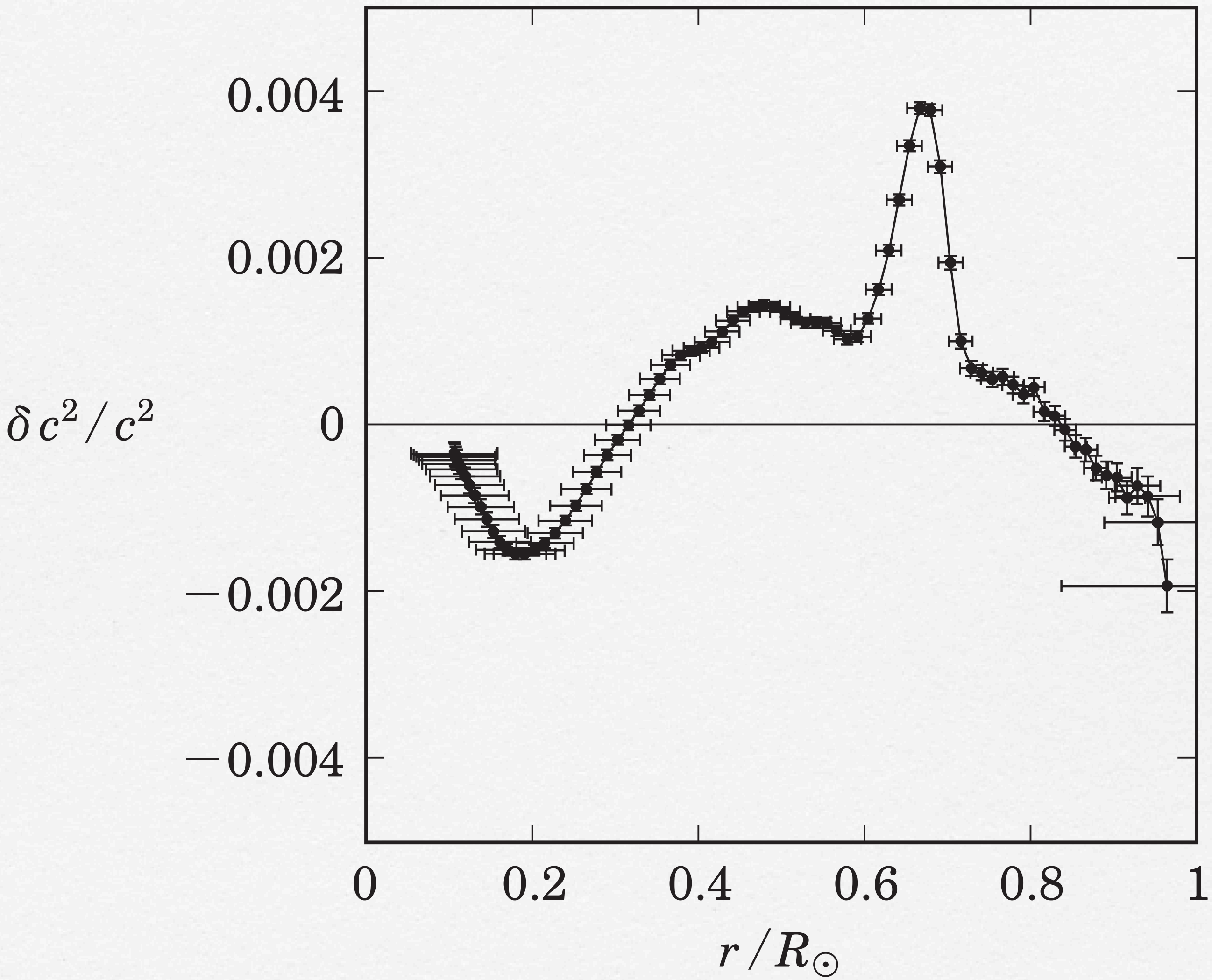

The differences are tiny, but meaningful!

Internal Rotation of the Sun

- Driving force of Magnetic Dynamos
- Driving force of Solar Activities
- Influence on Solar Structure & Evolution

Influence of rotation

$$\frac{\partial v}{\partial t} + (v \cdot \nabla)v + 2\Omega_0 \times v + \Omega_0 \times \Omega_0 \times r = -\nabla\Phi - \frac{1}{\rho}\nabla p$$

Linearized equation of motion:

$$\frac{\partial v'}{\partial t} + (v_0 \cdot \nabla)v' + (v' \cdot \nabla)v_0 + 2\Omega_0 \times v' = -\nabla\Phi' + \frac{\rho'}{\rho^2}\nabla p_0 - \frac{1}{\rho_0}\nabla p'$$

Coriolis force

Hence, the linearized equation of motion:

$$\mathcal{L}(\xi) - \omega^2 \xi + \omega \mathcal{M}(\xi) = 0$$

where

$$\mathcal{M}(\xi) := 2i[\Omega_0 \times \xi + (v_0 \cdot \nabla)\xi]$$

$$\mathcal{L}(\xi) - \omega^2\xi + \omega\mathcal{M}(\xi) = 0$$

Treat the influence of *M* as perturbations;

$$\rho = \rho^{(0)} + \rho^{(1)} + \cdots,$$

$$\xi = \xi^{(0)} + \xi^{(1)} + \cdots,$$

$$\omega = \omega^{(0)} + \omega^{(1)} + ...$$

$$\mathcal{L}^{(0)}\left(\xi^{(0)}\right) - \omega^{(0)2}\xi^{(0)} = 0$$

$$\mathcal{L}^{(0)}\left(\xi^{(1)}\right) + \mathcal{L}^{(1)}\left(\xi^{(0)}\right) - \omega^{(0)2}\xi^{(1)} - 2\omega^{(0)}\omega^{(1)}\xi^{(0)} + \omega^{(0)}\mathcal{M}^{(0)}\left(\xi^{(0)}\right) = 0$$

In the case of slow rotation (Coriols force dominant):

$$\boldsymbol{v}_0 = \boldsymbol{\Omega} \times \boldsymbol{r} = (0, 0, r\Omega \sin\theta)$$

$$\boldsymbol{\Omega} = [\Omega(r,\theta)\cos\theta, -\Omega(r,\theta)\sin\theta, 0]$$

Note that

$$\frac{\partial \boldsymbol{e}_r}{\partial \phi} = \boldsymbol{e}_\phi \sin\theta,$$

$$\frac{\partial \boldsymbol{e}_\theta}{\partial \phi} = \boldsymbol{e}_\phi \cos\theta,$$

$$\frac{\partial \boldsymbol{e}_\phi}{\partial \phi} = -\boldsymbol{e}_r \sin\theta - \boldsymbol{e}_\theta \cos\theta,$$

Then

$$\begin{aligned}
\frac{1}{2}\boldsymbol{\xi}^*_{m''} \cdot \mathcal{M}^{(0)}(\boldsymbol{\xi}_m) \quad = \quad & -m\Omega\boldsymbol{\xi}^*_{m''} \cdot \boldsymbol{\xi}_m - i(\Omega + \Omega_0)\xi^*_{m'',r}\xi_{m,\phi} \sin\theta \\
& -i(\Omega + \Omega_0)\xi^*_{m'',\theta}\xi_{m,\phi} \cos\theta \\
& +i(\Omega + \Omega_0)\xi^*_{m'',\phi}(\xi_{m,r} \sin\theta + \xi_{m,\theta} \cos\theta).
\end{aligned}$$

$$\boldsymbol{\xi}^{(0)} = \sum_{m=-l}^{l} \alpha_m \boldsymbol{\xi}_{nlm}$$

$$\boldsymbol{\xi}^{(1)} = \sum_{m'} {\sum_{n'l'}}' \beta_{n'l'm'} \boldsymbol{\xi}_{n'l'm'} + \sum_{l'm'} \gamma_{l'm'}(r) \boldsymbol{\eta}_{l'm'}$$

$$\boldsymbol{\eta}_{l'm'} \equiv \frac{1}{[l'(l'+1)]^{1/2}} \left(0, \frac{1}{\sin\theta}\frac{\partial}{\partial\phi}, -\frac{\partial}{\partial\theta}\right) \mathrm{Y}_{l'}^{m'}(\theta,\phi)$$

Secular equation (Coriolis force dominant) :

$$\boxed{\sum_{m=-l}^{l} \left(\mathcal{M}_{m''m} - \omega^{(1)}\delta_{m''m}\right)\alpha_m = 0}$$

where $$\mathcal{M}_{m''m} \equiv \frac{1}{2I_{nl}} \int_0^M \boldsymbol{\xi}^*_{nlm''} \cdot \mathcal{M}^{(0)}(\boldsymbol{\xi}_{nlm}) dM_r,$$

$$I_{nl} \equiv \int_0^M |\boldsymbol{\xi}_{nlm}|^2 dM_r$$

$$
\begin{aligned}
\frac{1}{2}\int_0^M \boldsymbol{\xi}^*_{nlm''}\cdot\mathcal{M}^{(0)}(\boldsymbol{\xi}_{nlm})dM_r \quad = \quad & \delta_{m''m} m \times \left\{ \Omega_0 \int_0^R \rho(r) r^2 \left(2\xi_r\xi_h + \xi_h^2\right) dr \right.\\
& + \frac{2l+1}{2}\frac{(l-|m|)!}{(l+|m|)!}\int_{\theta=0}^{\pi}\int_{r=0}^{R}\rho(r)r^2\Omega(r,\theta)\\
& \times \left[\left(-\xi_r^2 + 2\xi_r\xi_h\right)(P_l^m)^2\right.\\
& \left.\left. + \xi_h^2\left[2P_l^m\frac{dP_l^m}{d\theta}\frac{\cos\theta}{\sin\theta} - \left(\frac{dP_l^m}{d\theta}\right)^2 - \frac{m^2}{\sin^2\theta}(P_l^m)^2\right]\right]\right.\\
& \left. dr\sin\theta d\theta \right\}
\end{aligned}
$$

$$
\int_0^M |\boldsymbol{\xi}^{(0)}|^2 dM_r = \int_0^R \rho(r) r^2 \left[\xi_r^2 + l(l+1)\xi_h^2\right] dr
$$

Hence

$$
\boxed{\mathcal{M}_{m''m} = \omega^{(1)\mathrm{rot}}\delta_{m''m}}
$$

$$
\boldsymbol{\omega_m}^{\mathbf{(1)rot}} = m \times \left\{ \Omega_0 \int_0^R \rho(r) r^2 \left(2\xi_r \xi_h + \xi_h^2\right) dr \right.
$$

$$
+ \frac{2l+1}{2} \frac{(l-|m|)!}{(l+|m|)!} \int_{r=0}^{R} \rho(r) r^2 \left[\int_{\theta=0}^{\pi} \left(P_l^m\right)^2 \left\{ \Omega(r,\theta) \sin\theta \right. \right.
$$

$$
\left. \left. \left. \times \left(2\xi_r\xi_h - \xi_r^2 + \xi_h^2[1 - l(l+1)]\right) - \left(\frac{3}{2} \frac{\partial \Omega}{\partial \theta} \cos\theta + \frac{1}{2} \frac{\partial^2 \Omega}{\partial \theta^2} \sin\theta \right) \xi_h^2 \right\} d\theta \right] dr \right\}
$$

$$
\times \left[\int_0^R \rho(r) r^2 \left[\xi_r^2 + l(l+1)\xi_h^2\right] dr \right]^{-1}
$$

In the case of rigid rotation:

$$
\boldsymbol{\omega_m^{(1)\mathrm{rot}}}\Big|_{\textbf{inertial frame}} = -\boldsymbol{m(1 - C_{nl})\Omega}
$$

$$
C_{nl} = \frac{\int_0^R \rho r^2 \left[2\xi_r \xi_h + \xi_h^2\right] dr}{\int_0^R \rho r^2 \left[\xi_r^2 + l(l+1)\xi_h^2\right] dr}
$$

Running summary

- The $(2l+1)$-fold frequency degeneracy is resolved by rotation.
- In a case of uniform slow rotation, the perturbation in frequency due to the Coriolis force is proportional to the rotational angular velocity and to the azimuthal order m.
- In the case of $\Omega=\Omega(r)$, the perturbation in frequency is again linearly proportional to m.

Solar surface latitudinal differential rotation.

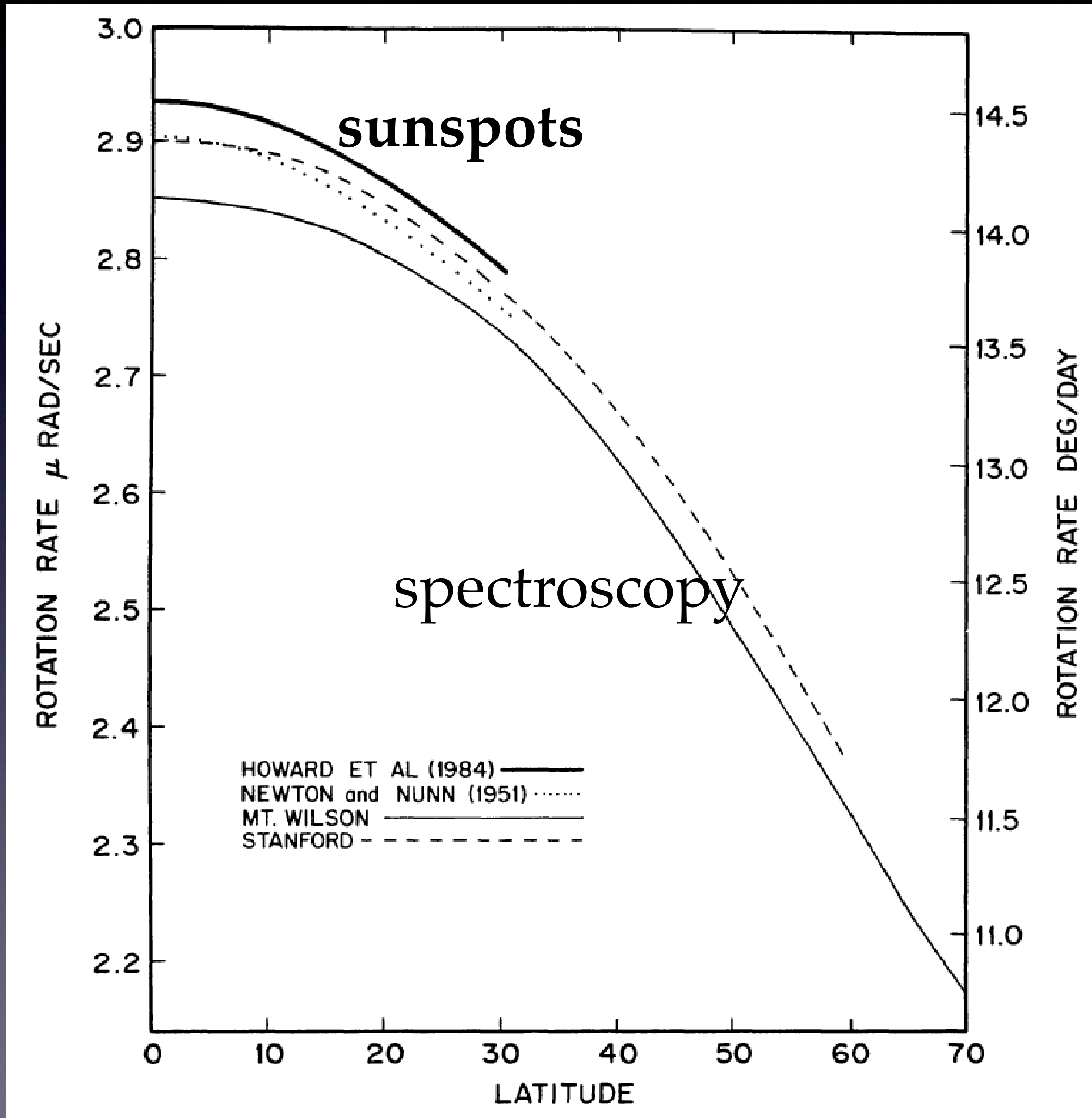

Degeneracy lifts -> m-splitting

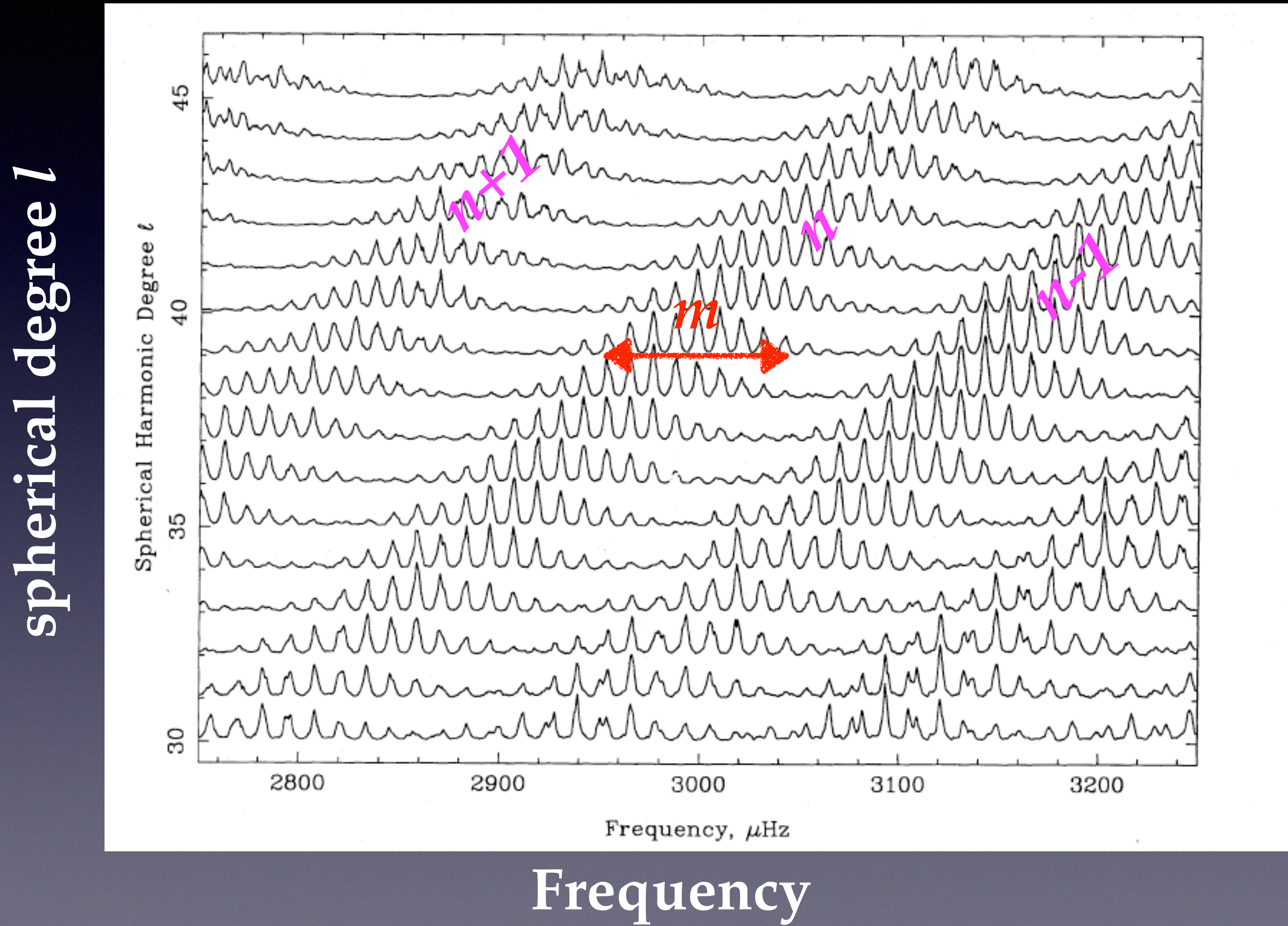

Observational development : ultra-high precision

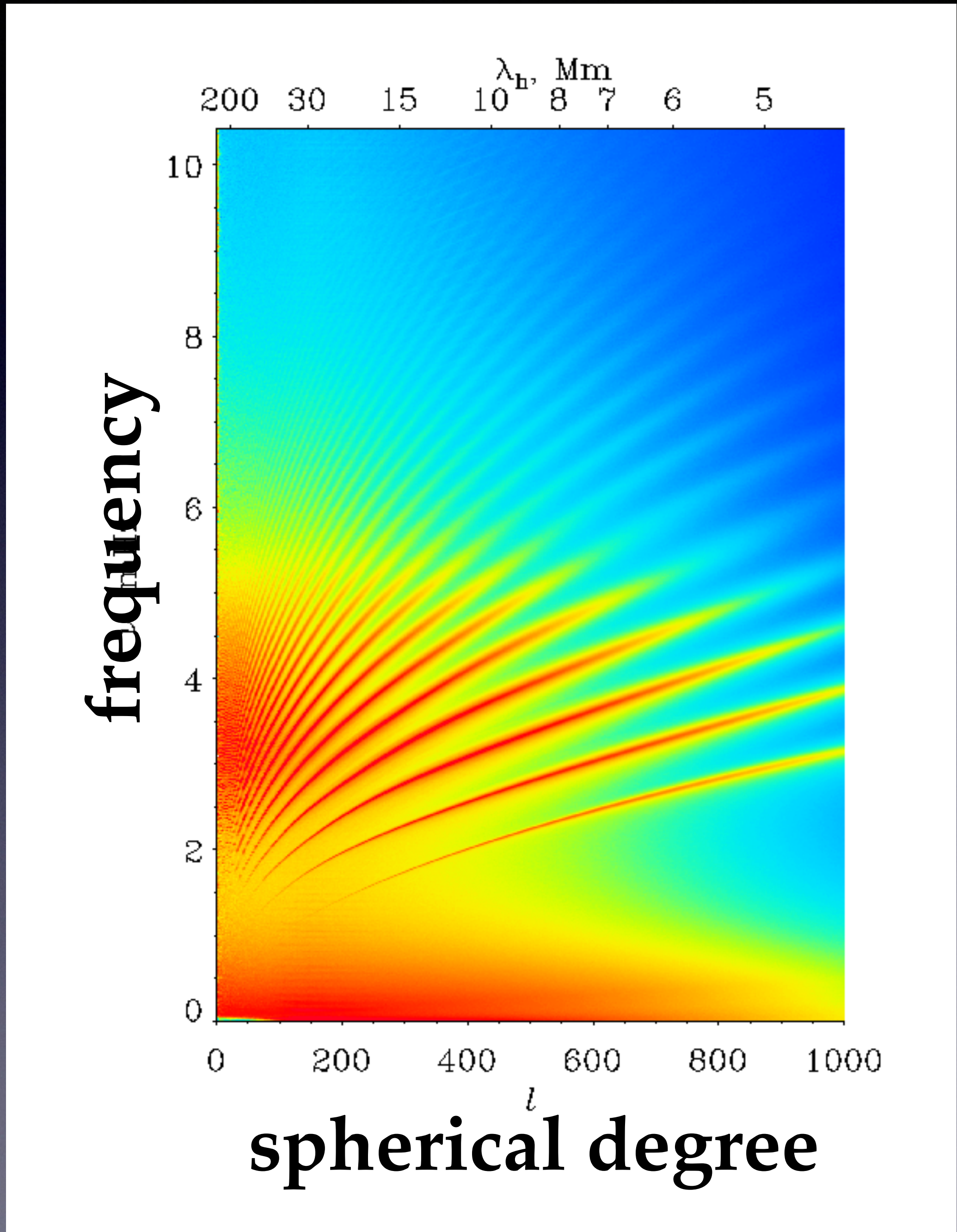

SOHO/MDI

color code: amplitude

Frequency

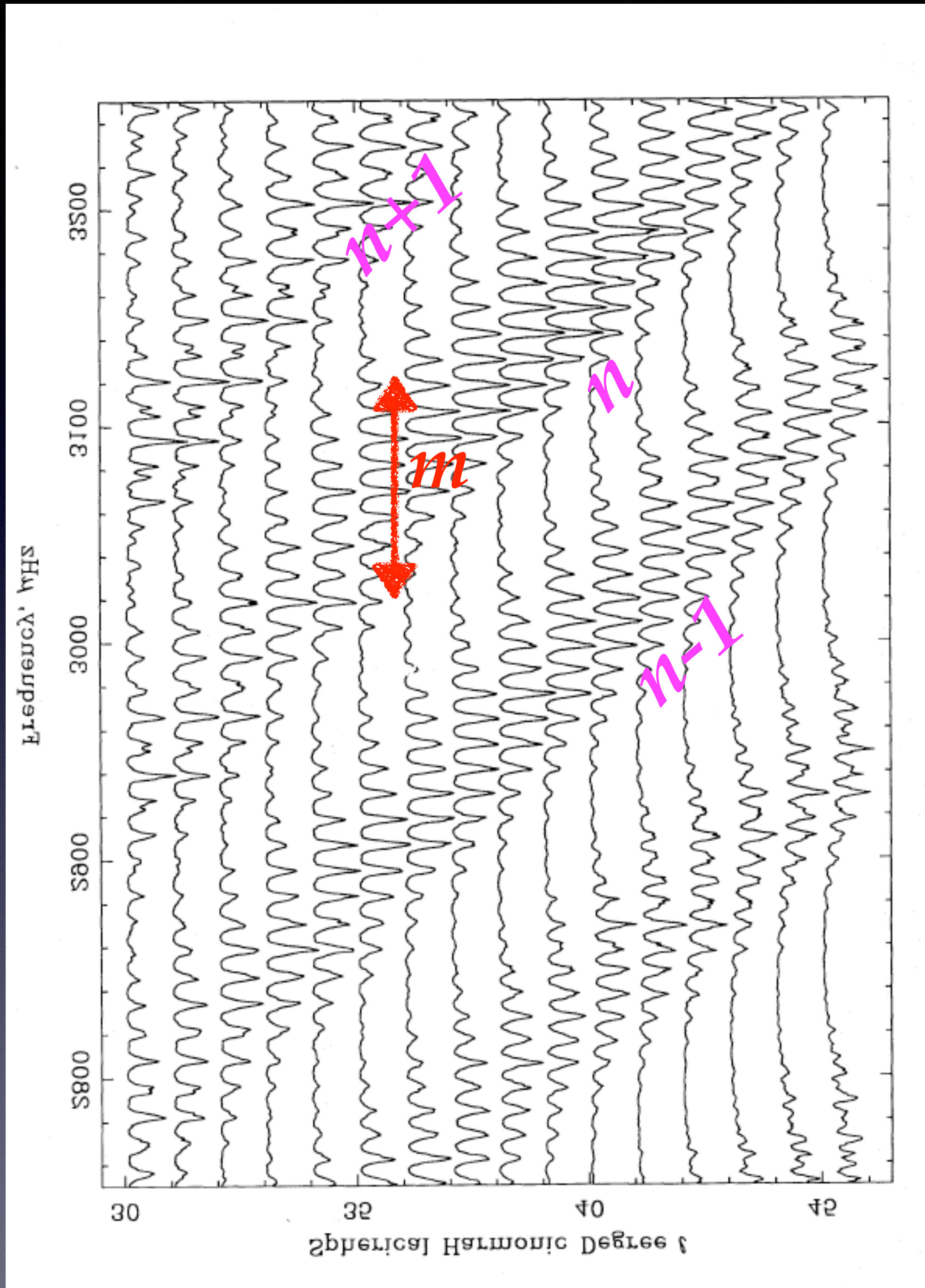

spherical degree *l*

The inclination is determined by the averaged rotation rate, while the S-shape deviation from straight lines indicate latitudinal dependence of the internal rotation.

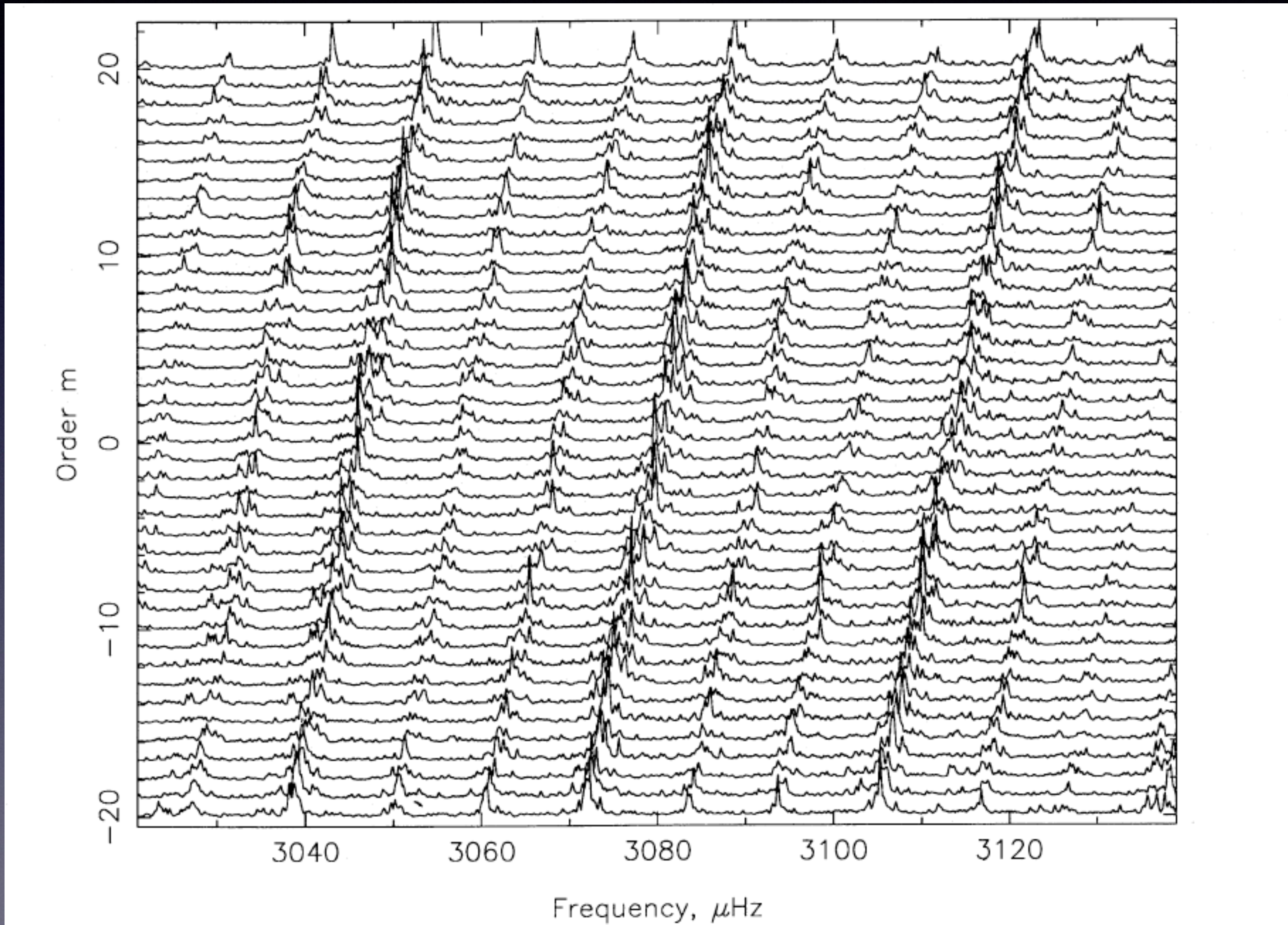

m / l

Frequency

$$\boldsymbol{\omega_m}^{\mathbf{(1)rot}} = m \times \left\{ \Omega_0 \int_0^R \rho(r) r^2 \left(2\xi_r \xi_h + \xi_h^2 \right) dr \right.$$
$$+ \frac{2l+1}{2} \frac{(l-|m|)!}{(l+|m|)!} \int_{r=0}^R \rho(r) r^2 \left[\int_{\theta=0}^\pi \left(P_l^m\right)^2 \{ \Omega(r,\theta) \sin\theta \right.$$
$$\left.\left. \times \left(2\xi_r\xi_h - \xi_r^2 + \xi_h^2[1 - l(l+1)] \right) - \left(\frac{3}{2} \frac{\partial\Omega}{\partial\theta} \cos\theta + \frac{1}{2} \frac{\partial^2\Omega}{\partial\theta^2} \sin\theta \right) \xi_h^2 \right\} d\theta \right] dr \right\}$$
$$\times \left[\int_0^R \rho(r) r^2 \left[\xi_r^2 + l(l+1)\xi_h^2 \right] dr \right]^{-1}$$

A set of $\boldsymbol{\omega_{nlm}}^{\mathbf{(1)rot}}$ is regarded as integral equations to determine the 2D internal rotation profile.

Inversion for rotation

<u>perturbation theory</u>

Integral equation :

$$\delta\omega_{n,l,m} = m(1 - C_{n,l}) \int_0^R K_{n,l}(r)\Omega(r)dr$$

$$C_{n,l} = \frac{\int_0^R \xi_h(2\xi_r + \xi_h)r^2\rho dr}{\int_0^R [\xi_r^2 + l(l+1)\xi_h^2]r^2\rho dr}$$

Kernel :

$$K_{n,l} = \frac{[\xi_r^2 + l(l+1)\xi_h^2 - 2\xi_r\xi_h - \xi_h^2]\rho r^2}{\int_0^R [\xi_r^2 + l(l+1)\xi_h^2 - 2\xi_r\xi_h - \xi_h^2]\rho r^2 dr}$$

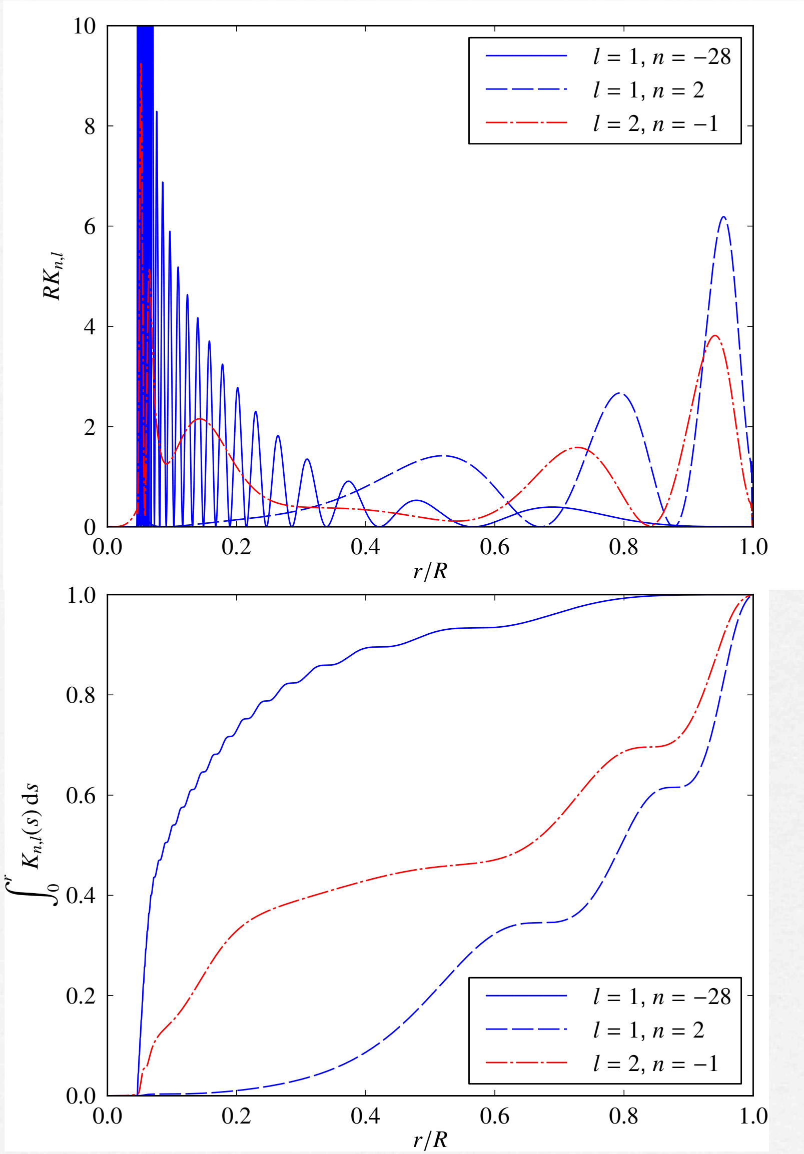

Internal rotation rate

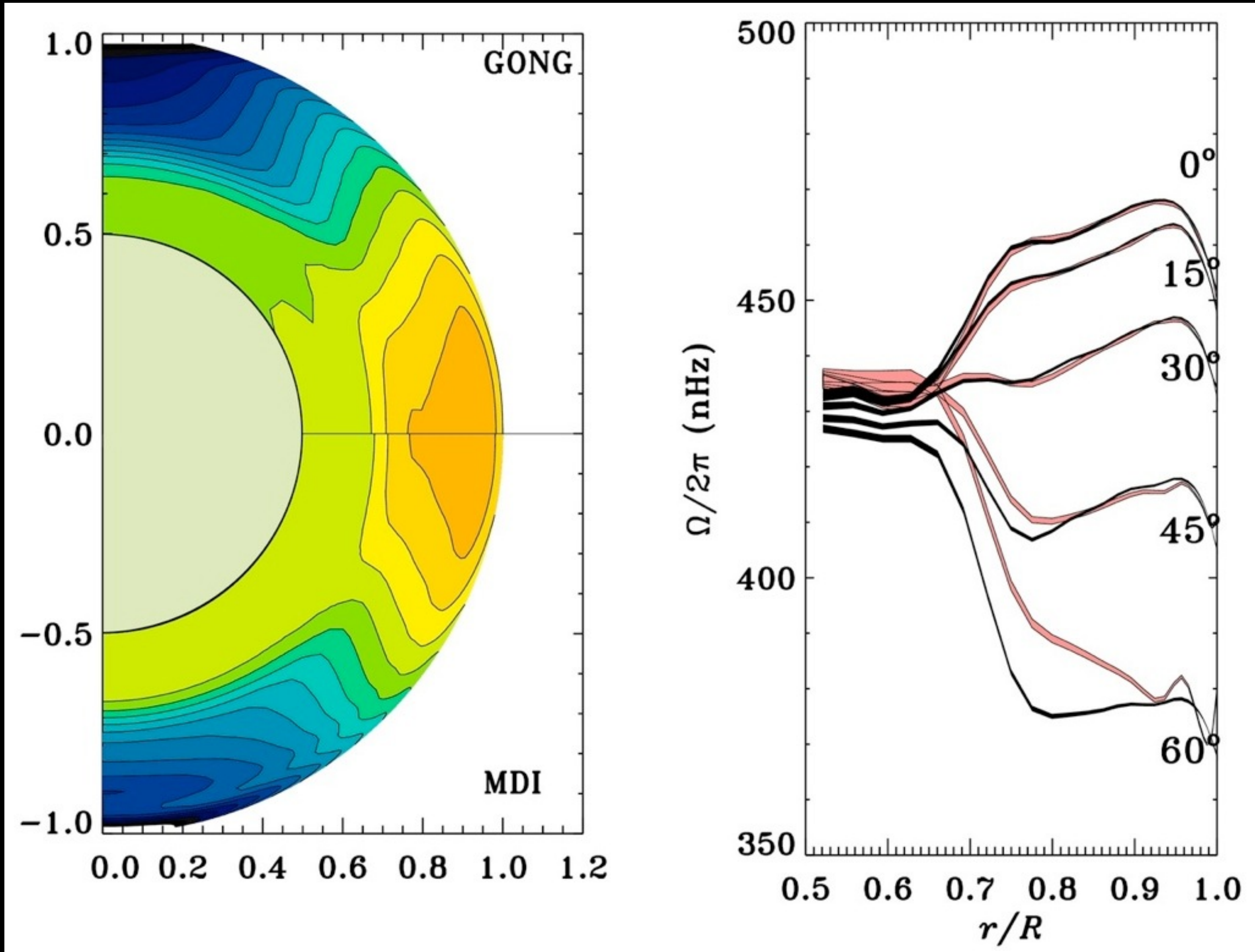

Contrary to the solar case, detectable pulsation modes are limited to low degree (l=0-3) modes.

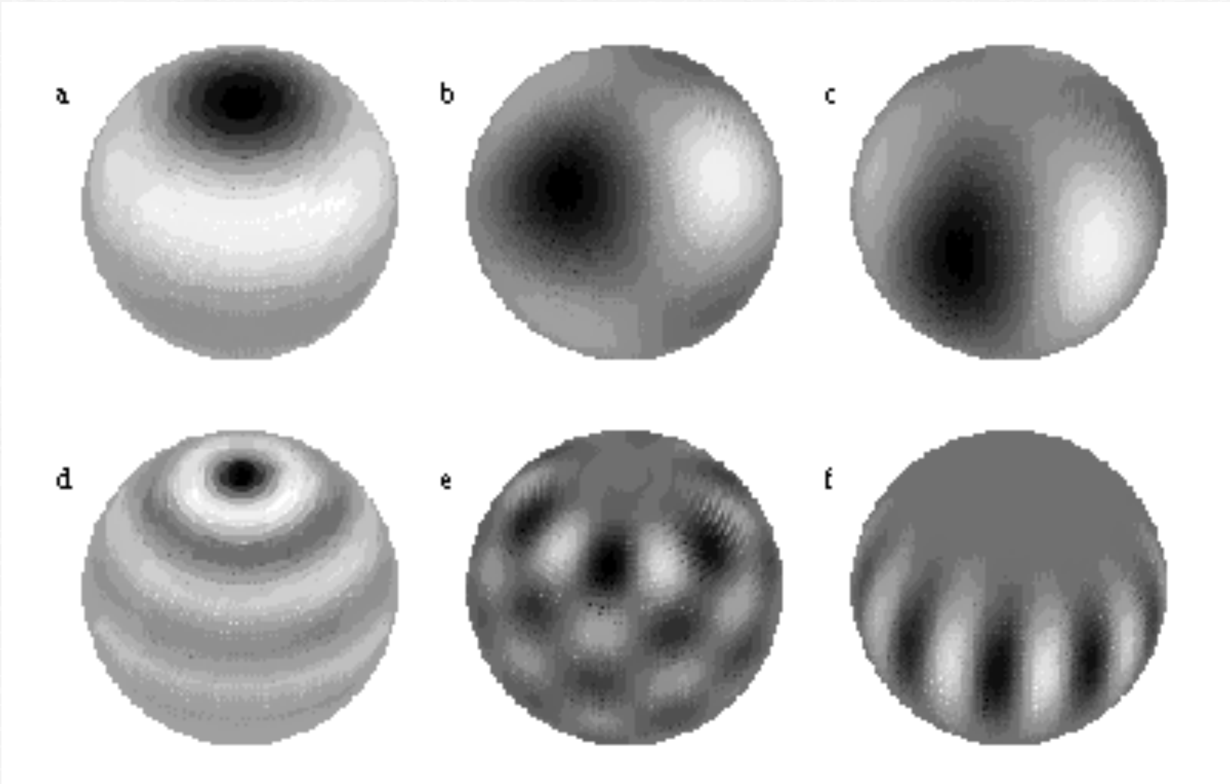

Two types of modes

- Acoustic waves
- restoring force = gaseous pressure
- high frequency
- stellar envelope

- Gravity waves
- restoring force = buoyancy
- low frequency
- stellar deep core

perturbation theory

$$\delta\omega_{n,l,m} = m(1 - C_{n,l}) \int_0^R K_{n,l}(r)\Omega(r)dr$$

$$C_{n,l} = \frac{\int_0^R \xi_h(2\xi_r+\xi_h)r^2\rho dr}{\int_0^R[\xi_r^2+l(l+1)\xi_h^2]r^2\rho dr}$$

$$K_{n,l} = \frac{[\xi_r^2+l(l+1)\xi_h^2-2\xi_r\xi_h-\xi_h^2]\rho r^2}{\int_0^R[\xi_r^2+l(l+1)\xi_h^2-2\xi_r\xi_h-\xi_h^2]\rho r^2 dr}$$

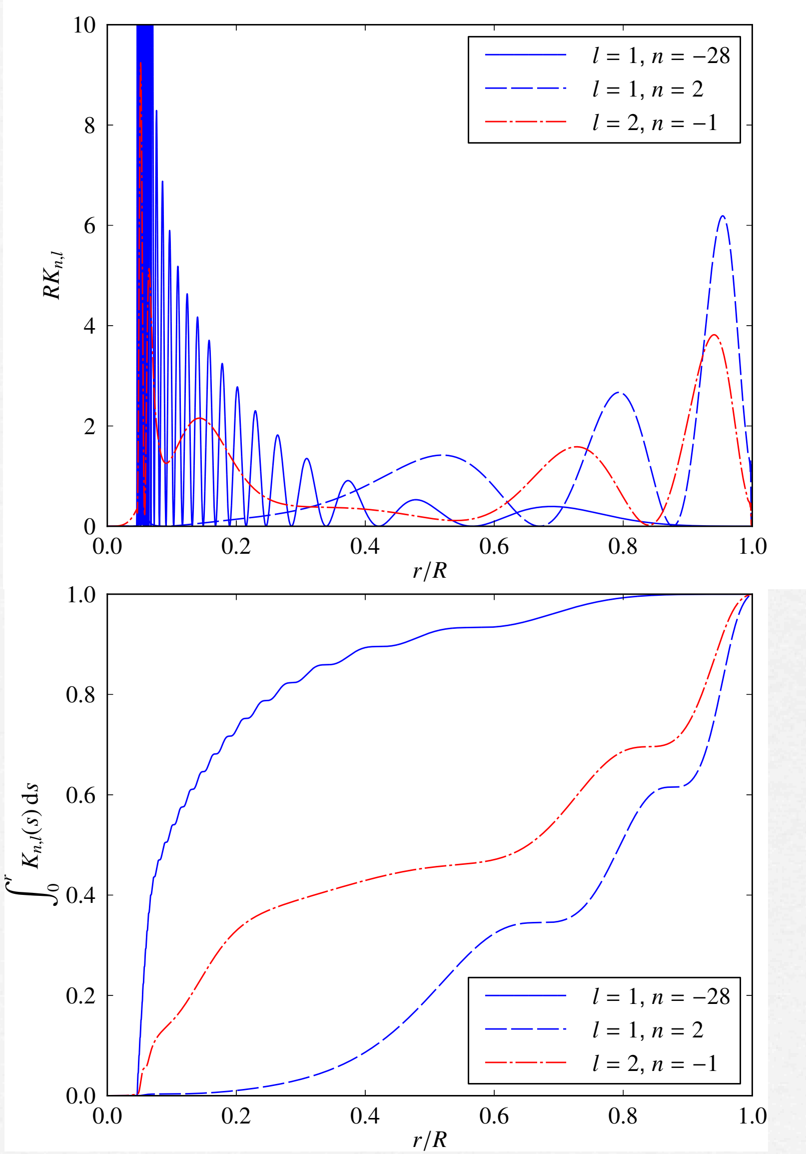

Sun as a Star

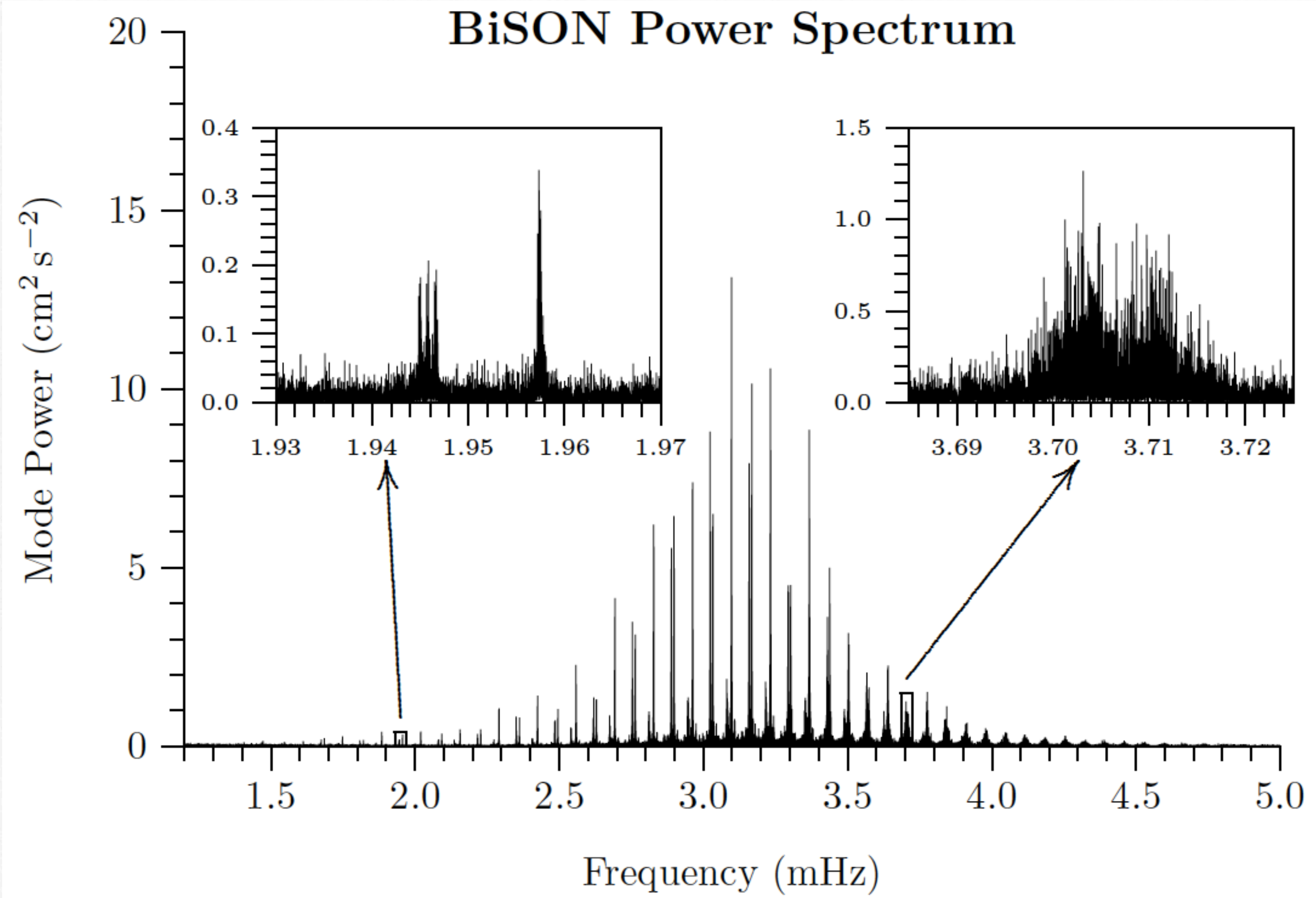

http://bison.ph.bham.ac.uk

Solar-like stars:
convection excites acoustic modes

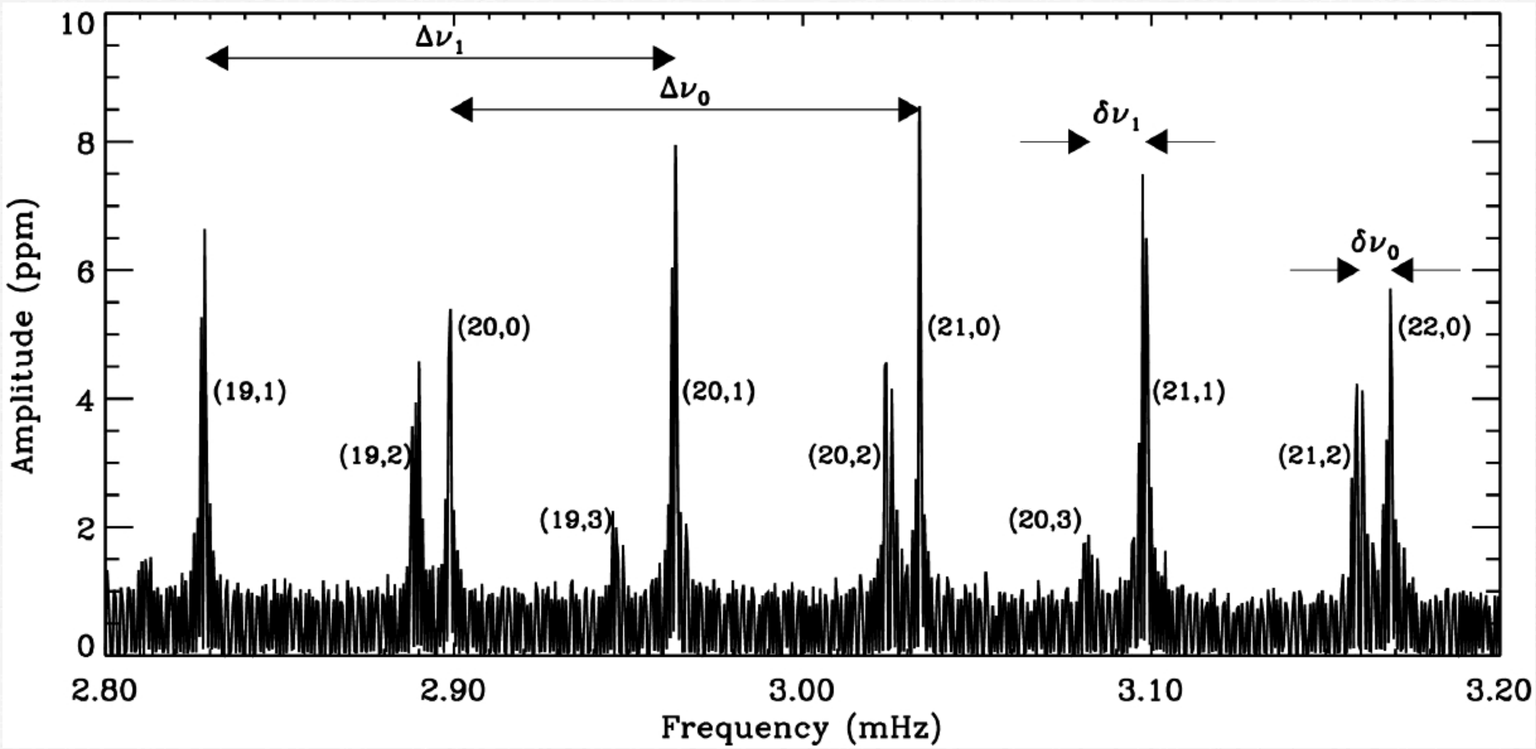

$$\Delta\nu \propto (M/R^3)^{1/2} = M^{1/2}R^{-3/2}$$

$$\nu_{\text{max}} \propto g\, T_{\text{eff}}^{-1/2} \propto MR^{-2}T_{\text{eff}}^{-1/2}$$

$$\therefore R \propto \nu_{\text{max}}\, \Delta\nu^{-2}$$

$$M \propto \nu_{\text{max}}^{3}\, \Delta\nu^{-4}$$

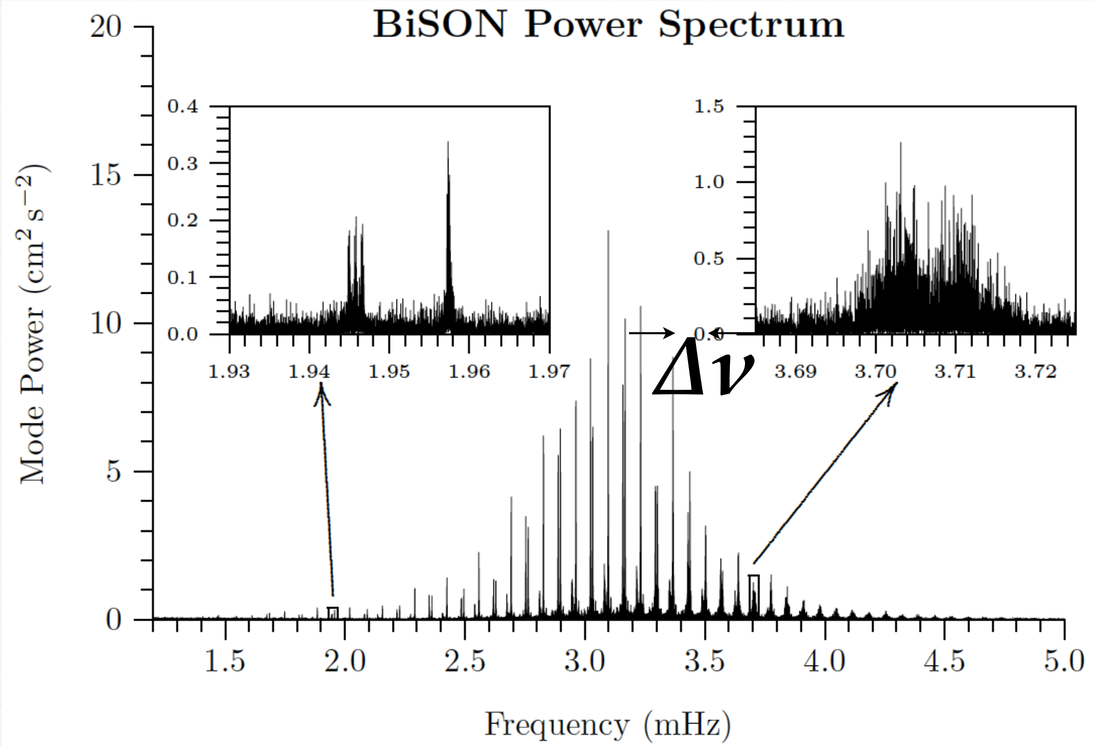

http://bison.ph.bham.ac.uk

acoutic mode：

$$\nu_{nl} \simeq \Delta\nu\left(n+l/2+\varepsilon\right) - d_{nl}$$

$$\Delta\nu = \left[2\int c^{-1}dr\right]^{-1}$$

d_{nl} : sensitive to the core

frequency ~ (sound travel time from the center to the surface)$^{-1}$
~ $(GM/R^3)^{1/2}$

sound wave: fast in the deep interior, less sensitive to the core

refraction due to the temperature gradient induces the sensibility to the core, evolution stage small spacing $\delta\nu$

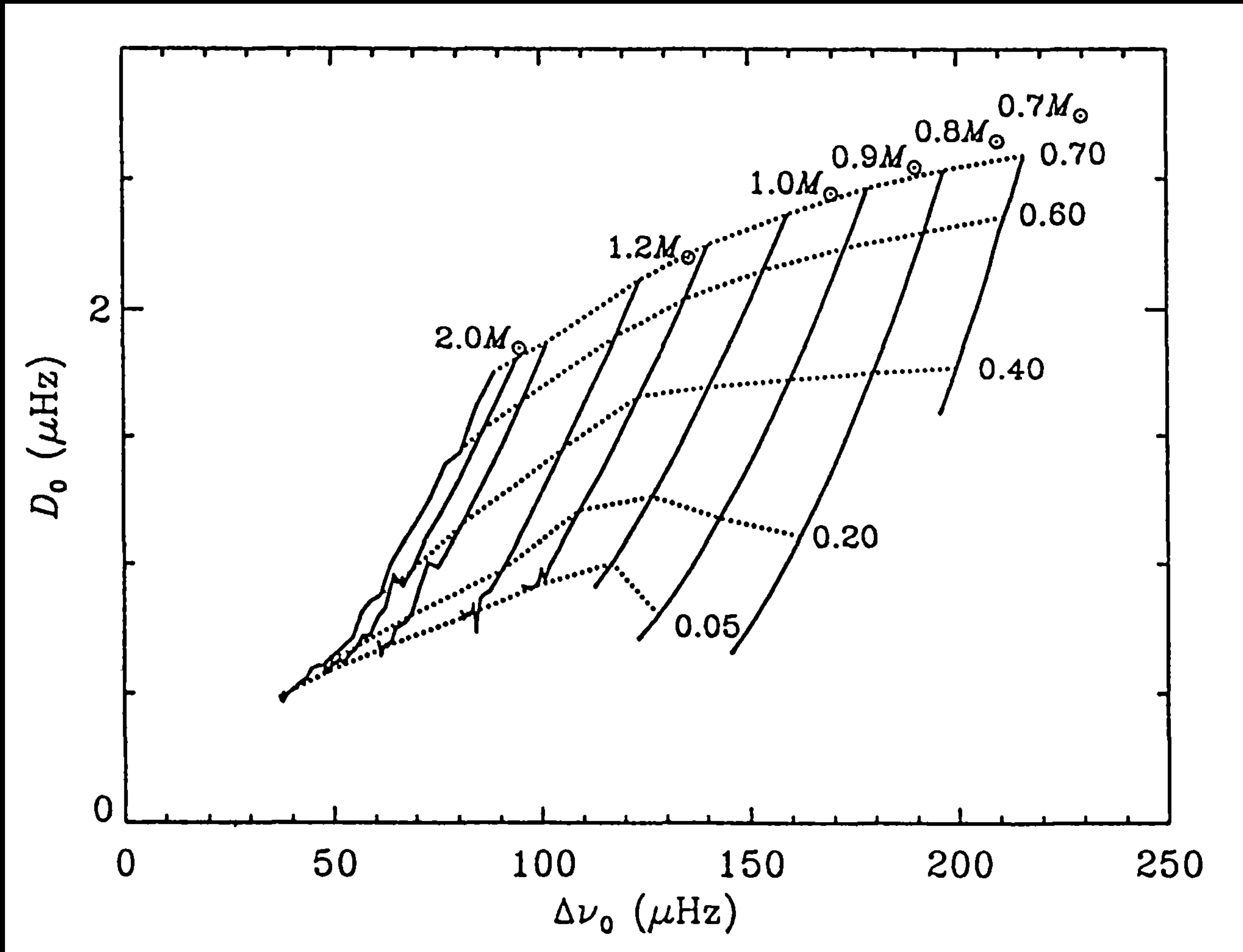

large spacing $\Delta\nu$

Christensen-Dalsgaard, J.1993, ASPC, 42, 397

Solar-like oscillations detected by *Kepler*

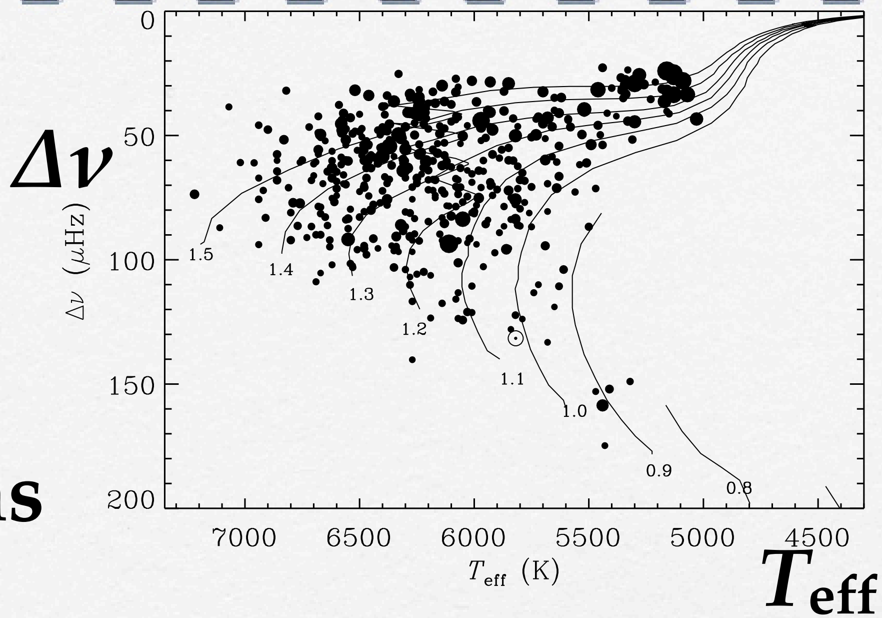

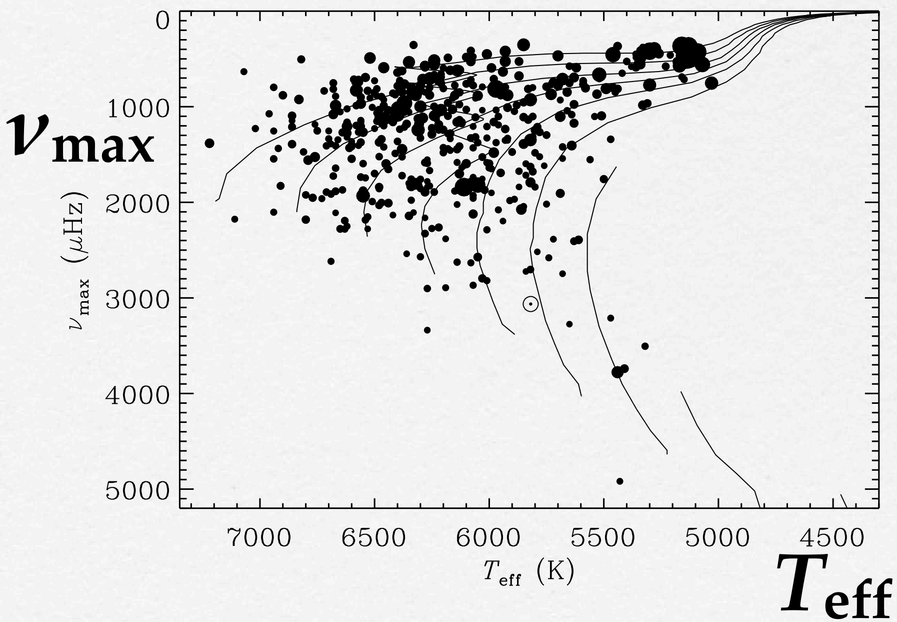

W. J. Chaplin 2012, ASPC, 462, 527

Excitation mechanisms

- Self-excitation
  - Thermal overstability:

    opacity mechanism working in an ionization zone
  - Stochastic excitation due to turbulence:

    waves generated by turbulence resonate in the cavity of a whole star

valve mechanism

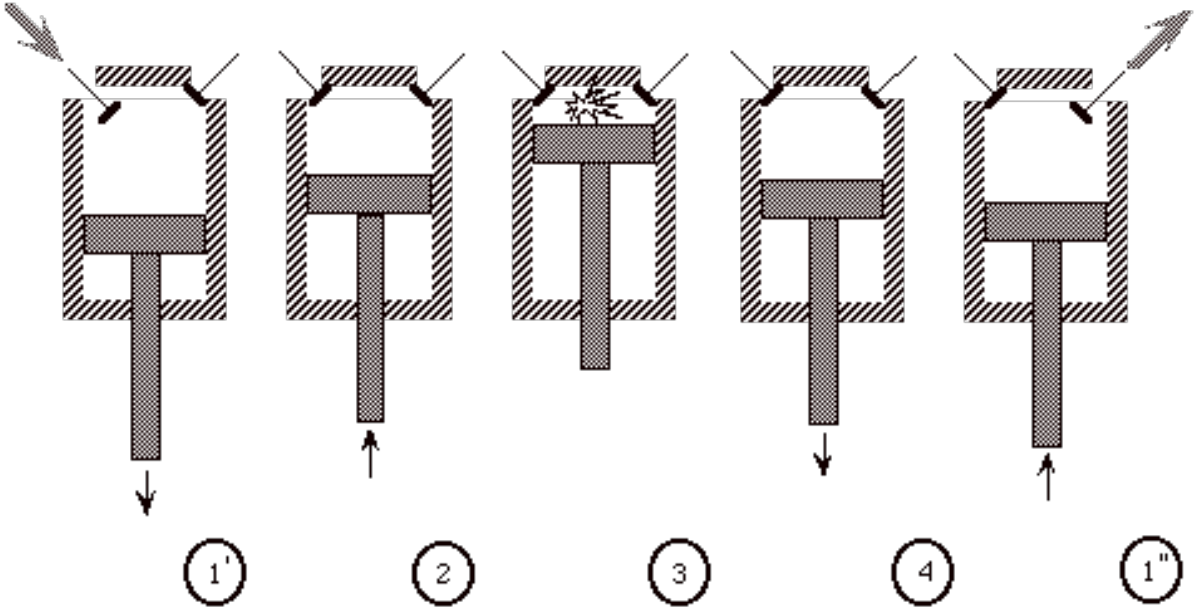

by analogy to car engines

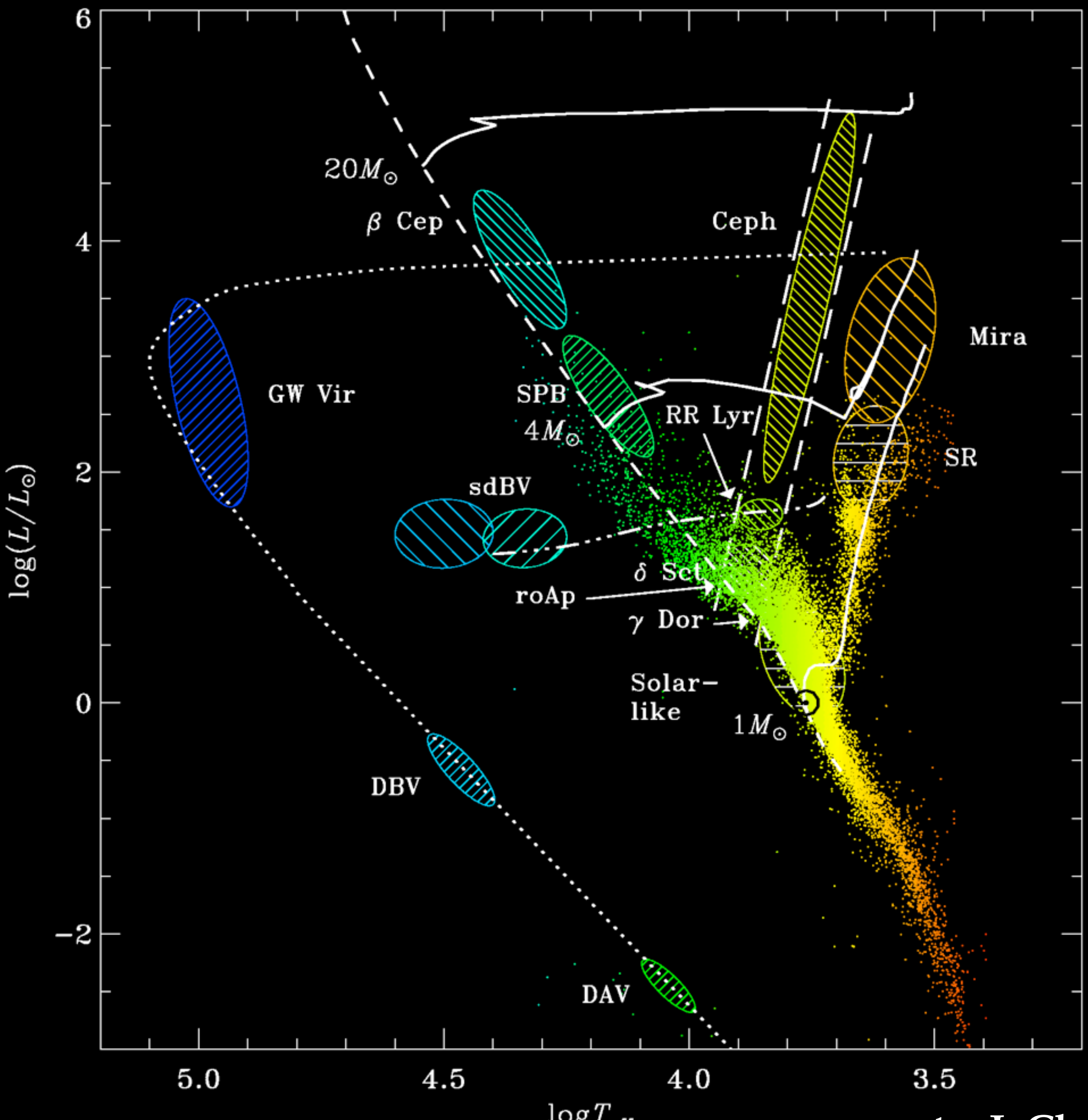

78

coursety: J. Christensen-Dalsgaard

recent progress

- Stellar rotation leads to frequency splittings.
- Acoustic modes tell us rotation of stellar outer envelope.
- Gravity modes tell us rotation of stellar deep core.
- To our surprise, core-to-envelope spin rate ratio is small.
- This implies the presence of very efficient angular momentum transfer / mixing.
- *Internal rotation of stars became observational science.*

Arthur S. Eddington

At first sight it would seem that the deep interior of the sun and stars is less accessible to scientific investigation than any other region of the universe. Our telescopes may probe farther and farther into the depths of space; but how can we ever obtain certain knowledge of that which is hidden behind substantial barriers? What appliance can pierce through the outer layers of a star and test the conditions within?

IV. Asteroseismic New Insights to Stellar Rotation

Stellar rotation is measured from spectroscopic line broadening.

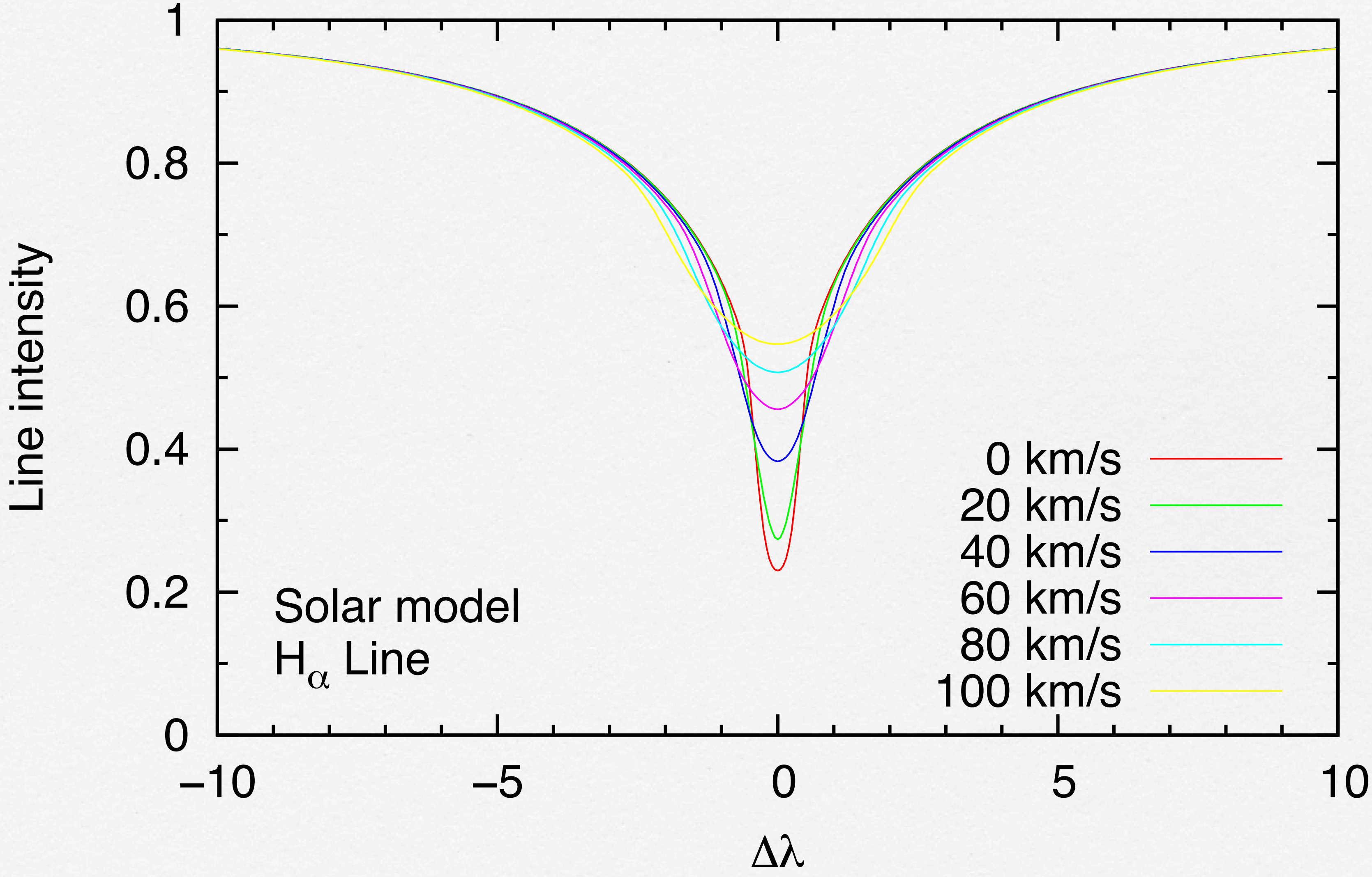

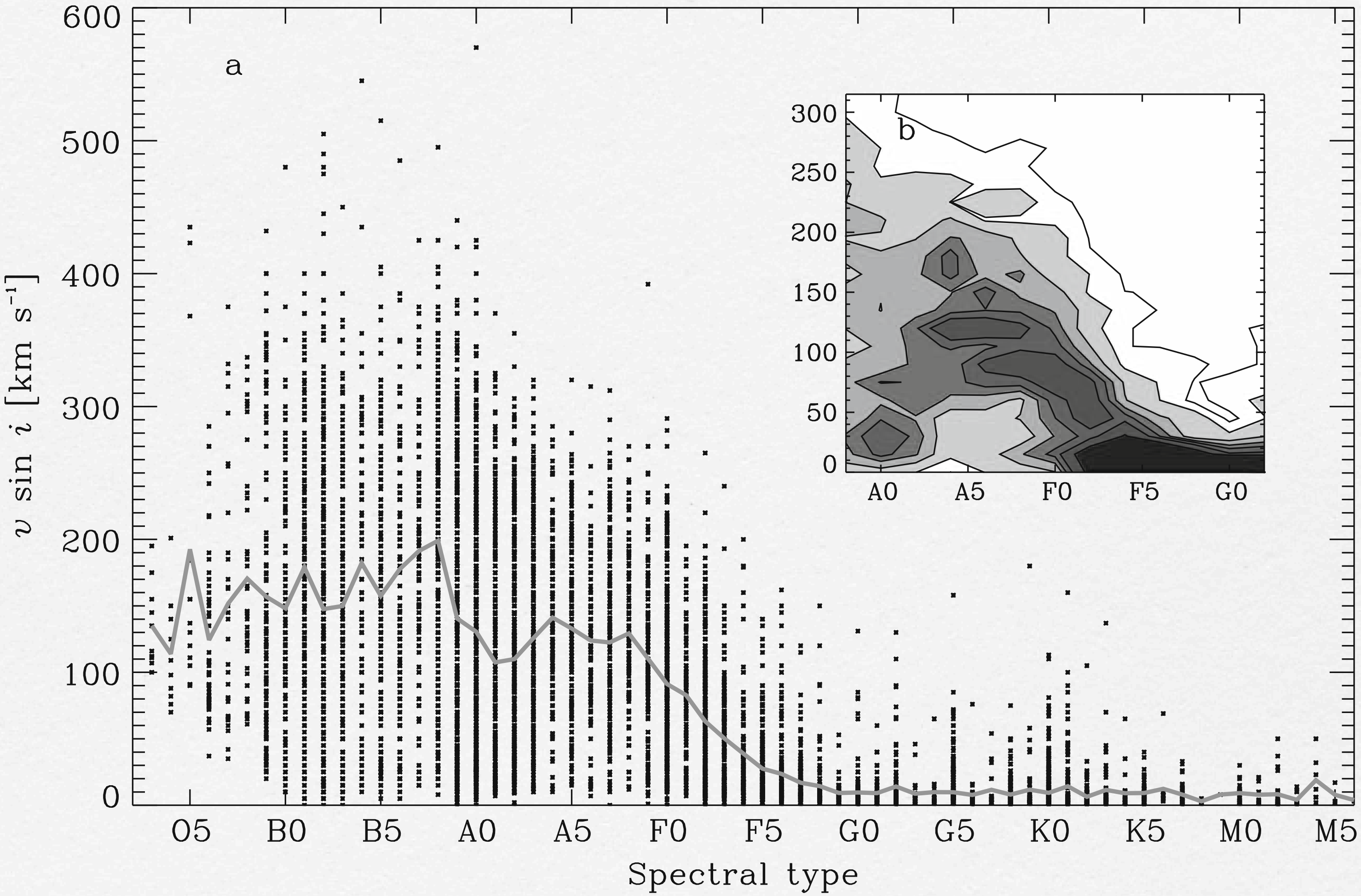

F. Royer 2009, Lecture Notes in Phys., 765, 207

Some thoughts

- Helioseismology opened a new way to see the invisible internal rotation of the Sun, which had had no hope to see it.
- Surprisingly, the radiative core of the Sun was found to be rotating uniformly and slowly.
- Ultimate compact objects, neutron stars and pulsars, are rotating fast indeed, but more slowly than the case of local angular momentum conserved.
- Hence, angular momentum in a star must be lost substantially during stellar evolution.
- Mass-loss phase at RGB or AGB has been regarded as such a candidate.
- But, the Sun, as a main sequence star, seems to have already lost its angular momentum.
- It is desirable to see evolution of stellar rotation.

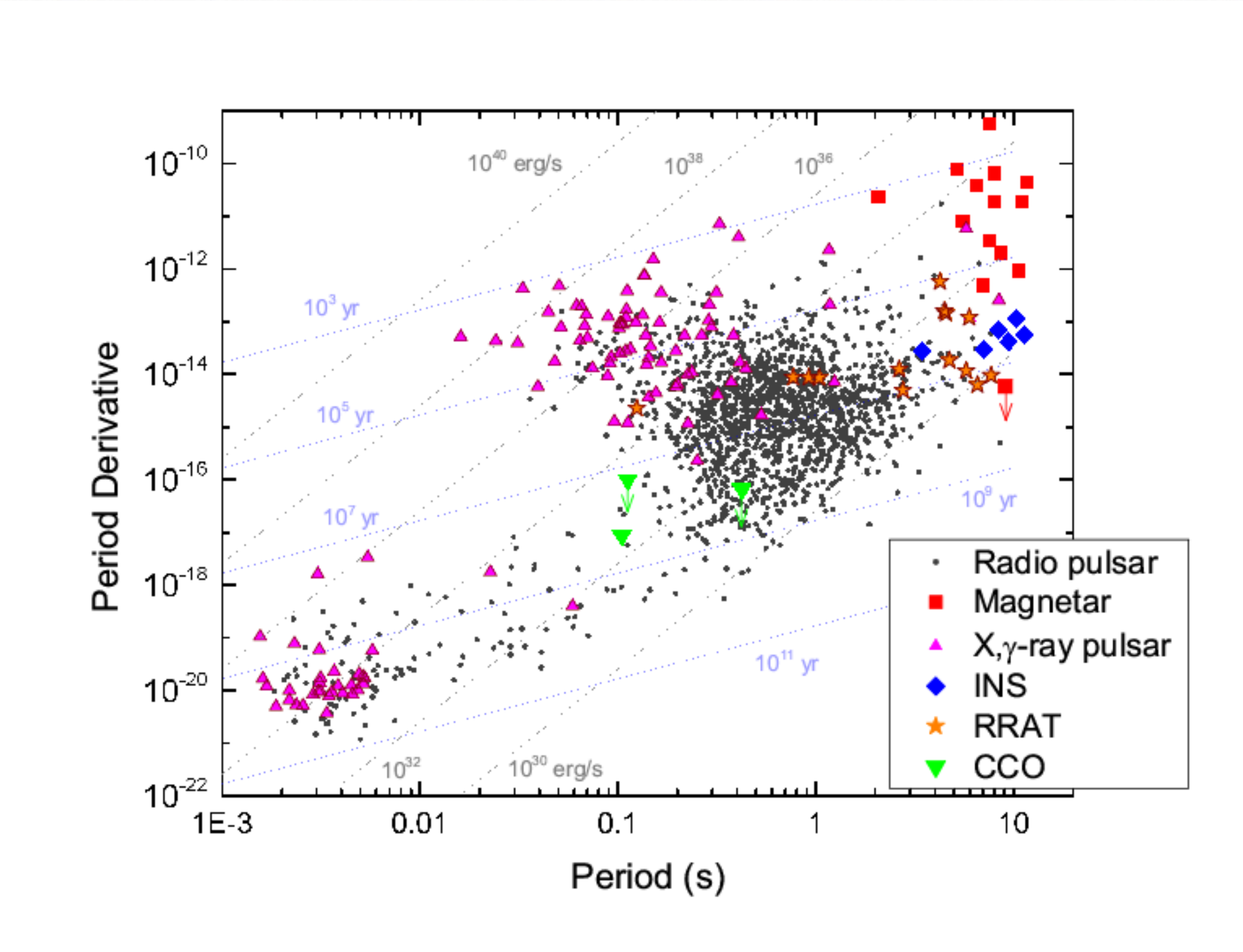

Remarks: INS = Isolated Neutron Stars, RRAT = Rotating Radio Transients, CCO = Compact Central Objects

from http://inspirehep.net/record/1217663/plots

Some thoughts

- In the case of distant stars, the photometrically detectable modes are limited only to very low degree modes, such as l=0~2 or 3.
- Hard to see the S-shape form of $\Delta\nu$ as a function of m / l.
- Visibility of the rotational splitting is highly dependent on the inclination angle to the line-of-sight.
- In the case of solar-like stars, m-modes are expected to be equally excited.
- In the case of solar-like stars, the rotational splitting is likely to be small (because of slow rotation), while turbulence makes the spectroscopic lines broad.

Doppler measurement with integrated light

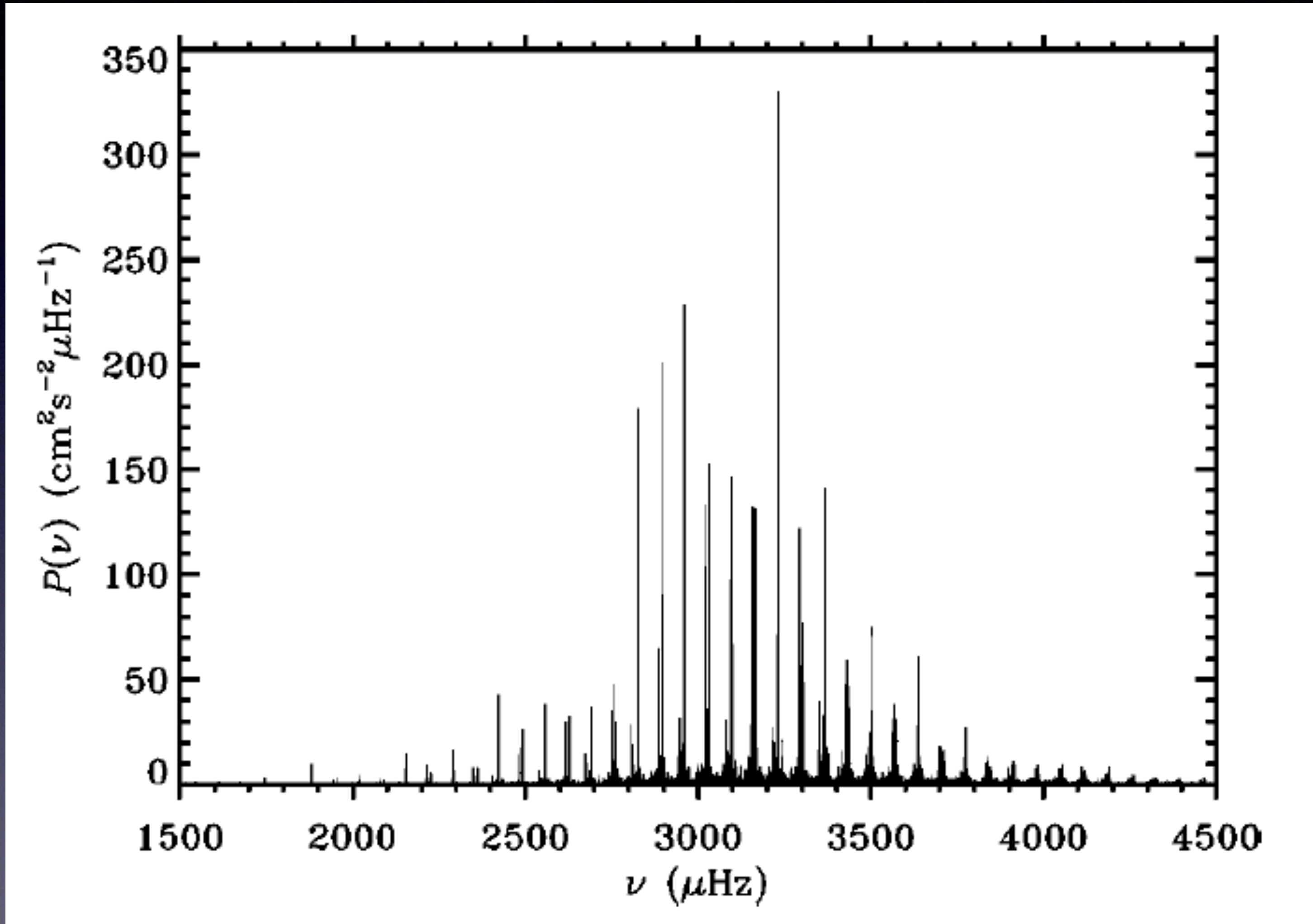

a clear comb structure = evidence for low degree *l* high order *n* p-modes

The inclination is determined by the averaged rotation rate, while the S-shape deviation from straight lines indicate latitudinal dependence of the internal rotation.

m / l

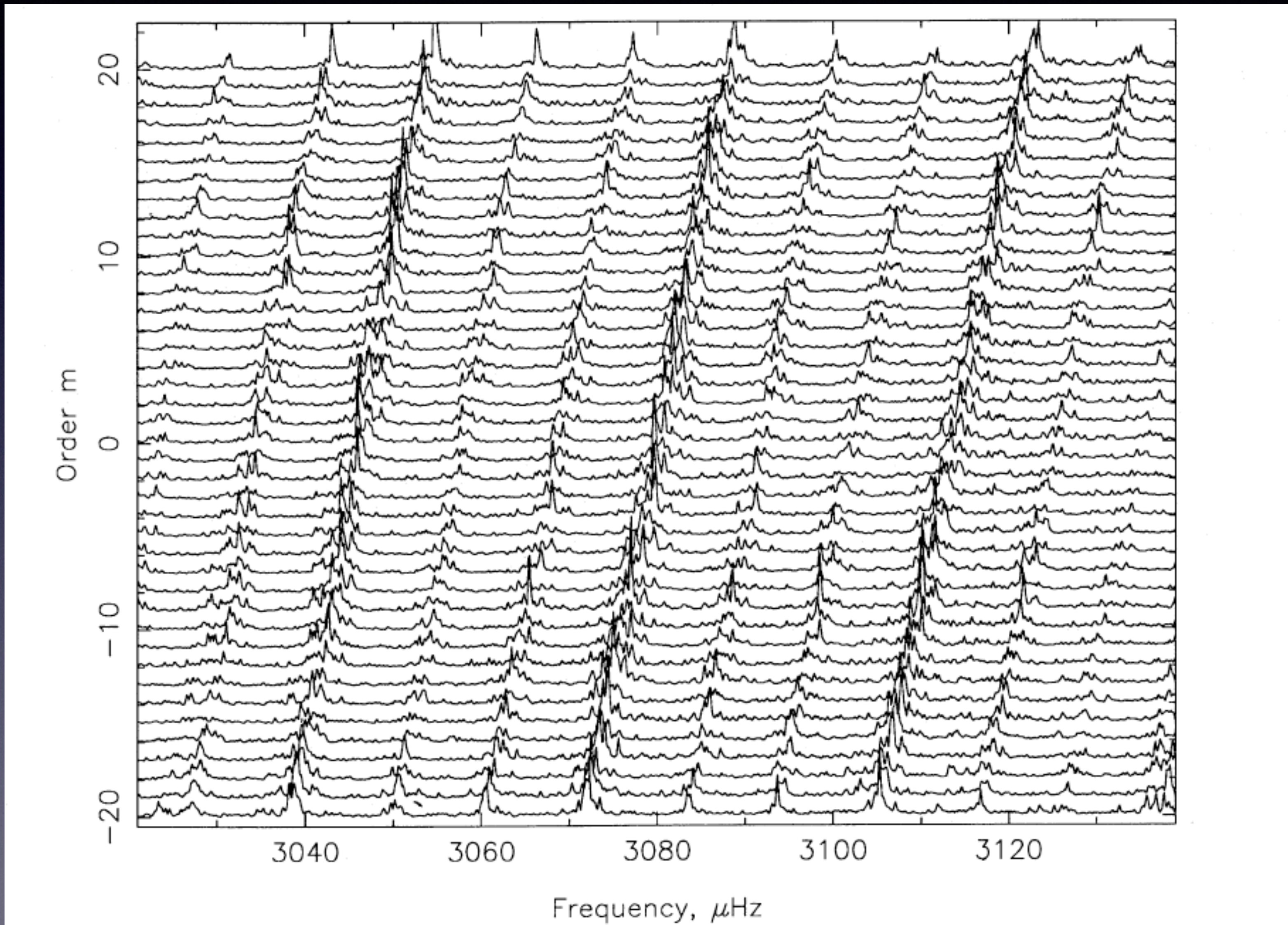

Frequency

Visibility of rotational multiplets is highly sensitive to the stellar inclination.

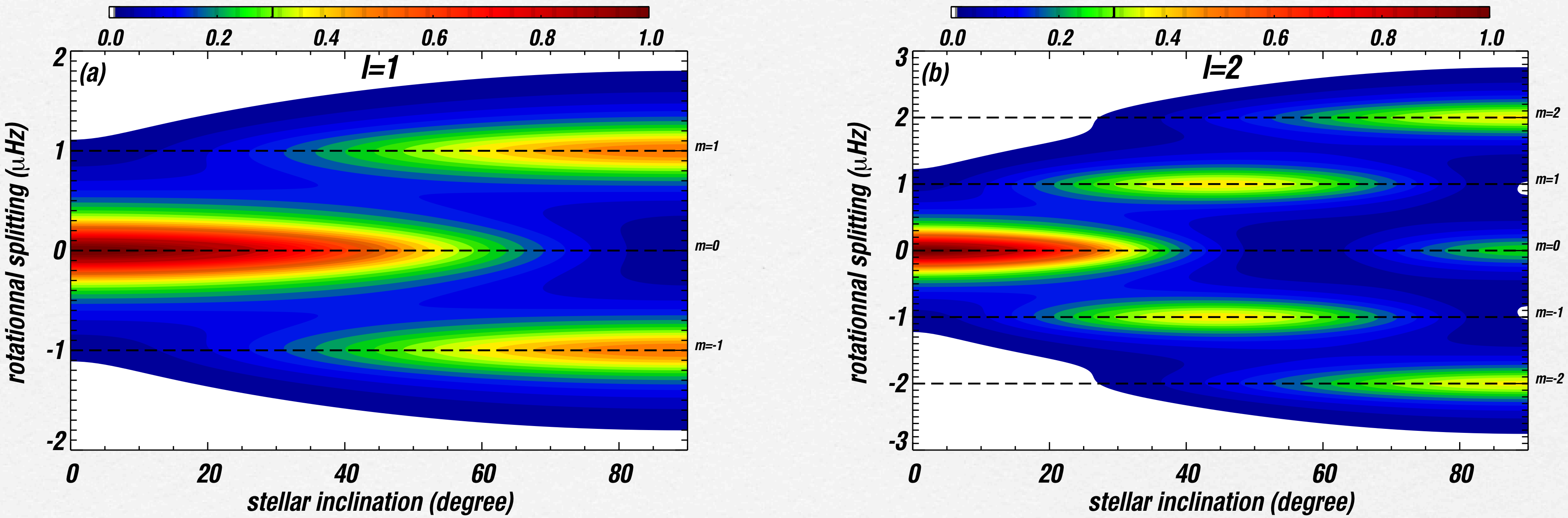

Benomar, O., Masuda, K., Shibahashi, H., Suto, Y. 2014, PASJ, 66, 94

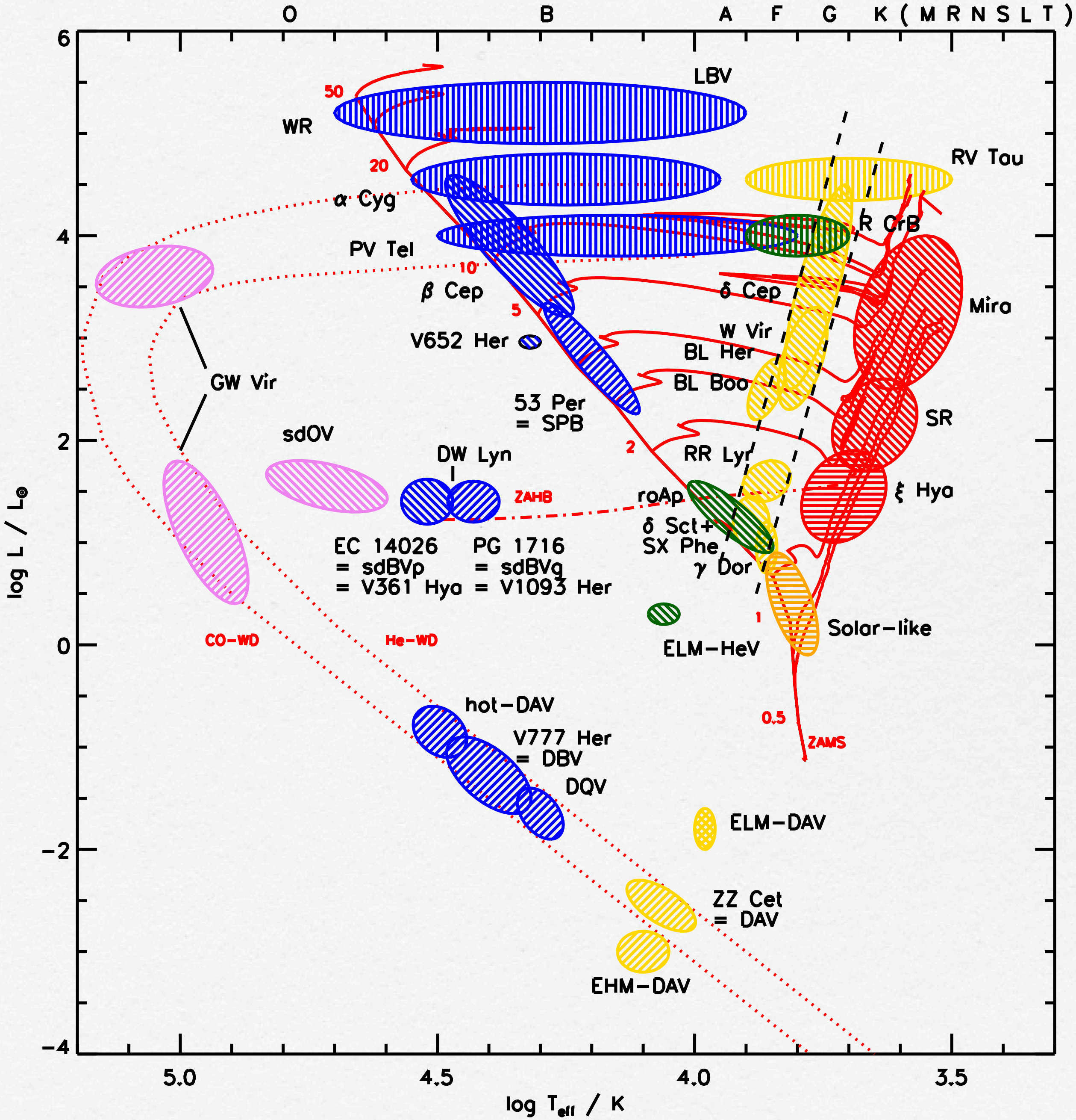

Credit: C. S. Jeffery

Some thoughts

- In the case of early-type stars, the amplitudes of *m*-components may be dependent on the excitation mechanism, so may be different each other.
- In the case of early-type stars, there is a possibility of hybrid stars pulsating with both p- and g-modes. They may provide information from the core to the envelope.
- Let us look for good examples among the *Kepler* stars.

An Example of Hybrid Stars
KIC11145123

T_{eff} = 8050 +/- 200 K

log g (cgs) = 4.0 +/- 0.2

a hybrid δ Sct / γ Dor star

KIC11145123

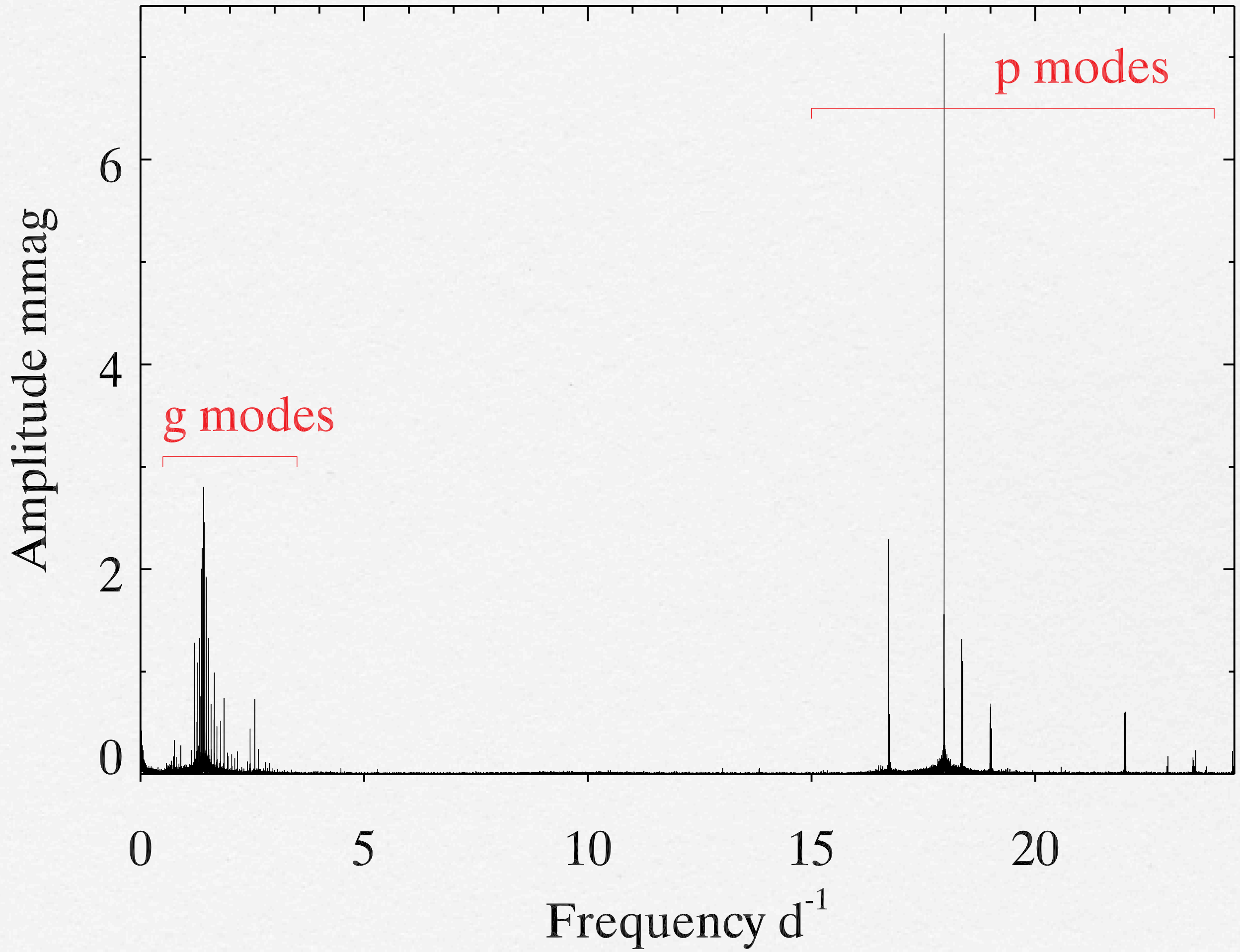

Kurtz, D. W., Saio, H., Takata, M., Shibahashi, H., Murphy, S. J., Sekii, T. 2014, MNRAS, 444, 102

KIC11145123

g modes

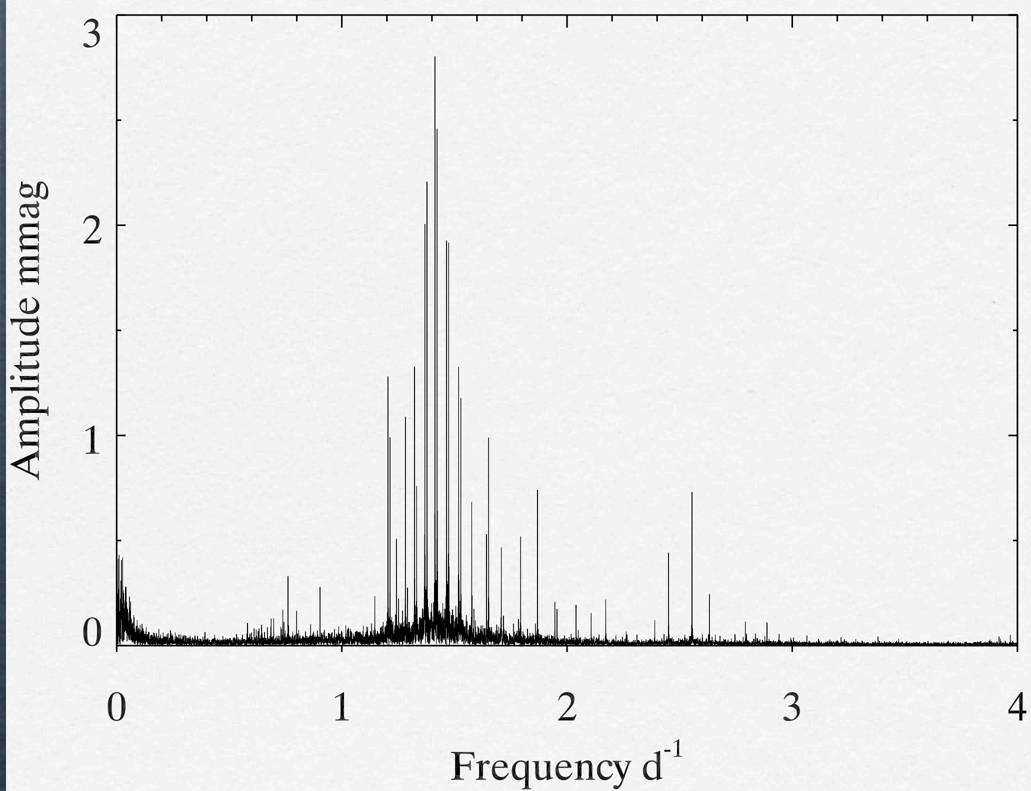

p modes

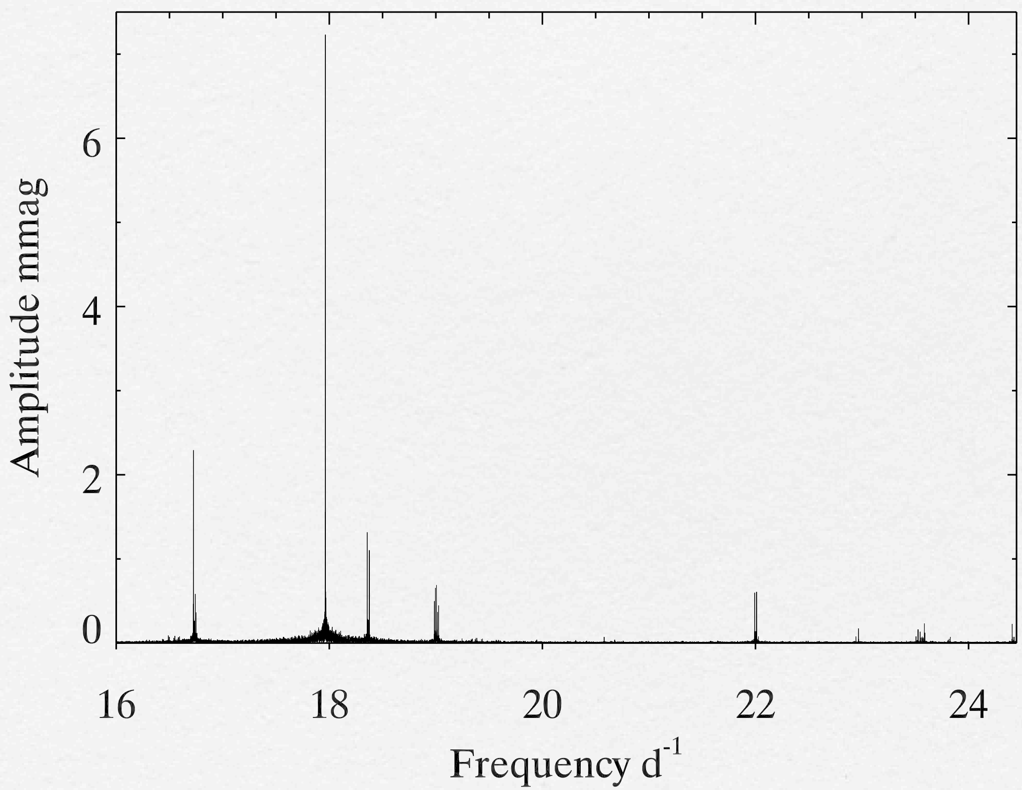

Kurtz, D. W., Saio, H., Takata, M., Shibahashi, H., Murphy, S. J., Sekii, T. 2014, MNRAS, 444, 102

KIC11145123

g modes

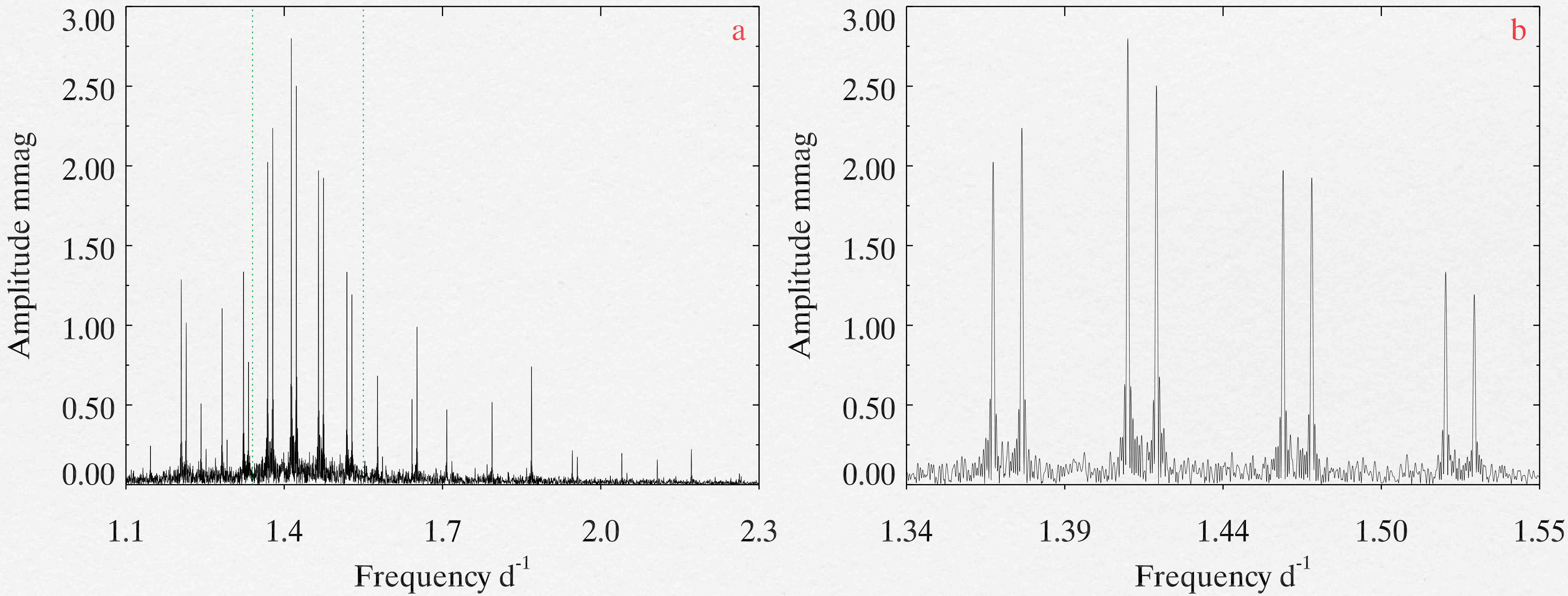

Kurtz, D. W., Saio, H., Takata, M., Shibahashi, H., Murphy, S. J., Sekii, T. 2014, MNRAS, 444, 102

KIC11145123

p modes

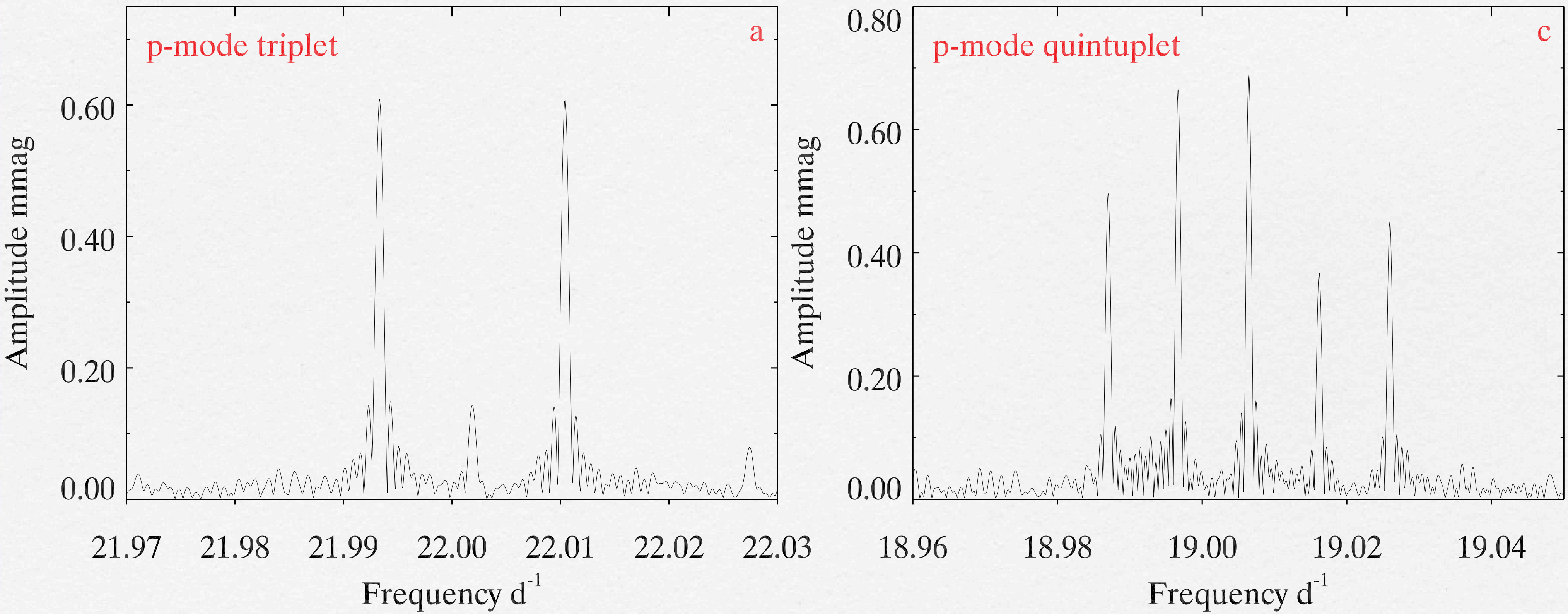

Kurtz, D. W., Saio, H., Takata, M., Shibahashi, H., Murphy, S. J., Sekii, T. 2014, MNRAS, 444, 102

Inversion for rotation

<u>perturbation theory</u>

Integral equation :

$$\delta\omega_{n,l,m} = m(1 - C_{n,l}) \int_0^R K_{n,l}(r)\Omega(r)dr$$

$$C_{n,l} = \frac{\int_0^R \xi_h(2\xi_r+\xi_h)r^2\rho dr}{\int_0^R[\xi_r^2+l(l+1)\xi_h^2]r^2\rho dr}$$

Kernel :

$$K_{n,l} = \frac{[\xi_r^2+l(l+1)\xi_h^2-2\xi_r\xi_h-\xi_h^2]\rho r^2}{\int_0^R[\xi_r^2+l(l+1)\xi_h^2-2\xi_r\xi_h-\xi_h^2]\rho r^2 dr}$$

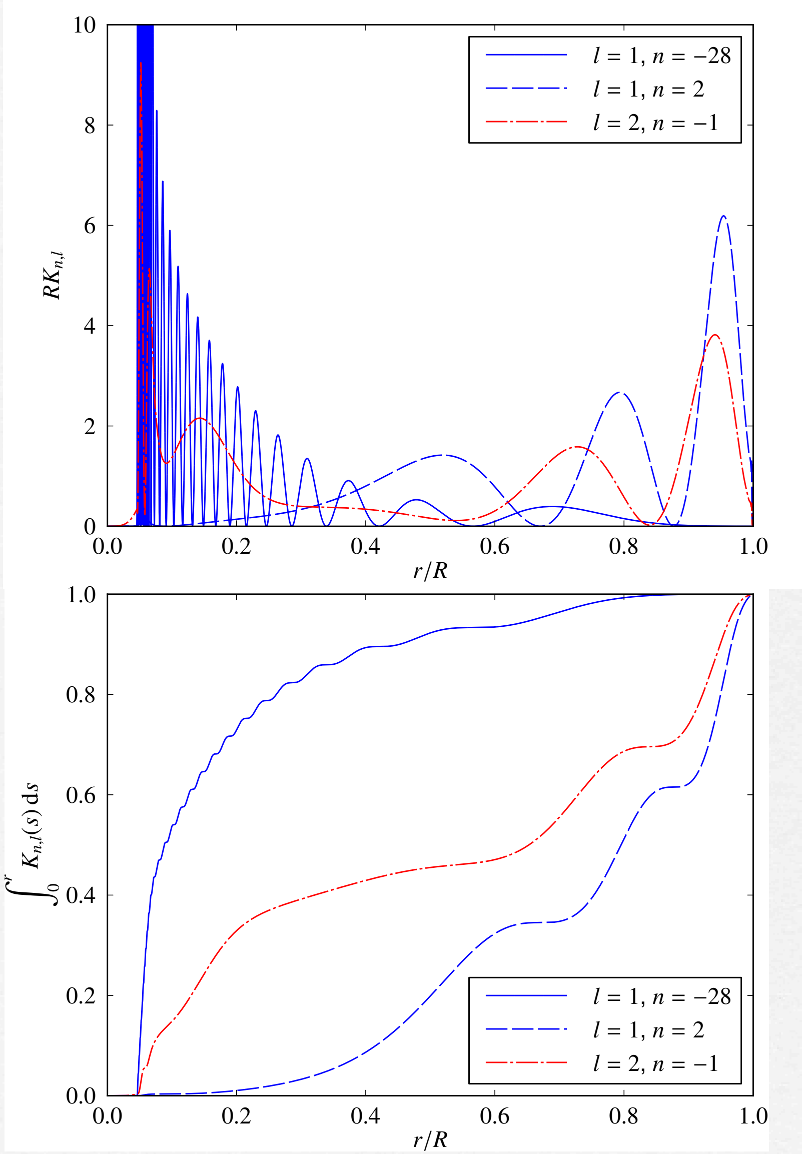

Kurtz, D. W., Saio, H., Takata, M., Shibahashi, H., Murphy, S. J., Sekii, T. 2014, MNRAS, 444, 102

The Ledoux constant :

$$C_{n,l} = \frac{\int_0^R \xi_h (2\xi_r + \xi_h) r^2 \rho dr}{\int_0^R [\xi_r^2 + l(l+1)\xi_h^2] r^2 \rho dr}$$

High-order p-modes :

$|\boldsymbol{\xi}_\mathrm{h}| \ll |\boldsymbol{\xi}_\mathrm{r}|$

then $C_{nl} \longrightarrow 0$

High-order g-modes :

$|\boldsymbol{\xi}_\mathrm{r}| \ll |\boldsymbol{\xi}_\mathrm{h}|$

then $C_{nl} \longrightarrow 1/l(l+1)$

$C_{nl} = 1/2$ for $l = 1$

$1/6$ for $l = 2$

The observed splitting of g-modes is ~0.005 d^{-1}, while the observed splitting is ~0.01 d^{-1}.

So, it is concluded that the star is almost uniformly rotating with P_{rot} ~ 100 d. *This conclusion is model independent.*

Two-zone model of internal rotation

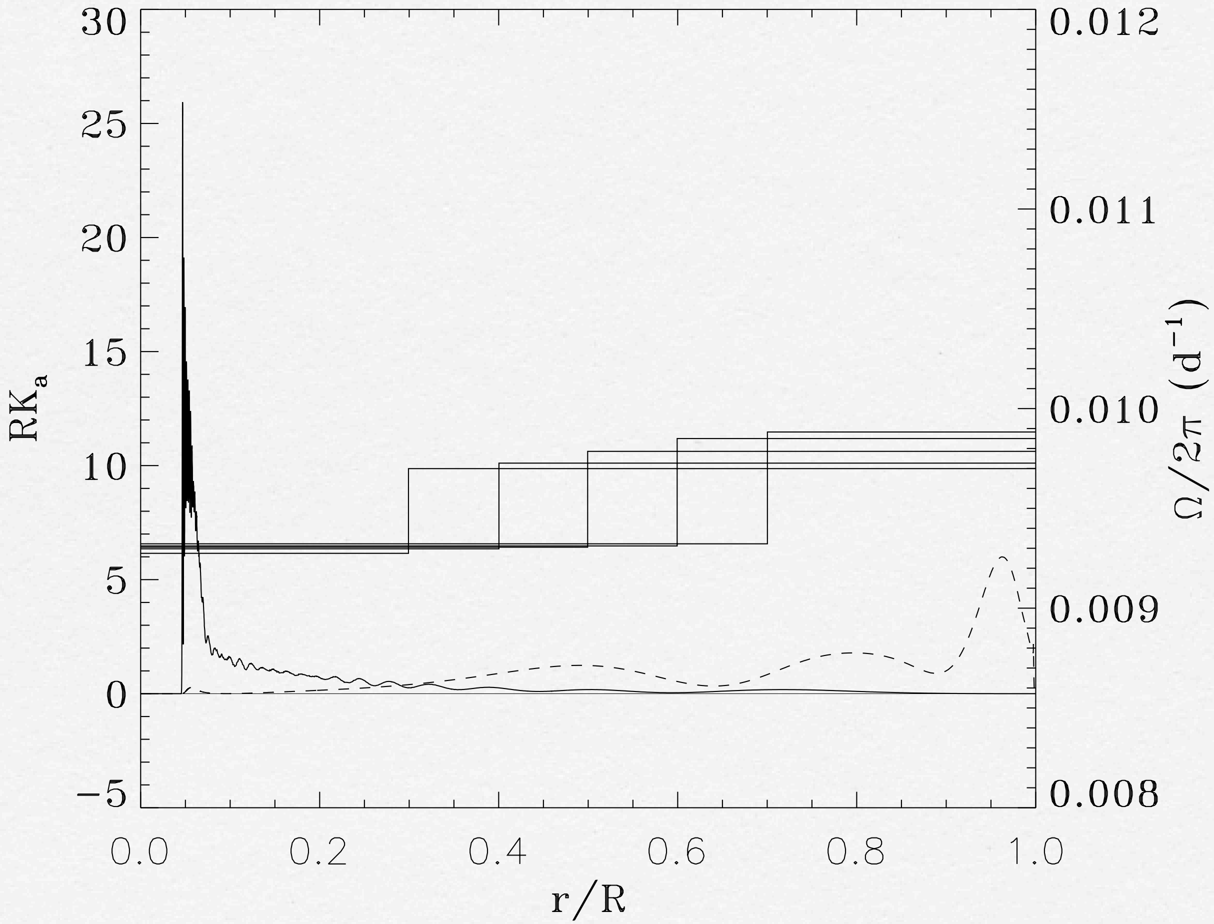

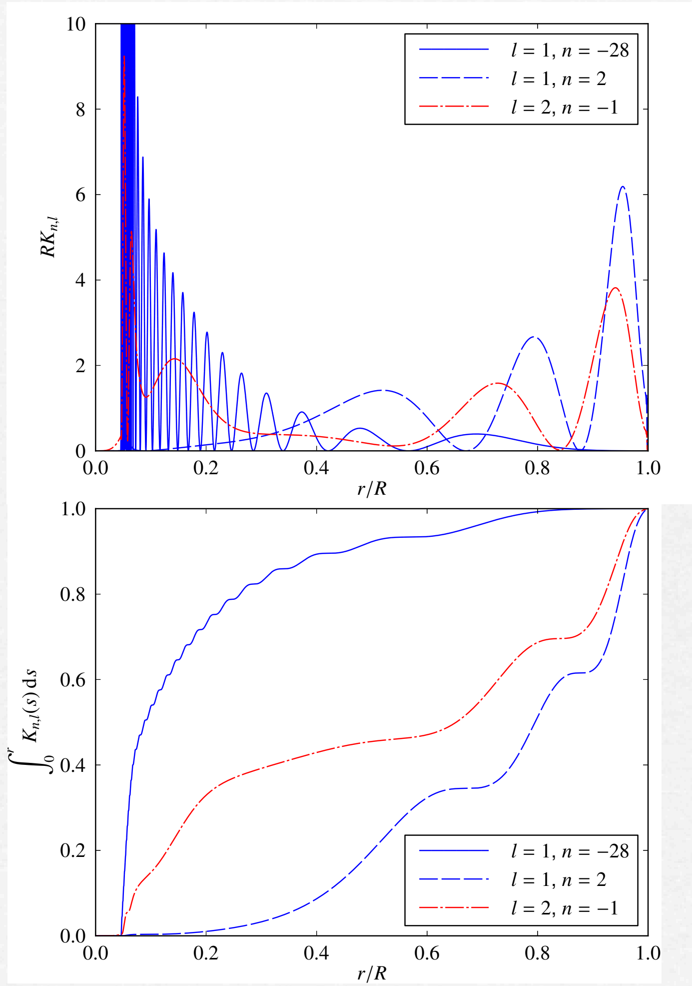

Kurtz, D. W., Saio, H., Takata, M., Shibahashi, H., Murphy, S. J., Sekii, T. 2014, MNRAS, 444, 102

gravity mode: $P_{nl} = [l(l+1)]^{1/2} P_0(n+l/2+\varepsilon)$, **where** $P_0 := \int_c^R N/r\, dr$

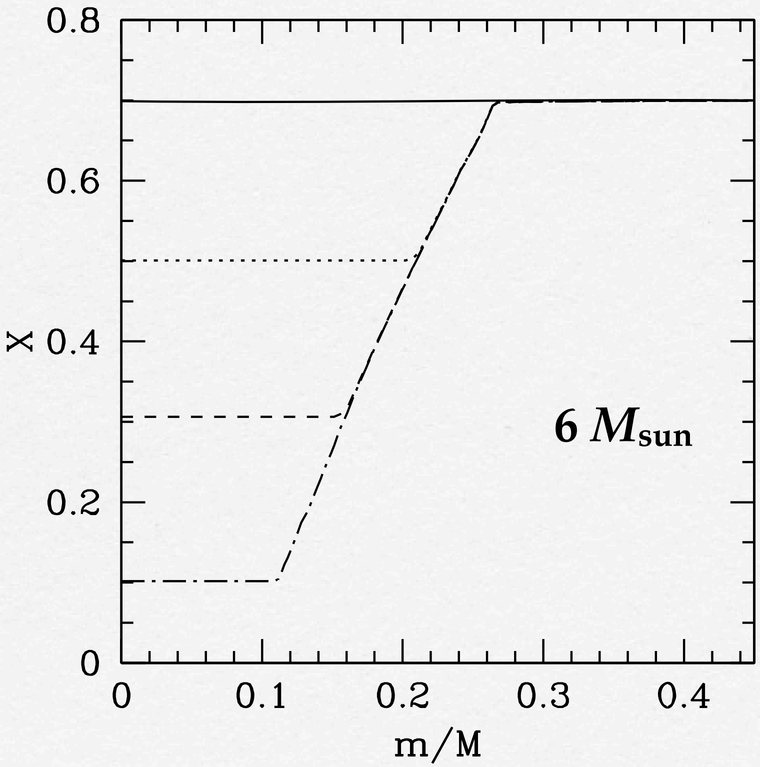

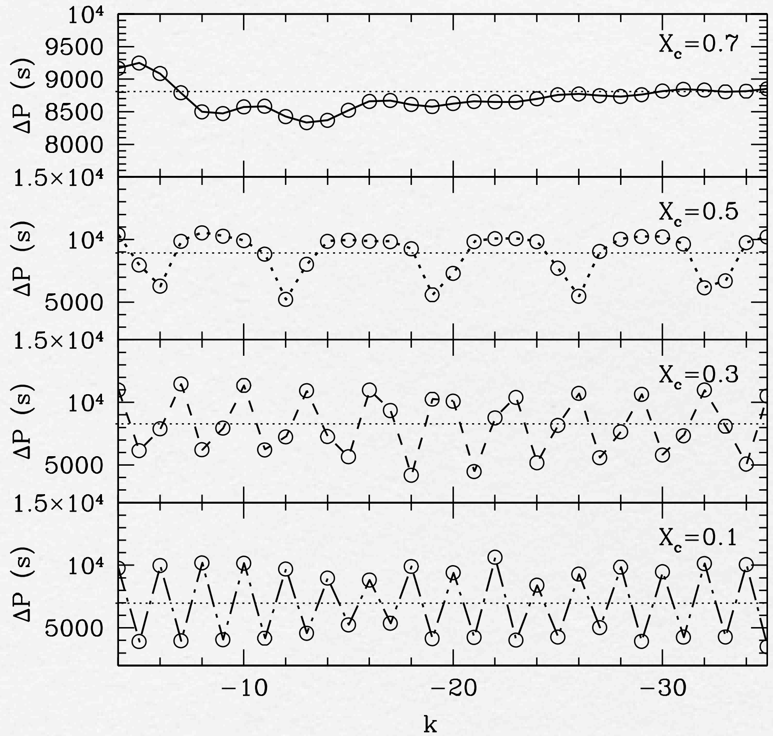

The period separation is sensitive to the chemically inhomogeneous zone.

Miglio, A., Montalbán, J., Noels, A., & Eggenberger, P. 2008, MNRAS, 386, 1487

Evolutionary stage of the star

Useful information :

- Period separation of g-modes —- sensitive to the μ-zone
- Frequencies of singlet p-modes

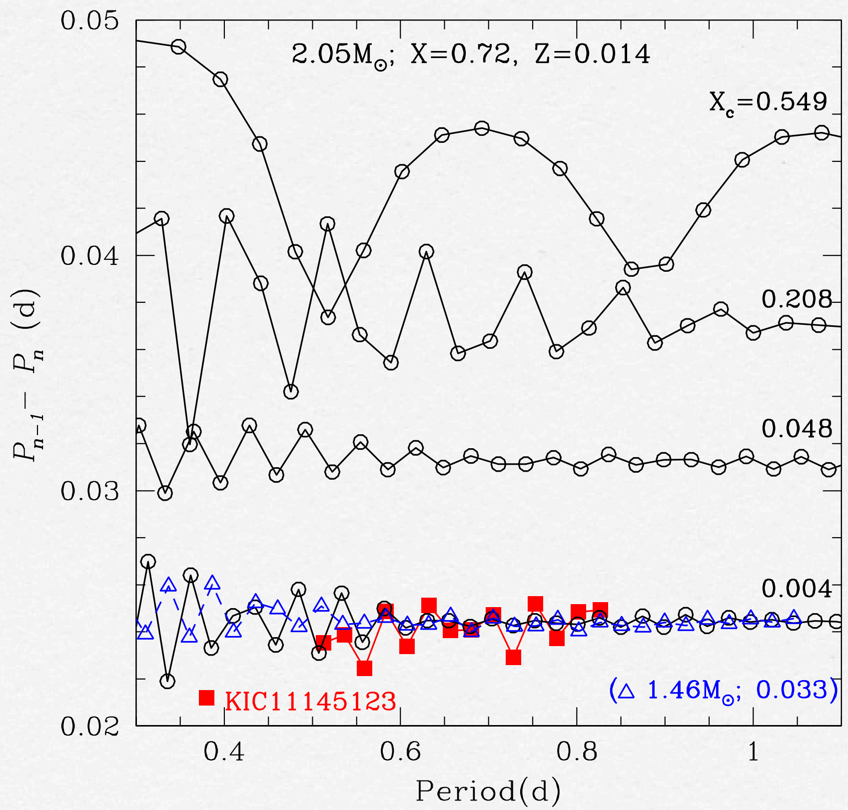

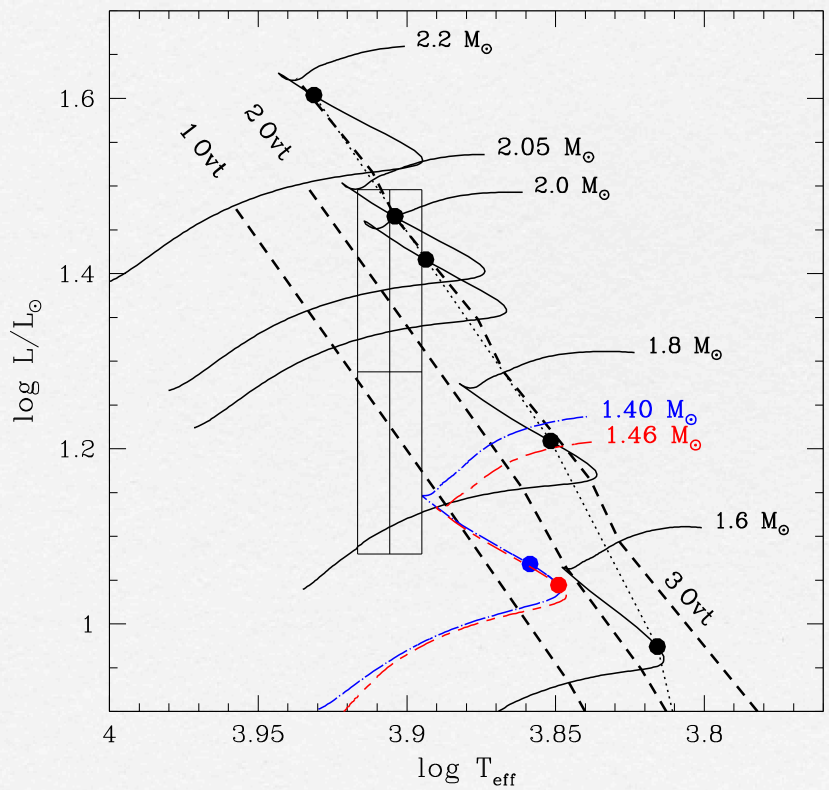

Kurtz, D. W., Saio, H., Takata, M., Shibahashi, H., Murphy, S. J., Sekii, T. 2014, MNRAS, 444, 102

Another similar hybrid δSct / γDor star : KIC 9244992

Saio, H., Kurtz, D.W., Takata, M., Shibahashi, H., Murphy, S.J., Sekii, T., Bedding, T.R. 2015, MNRAS, 447, 3264

The impacts

- Internal rotation of stars became an observational astronomy.
- Two examples of the main-sequence stars were found to be almost uniformly rotating from core to surface, model independently.

Break

Asteroseismology of Giant Stars

gravity mode: $P_{nl} = [l(l+1)]^{1/2} P_0(n+l/2+\varepsilon)$**, where** $P_0 := \int_c^R N/r\, dr$

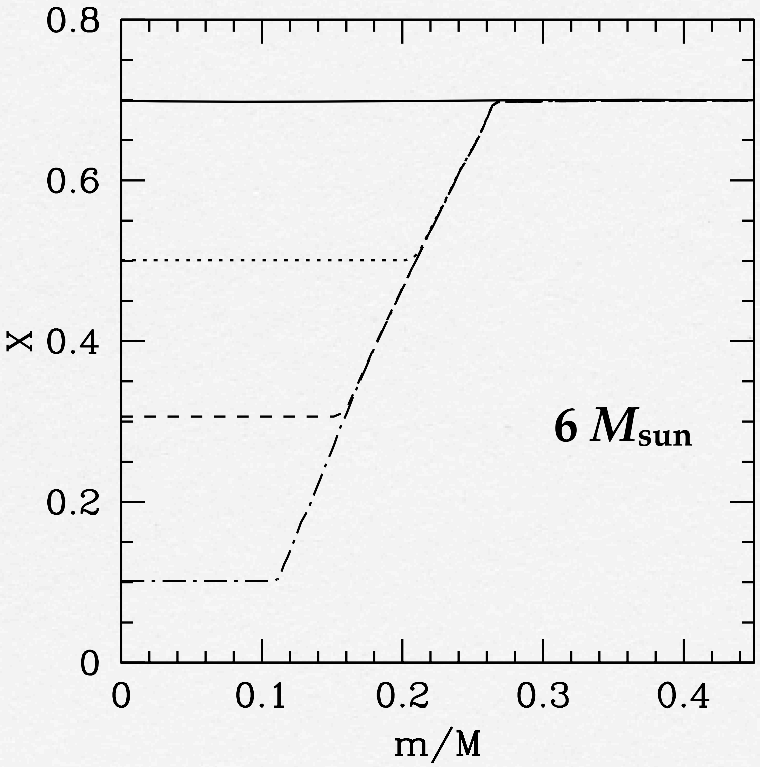

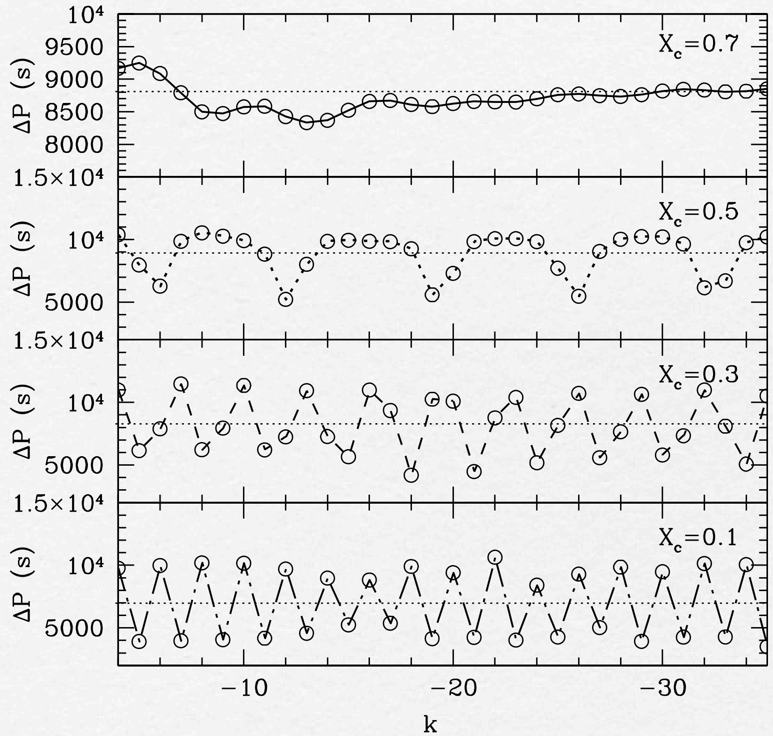

The period separation is sensitive to the chemically inhomogeneous zone.

Miglio, A., Montalbán, J., Noels, A., & Eggenberger, P. 2008, MNRAS, 386, 1487

Dramatic development of Asteroseismology of Red Giants

gravity wave：buoyancy as restoring force

buoyancy: stratification of light element above heavy element layer

practically, gravito-acoustic wave

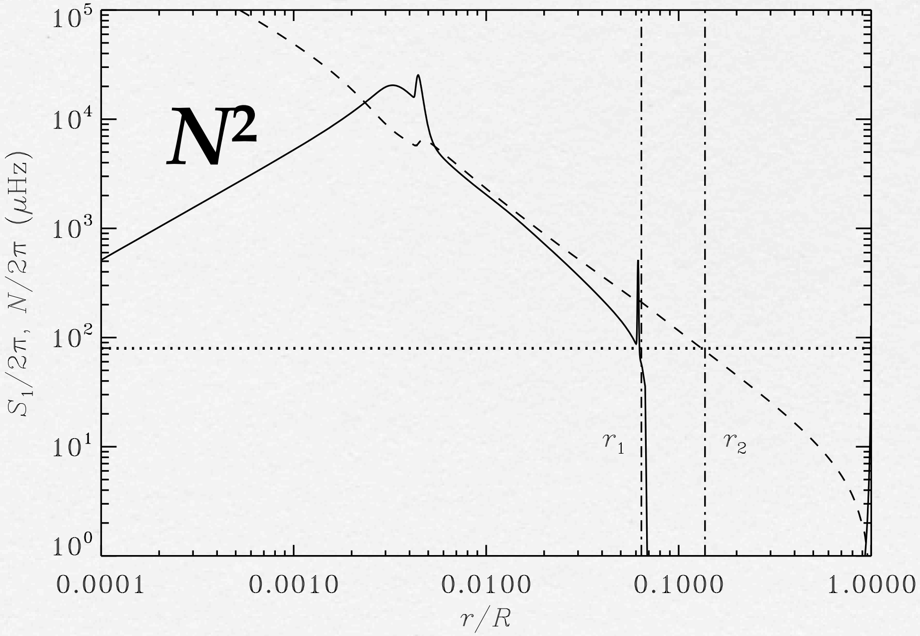

Christensen-Dalsgaard, J. 2012, ASPC, 462, 505

Red giants: propagation diagram

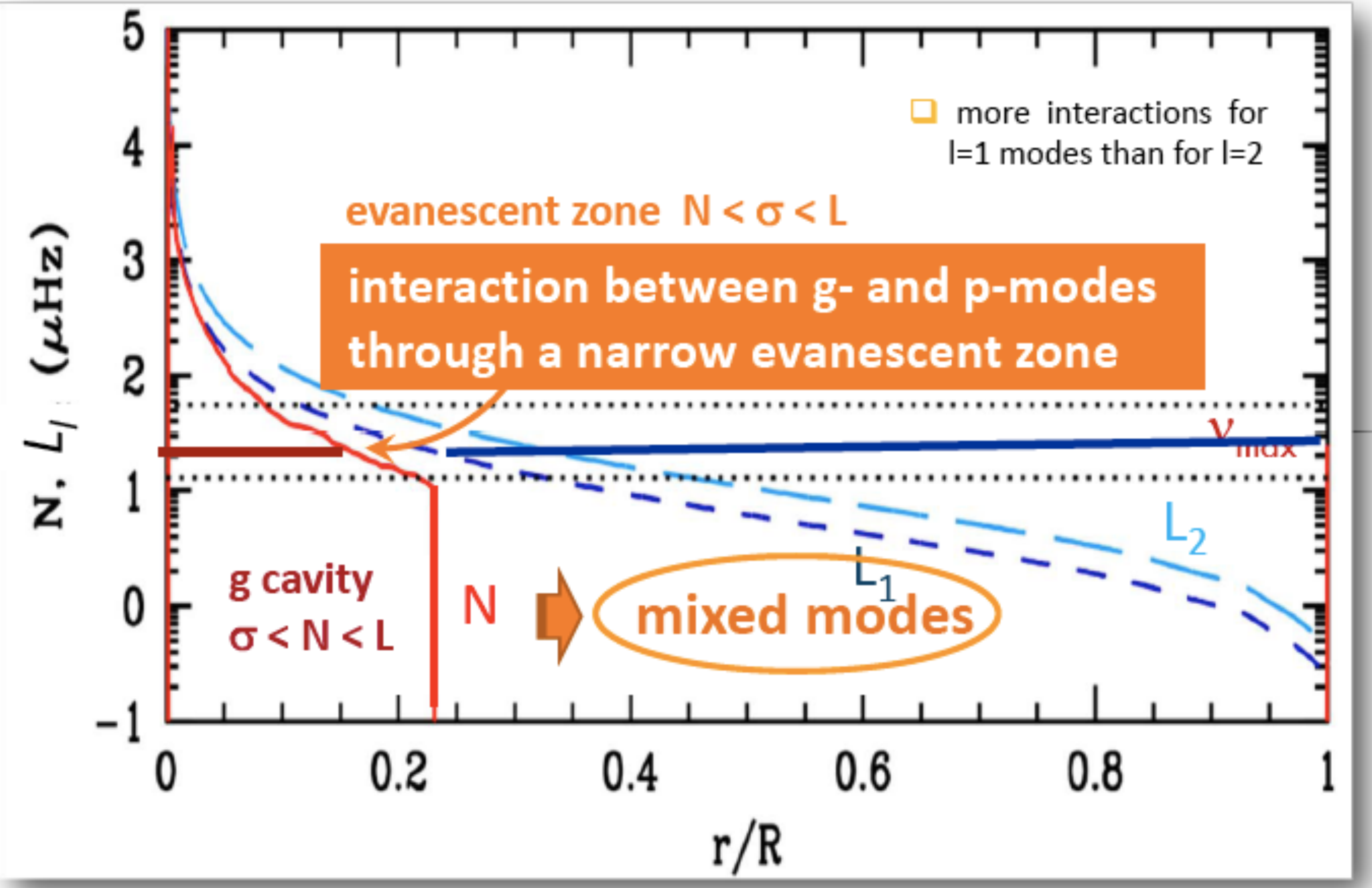

$$\nu_{nl} \simeq \Delta\nu\ (n+l/2+\varepsilon) - d_{nl}$$
$$\Delta\nu = [2\textstyle\int c^{-1}dr]^{-1}$$

mixed mode :
l=1 modes are sensitive both to stellar core and envelope and detectable

dual character :
acoustic wave in envelope, while gravity wave in core

probe for stellar core

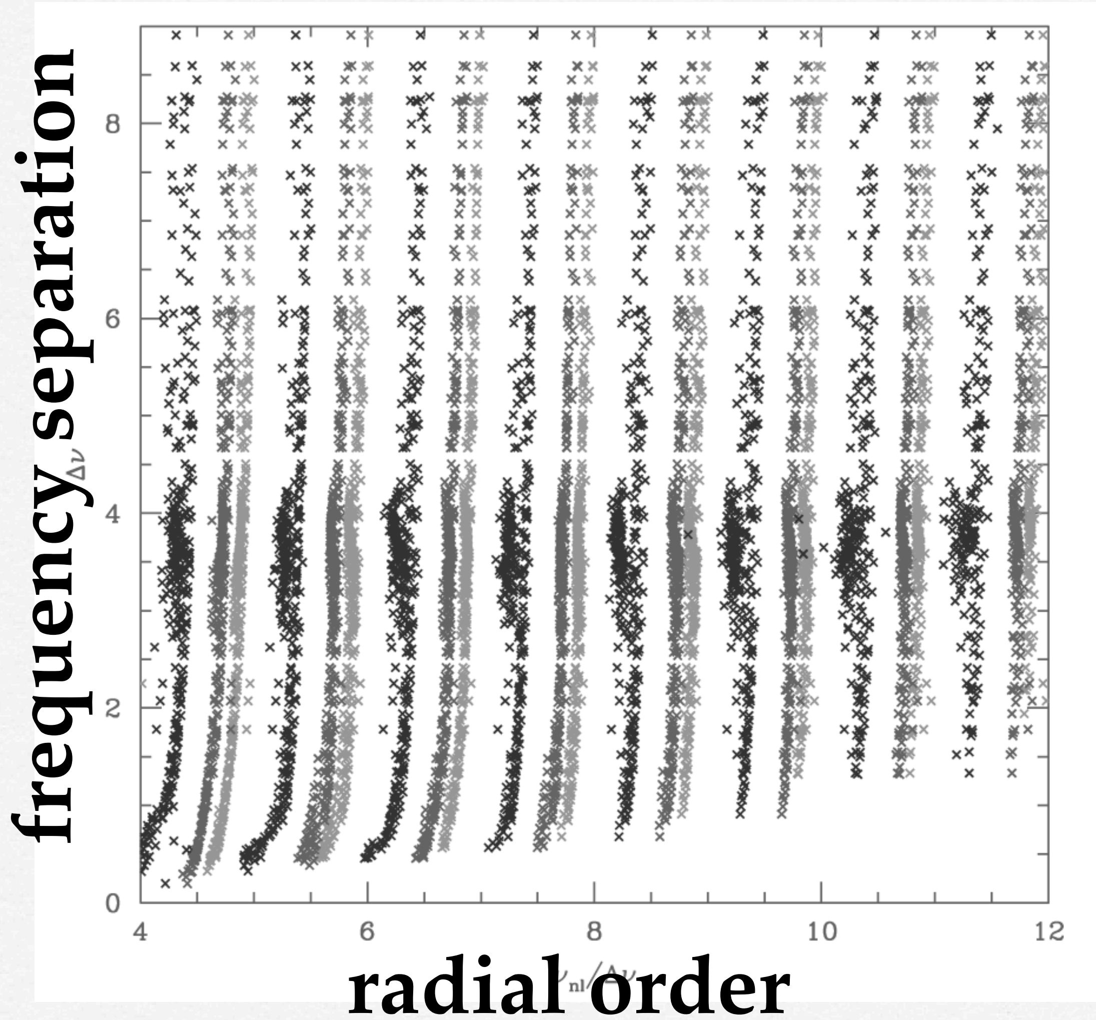

Montalban J. et al. 2010, ApJ 721 L182
Bedding T.R. et al. 2011, Nature 471 608
Beck P. et al. 2011, Nature doi:10.1038/nature10612

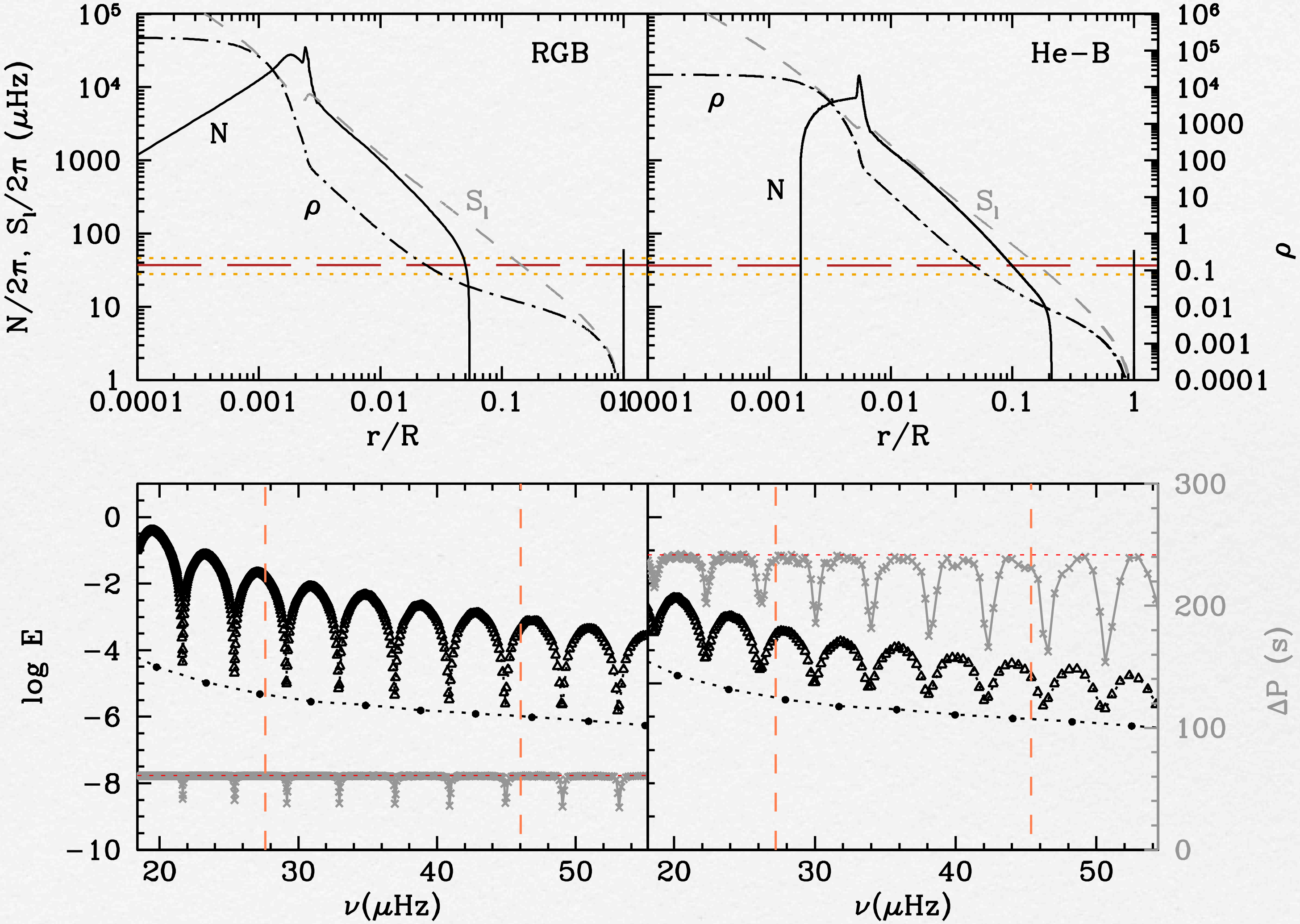

Montalbán, J., Miglio, A., Noels, A., Dupret, M.-A., Scuflaire, R., & Ventura, P. 2013, ApJ, 766, 118

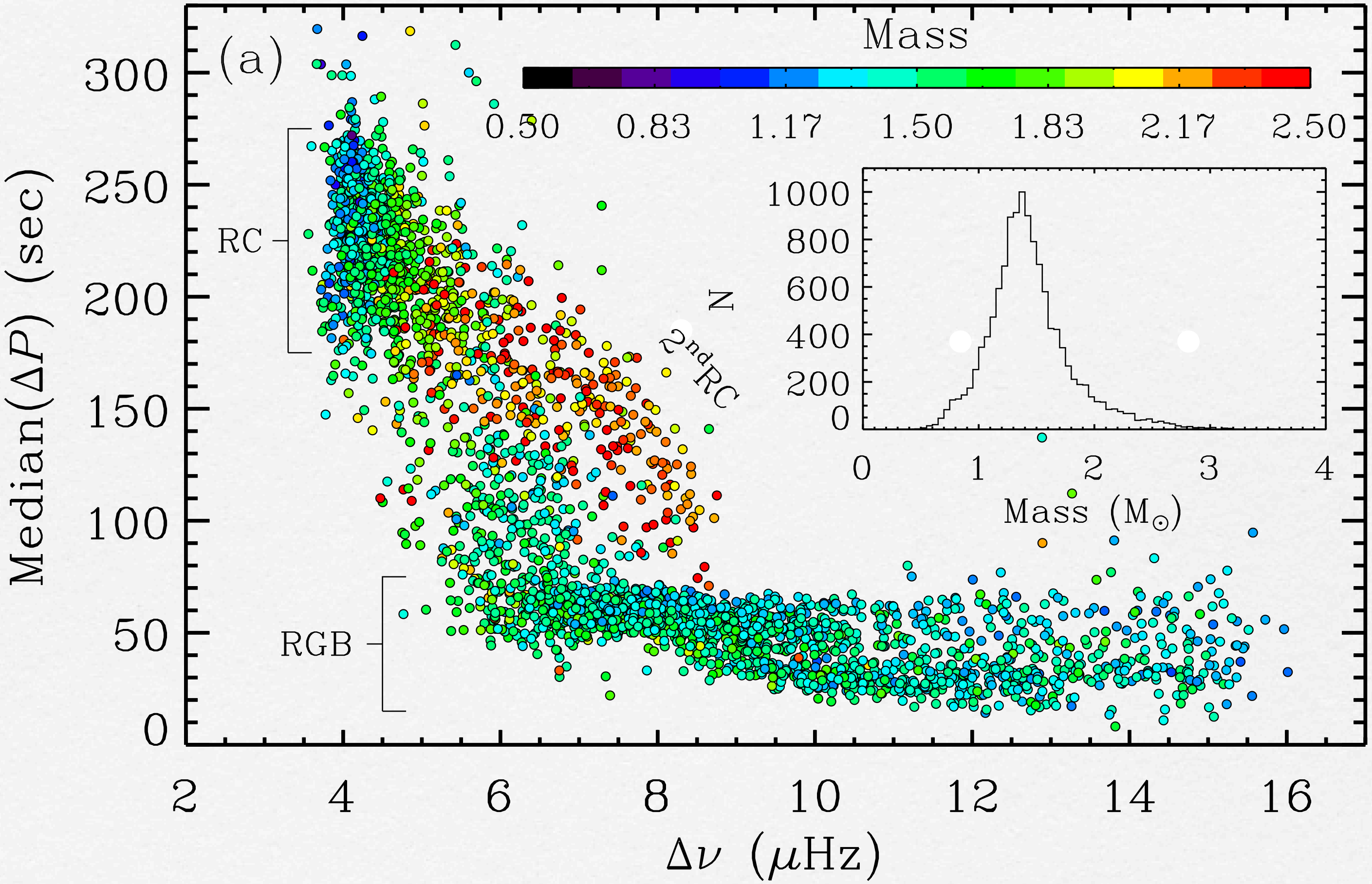

Stello, D., Huber, D., Bedding, T. R., et al. 2013, in ASP Conf. Ser., 479, 167

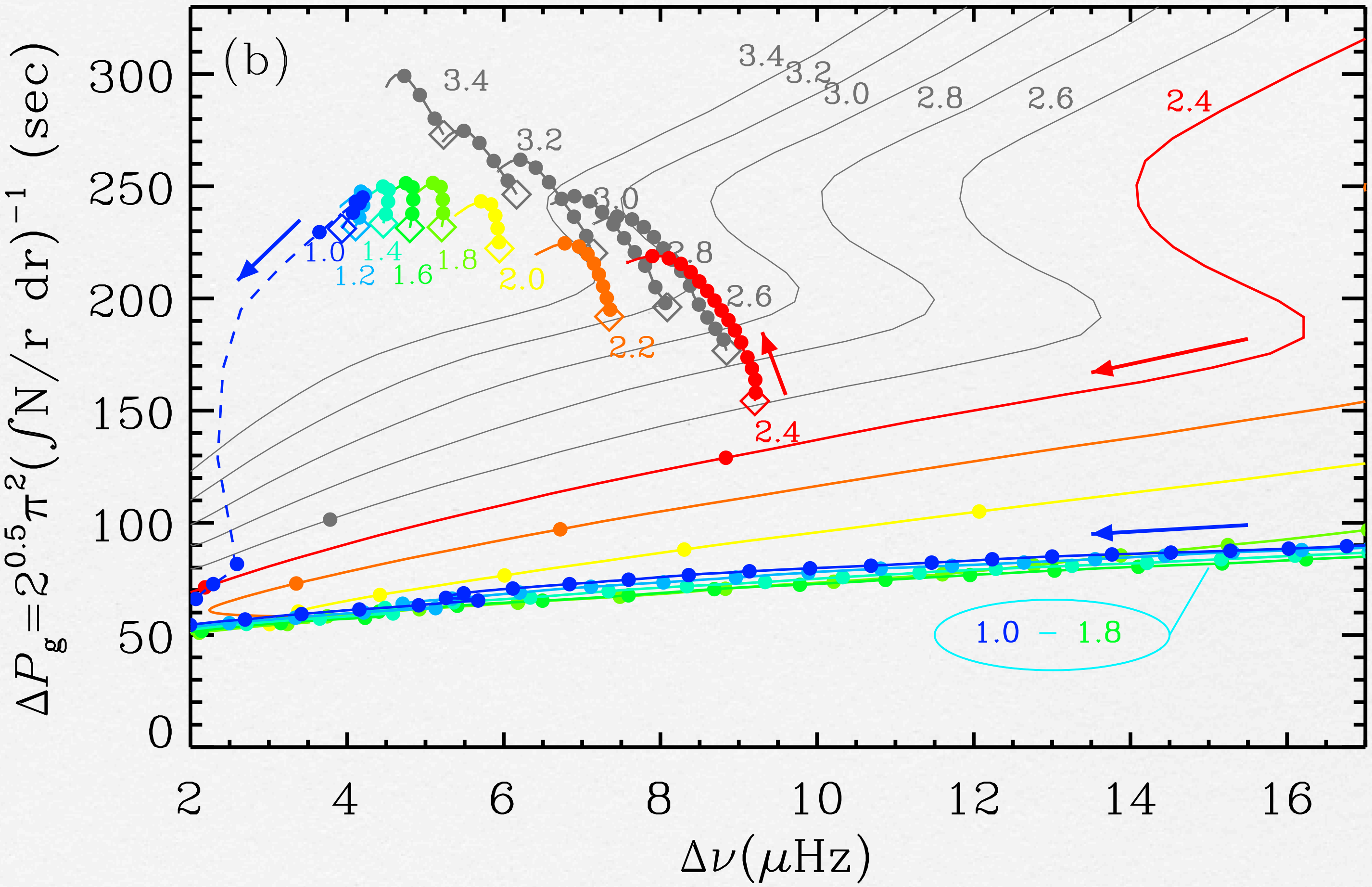

Stello, D., Huber, D., Bedding, T. R., et al. 2013, in ASP Conf. Ser., 479, 167

Period spacing as a function of frequency spacing

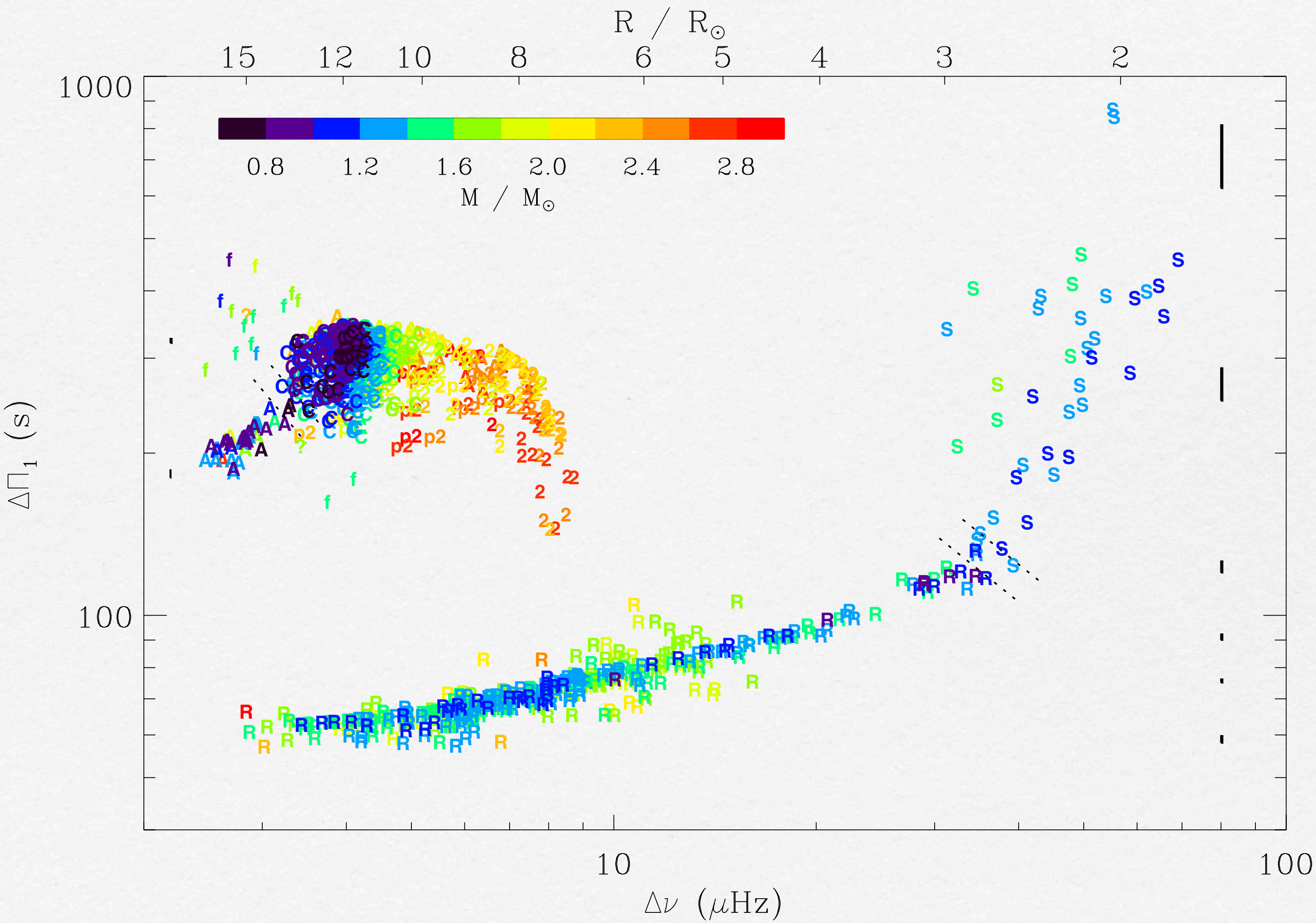

Mosser, B., Benomar, O., Belkacem, K., et al. 2014, A&A, 572, L5

Running Summary (a)

- **Dipole (*l*=1) mixed modes are very helpful to extract information of the deep interior of red giants.**
- **RGB and RC are distinguishable by asteroseismology, though they are overlapped each other on the HR diagram.**

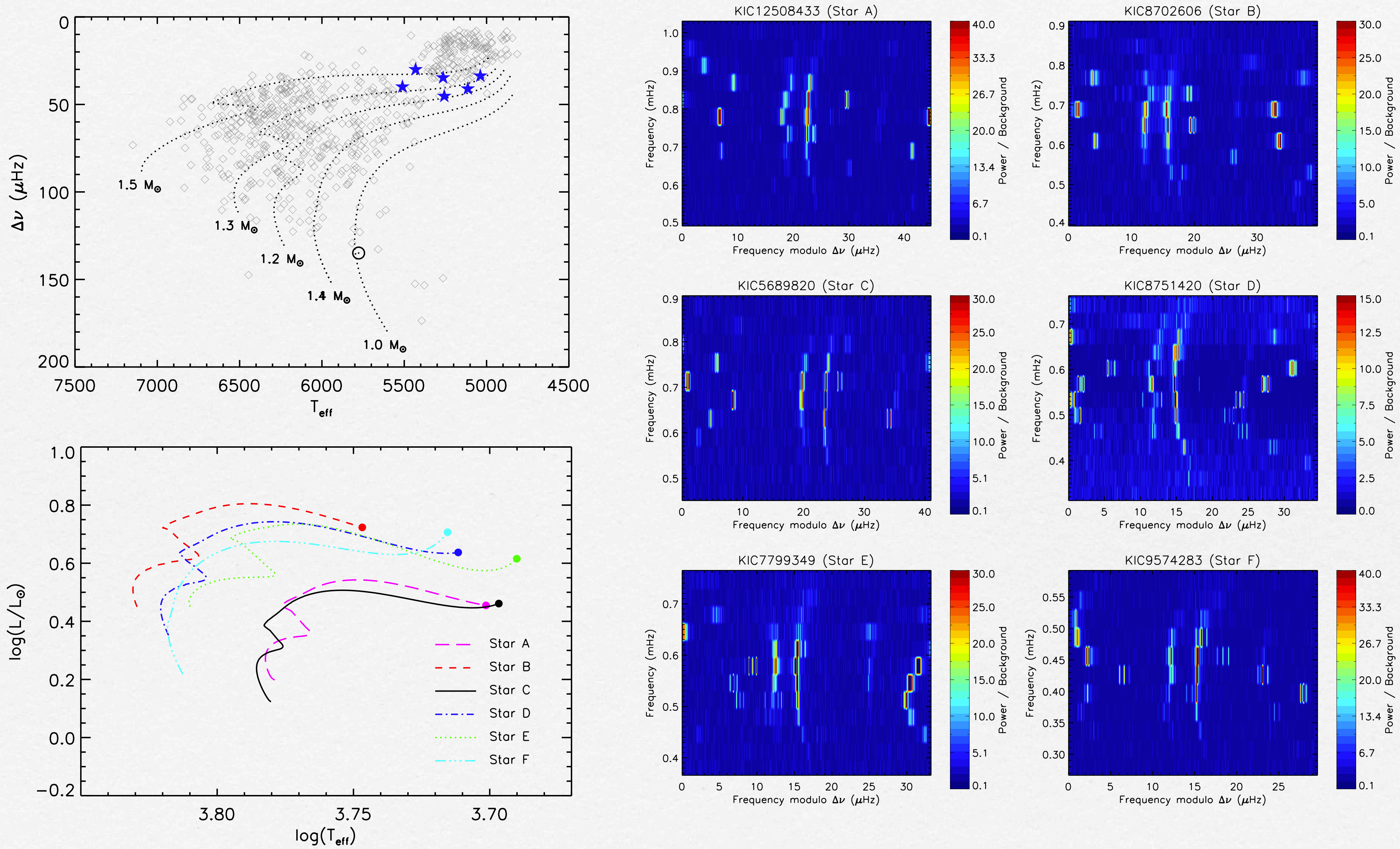

Delheuves, S., Doğan, G., Goupil, M.J., et al. 2014, A&A, 564, A27 splittings

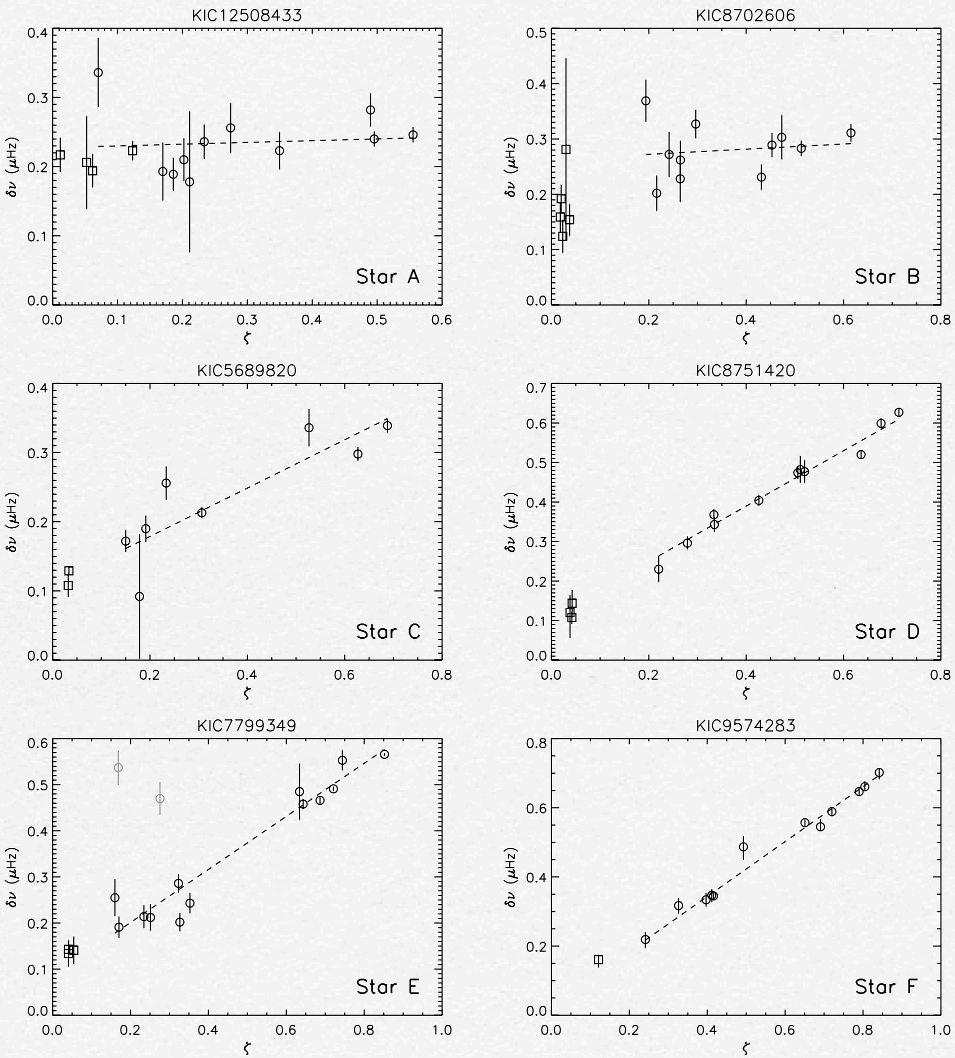

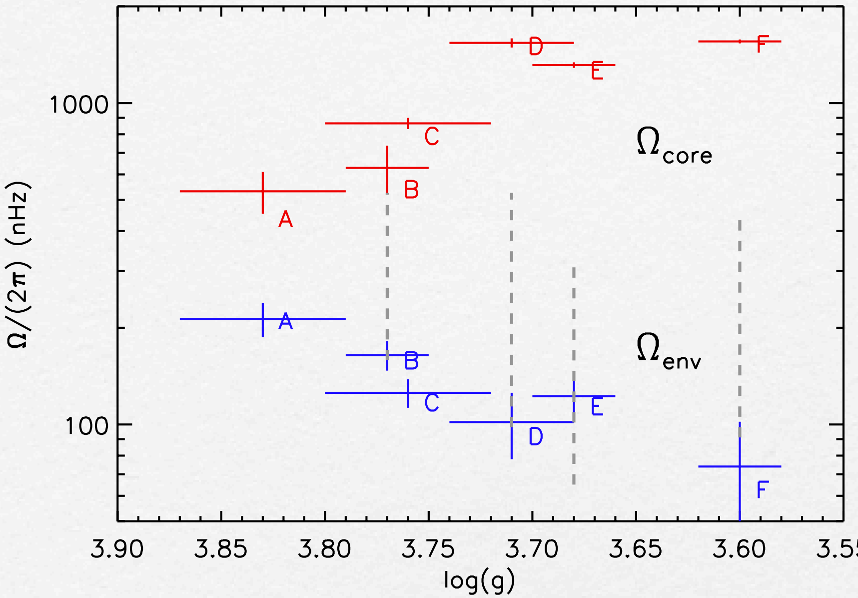

$$\zeta := \frac{KE(\text{g mode cavity})}{KE(\text{total})}$$

Delheuves, S., Doğan, G., Goupil, M.J., et al. 2014, A&A, 564, A27

Running Summary (b)

- **Subagents and RGB stars in the early stage show that the core rotates faster than the envelope, but the difference is only a factor of 5~10 —- *smaller than naively expected*.**

Some thoughts

- Ultimate compact objects, neutron stars and pulsars, are rotating fast indeed, but more slowly than the case of local angular momentum conserved.
- Hence, angular momentum in a star must be lost substantially during stellar evolution.
- Mass-loss phase at RGB or AGB has been regarded as such a candidate.
- But, subgiants and RGB stars in the early stage were found to be rotating with smaller contrast between the core and the envelope.It is desirable to see evolution of stellar rotation.
- Surprisingly, two main-sequence A stars were found to be rotating uniformly and slowly.
- So, how about main-sequence solar-like stars?

Solar-like oscillations are only low degree high-order p-modes. They are sensitive not only to the envelope but to the deep interior.

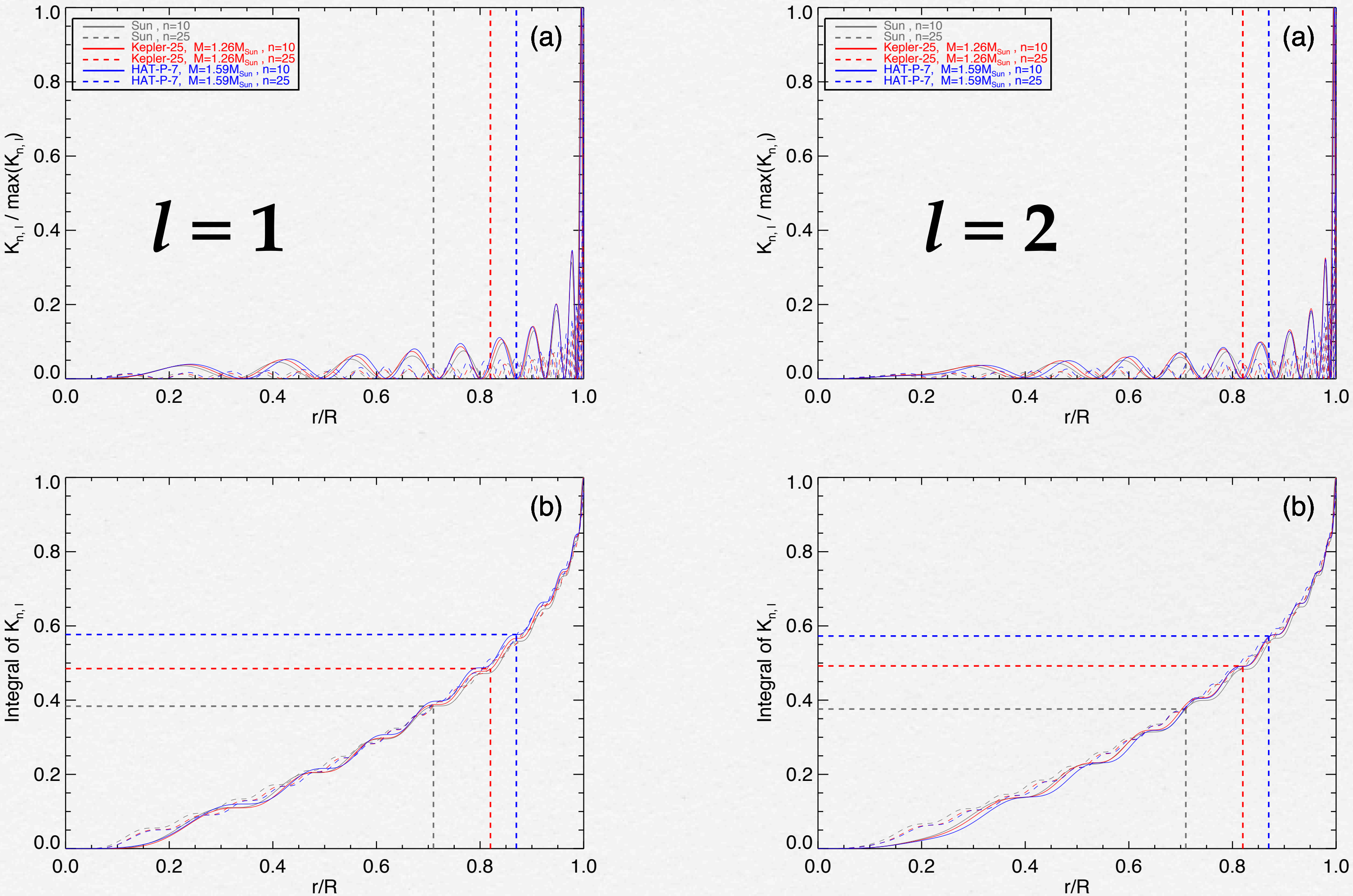

Benomar, O., Takata, M., Shibahashi, H., Ceillier, T, García, R. A. 2015, MNRAS, in press

$$\delta\omega_{n,l,m} = m(1 - C_{n,l}) \int_0^R K_{n,l}(r)\Omega(r)dr$$

$$=: m(1 - C_{n,l}) f_{n,l}$$

Separating contributions from the radiative core and the convective envelope,

$$\simeq I_{\mathrm{rad}} f_{\mathrm{rad}} + I_{\mathrm{conv}} f_{\mathrm{conv}}$$

Supposing the averaged rotation in the conv. env. is equal to the surface rotation rate,

$$\simeq I_{\mathrm{rad}} f_{\mathrm{rad}} + I_{\mathrm{conv}} f_{\mathrm{surf}}$$

Hence, from the seismically determined frequency splittings and the surface rotation rate,

$$\boxed{\langle f_{\mathrm{rad}} \rangle = f_{\mathrm{surf}} + \langle I_{\mathrm{rad}} \rangle^{-1} (f_{\mathrm{seis}} - f_{\mathrm{surf}})}$$

The surface rotation rate is estimated by

1. **spectroscopically measured $v_{eq}\sin i$,**
2. **semi-periodic luminosity variation due to probably starspots**

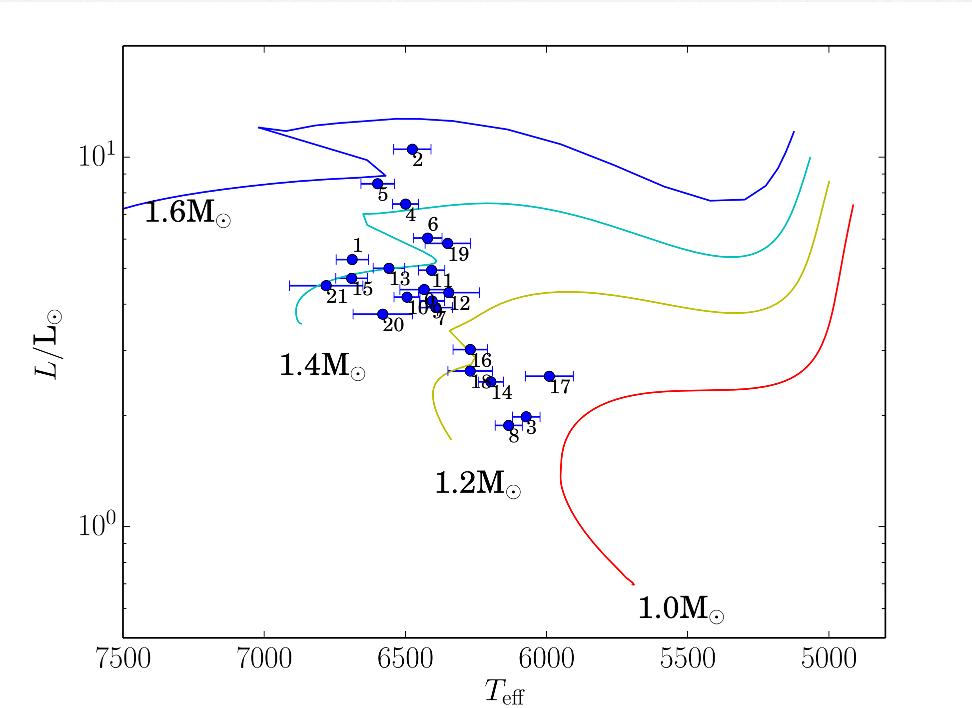

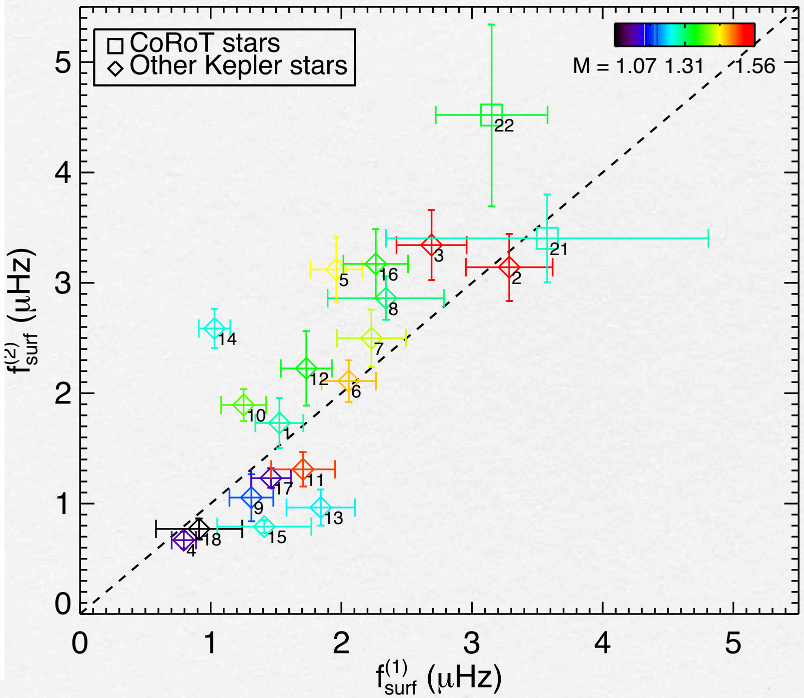

Benomar, O., Takata, M., Shibahashi, H., Ceillier, T, García, R. A. 2015, MNRAS, in press

The rotational splitting and the inclination angle are estimated in the form of a probability distribution function (pdf).

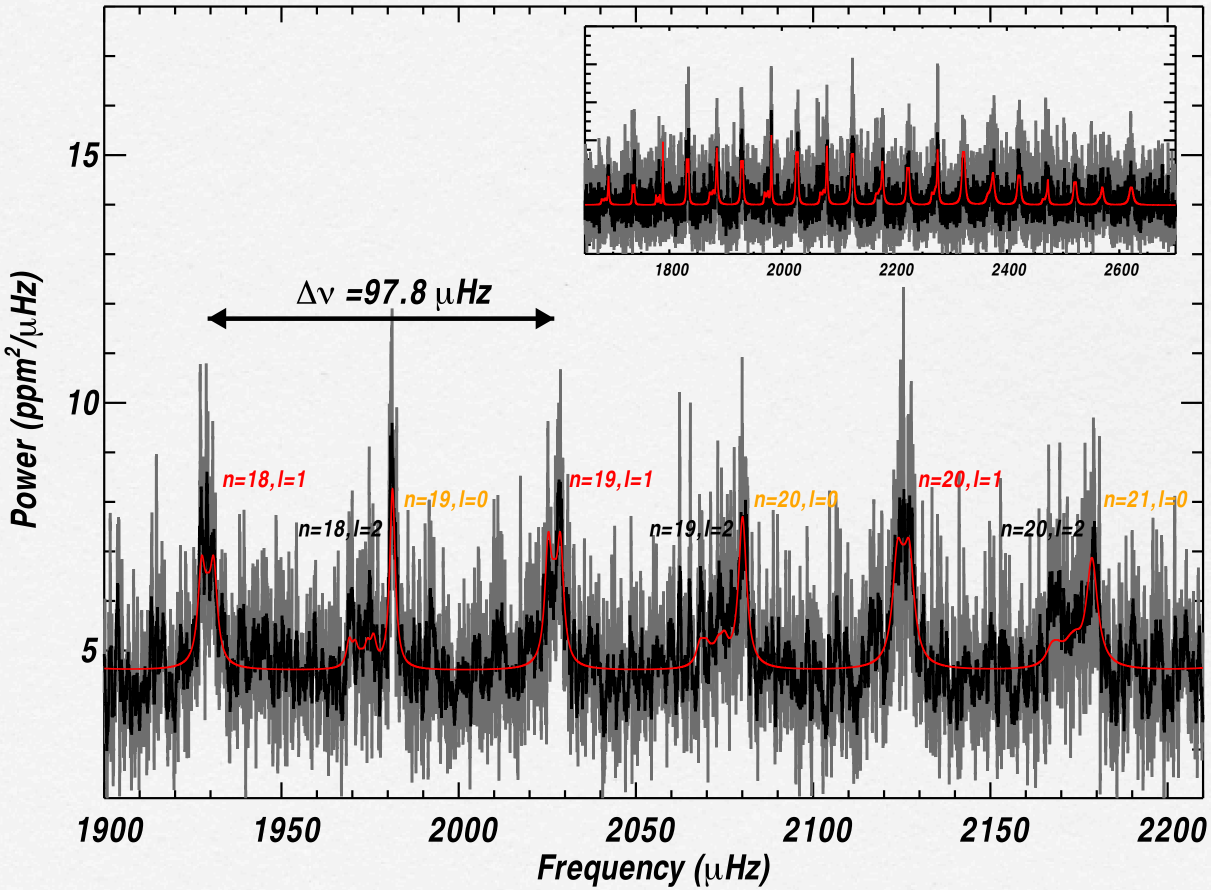

The rotational splitting and the inclination angle are estimated in the form of a probability distribution function (pdf).

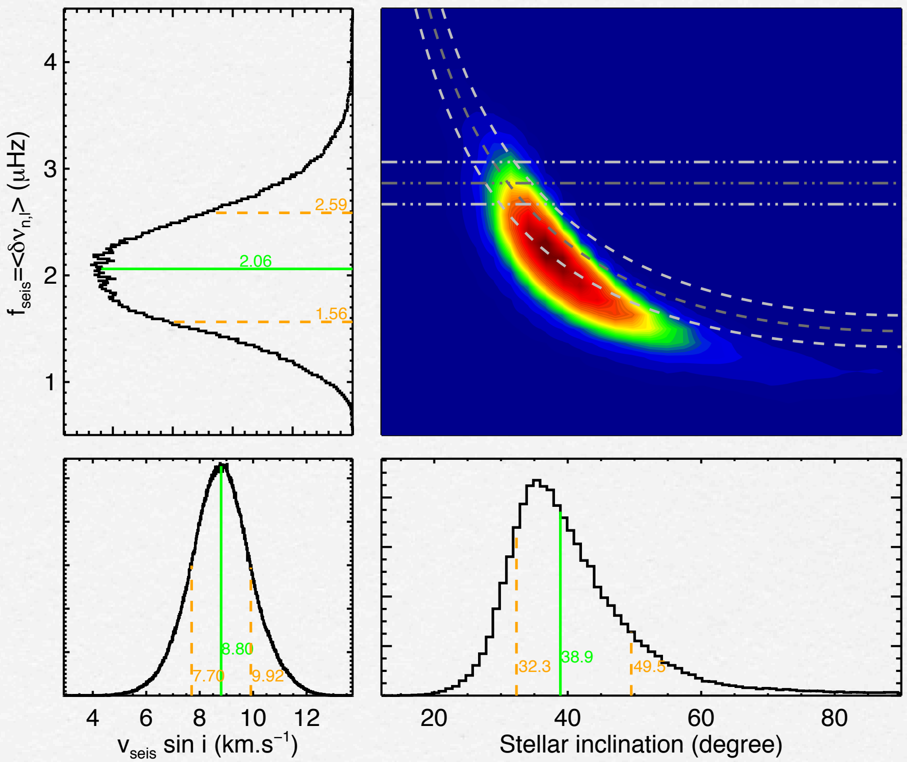

(a) KIC 7206837

Benomar, O., Takata, M., Shibahashi, H., Ceillier, T, García, R. A. 2015, MNRAS, in press

The difference between the surface rotation rate and the average rotation rate in the bulk of stars is small.

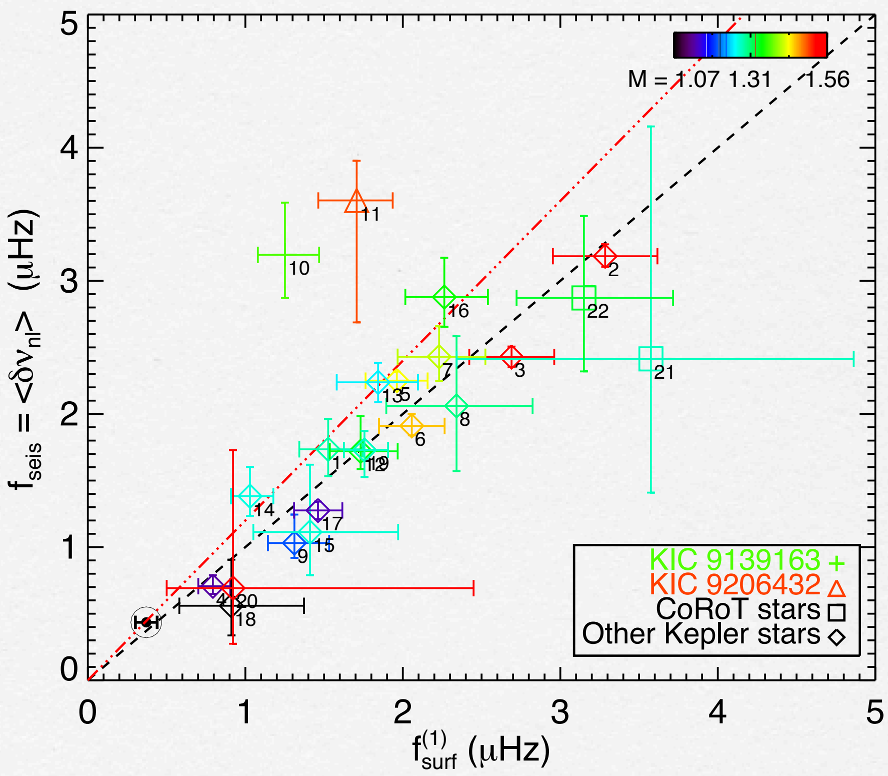

Benomar, O., Takata, M., Shibahashi, H., Ceillier, T, García, R. A. 2015, MNRAS, in press

Speculative conclusion

- Mass-loss phase at RGB or AGB has been suspected as a phase of dramatic change in stellar internal rotation.
- But, subgiants and RGB stars in the early stage were found to be rotating with smaller contrast between the core and the envelope.
- Surprisingly, two main-sequence A stars were found to be rotating uniformly and slowly.
- The main-sequence solar-like stars (including the Sun itself) were also found to be rotating nearly uniformly.
- An efficient process of angular momentum transport seems to operate during and/or before the main-sequence stage of stars?
- Internal rotation of stars is now a target of observational astronomy!

End of Lecture III-2